THE

LONDON EDINBURGH AND DUBLIN

PHILOSOPHICAL MAGAZINE

AND

JOURNAL OF SCIENCE.

[SEVENTH SERIES.]

NOVEMBER 1928.

XCIV. *The Escape of Heat from a Harmonically Oscillating Hot Wire.* *By* R. S. MAXWELL, *M.A.*, *B.Sc.**

1. INTRODUCTION.

THE problem of the escape of heat by free convection from a thin cylindrical wire at rest has been studied by Langmuir † and others, while King ‡ has carried out an exhaustive research, both theoretically and experimentally, on the case when the stationary wire is cooled by a stream of air passing it with a certain velocity, *i. e.* cooling by forced convection. When the wire is not at rest the problem is considerably more complicated, and up to the present no complete mathematical analysis has been brought forward. A considerable amount of experimental work has, however, been done on the subject by Tucker and Paris § in connexion with their Hot-Wire Microphone. They measured the escape of heat from the electrically-heated wire when subjected to an alternating air-current. The converse effect, that of a hot wire oscillating in still air, has been dealt with by Richards ‖. In both cases the wire is cooled,

* Communicated by Prof. A. W. Porter, F.R.S.

† Langmuir, Phys. Rev. xxxiv. pp. 401–422 (1912).

‡ King, Phil. Trans. Roy. Soc. A, ccxiv. pp. 373–430 (1914).

§ Tucker & Paris, Phil. Trans. Roy. Soc. A, ccxxi. pp. 389–430 (1921).

‖ Richards, Phil. Mag. xlv. pp. 926–934 (1923).

and consequently its resistance alters. It is shown that the change can be divided into two categories :—

(*a*) A lowering of the resistance of the whole wire. This is known as the steady drop.

(*b*) A periodic change of resistance.

The object of the present work is to investigate these two resistance changes under varying conditions, and also to bring forward, at any rate approximately, a mathematical theory which will explain the observed effects.

2. Experimental Work.

(a) *Steady Drop.*

(1) *Description of Apparatus.*

The experiments were made with the very fine platinum wire—diameter 0·0006 cm.—in the grid of a Tucker hot-wire

Fig. 1.

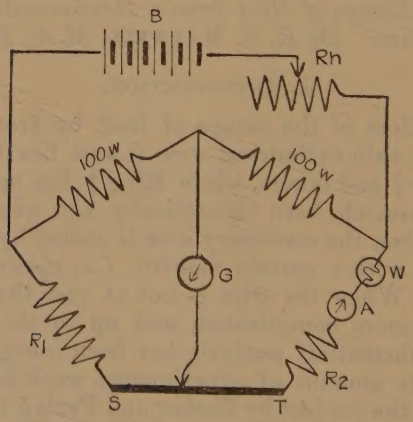

microphone. This grid was mounted on one prong of an electrically-maintained tuning-fork, and a compensating weight was mounted on the other prong, so that the fork would vibrate evenly. The tuning-fork and grid were completely enclosed in a large wooden box, so that all extraneous draughts were excluded.

The grid (W) was arranged in one arm of a Wheatstone's network, so that its resistance could be measured, and a milliammeter (A) was also included in the circuit. The electrical connexions are shown in fig. 1.

The method of taking observations was as follows. A rheostat (Rh) in the battery circuit was adjusted until the heating current through the grid had reached some definite value—say 30 milliamperes—when the fork was at rest, and the resistance of the grid was then measured. A long straight wire (ST) which had previously been calibrated, with an adjustable contact to the galvanometer, was used to obtain an accurate point of balance.

When the fork was set in vibration, the resistance of the grid decreased as it became cooled, and the new resistance was measured by balancing the network again. In order to prevent much alteration of the grid heating current, the total resistance $R_1 + R_2$ in the two resistance boxes was kept constant throughout a given series of readings.

The resistance of the grid was measured for various values of the amplitude of the fork, keeping the heating current constant. Nine such series of readings were taken for different values of the heating current : the resulting curves are shown in fig. 2.

The amplitudes were measured by means of a microscope with an eyepiece scale which was calibrated against a linear steel scale.

(2) *Numerical Calculations.*

(α) *Temperature.*—Within the accuracy covered by these experiments, there is a linear relationship connecting the resistance of the grid when at rest with the excess temperature of the hot wire of the grid over that of the surrounding atmosphere.

If R_0 = resistance of grid at atmospheric temperature and R_θ = resistance of grid at a temperature excess of θ_1 above that of the atmosphere, then

$$R = R_0(1 + \alpha\theta_1), \quad . \quad . \quad . \quad . \quad . \quad . \quad (1)$$

where α is the temperature coefficient of resistance of the wire of the grid.

Table I. shows the resistance of the grid when at rest for different heating currents. On extrapolating the resulting graph, it is found that the resistance of the grid at atmospheric temperature, *i. e* when no current is flowing in the wire, is 120 ohms.

The last column in the table gives the excess temperature (θ_1), calculated with the aid of equation (1) and assuming $\alpha = 0{\cdot}00367$ for platinum.

Fig. 2.

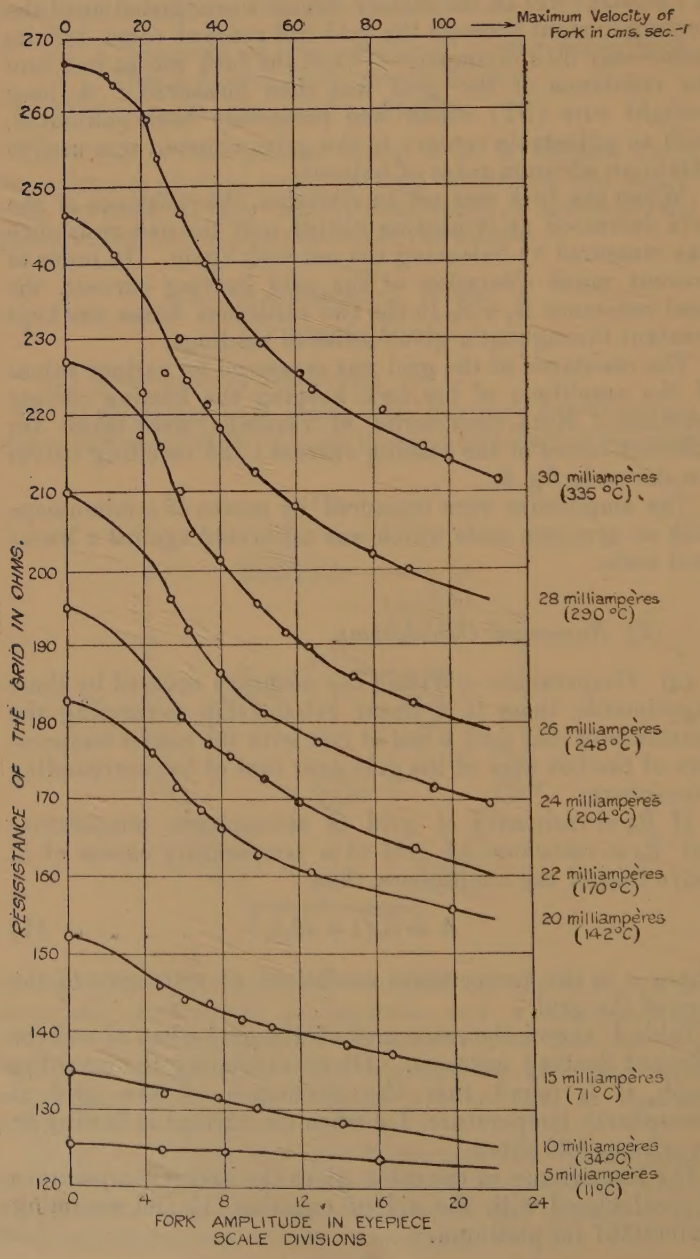
Maximum Velocity of Fork in cms. sec.⁻¹
0
20
40
60
80
100
270
260
250
240
230
220
210
200
190
180
170
160
150
140
130
120
RESISTANCE OF THE GRID IN OHMS.
30 milliampères (335 °C)
28 milliampères (290 °C)
26 milliampères (248 °C)
24 milliampères (204 °C)
22 milliampères (170 °C)
20 milliampères (142 °C)
15 milliampères (71 °C)
10 milliampères (34 °C)
5 milliampères (11 °C)
0
4
8
12
16
20
24
FORK AMPLITUDE IN EYEPIECE SCALE DIVISIONS

From the graph obtained on plotting $R\theta$ against θ_1 it is found that 1 ohm is equivalent to 2·24° C., *i. e.* that a decrease in the resistance of the grid of 1 ohm corresponds to a fall in temperature of the wire of 2·24° C.

(β) *Velocity.*—The change in the steady drop when the heating current is unaltered is due to the relative movement of wire and air, and is a function of the velocity of the wire through the air. This of course is not constant throughout the cycle, but the maximum velocity (V) can easily be found.

TABLE I.

Heating current (i), milliamps.	Resistance of grid when at rest (R), ohms.	Excess temperature above atmospheric (θ), °C.
30	267	335
28	247	290
26	228	248
24	210	204
22	195	170
20	183	142
15	152	71
10	135	34
5	125	11
(0)	(120)	—

If
$$\left.\begin{array}{l} n = \text{frequency of fork} \\ y_0 = \text{amplitude } ,, \quad ,, \\ \text{V} = 2\pi n y_0. \end{array}\right\} \quad \text{and} \quad \text{then} \qquad \ldots\ldots (2)$$

Now, the frequency of the fork used during the experiments was 96 vibrations per second. The eyepiece scale of the microscope was calibrated against a steel millimetre scale, and it was found that one eyepiece scale-division was equivalent to $7{\cdot}5 \times 10^{-3}$ cm. Therefore for one eyepiece scale-division

$$y_0 = 7{\cdot}5 \times 10^{-3} \text{ cm.}$$

$$\therefore \quad \text{V} = 2\pi \times 96 \times 7{\cdot}5 \times 10^{-3} \text{ cm.}$$

$$= 4{\cdot}52 \text{ cm. sec.}^{-1}$$

Values of the maximum velocity (V) for various values of the amplitude are given in Table II.

(γ) *Steady Drop.*—The experimental values found for the steady drop (Δ) from the graphs of fig. 2, with the help of Table I., are tabulated in Table II. for various known conditions of temperature and velocity.

TABLE II.

Experimental Values of Δ in °C. for Microphone Grid.

Amplitude.		Maximum Velocity (V) in cm. sec.$^{-1}$.	Temperature excess (θ_1) in ° C.								
Eyepiece scale-divisions.	cm.		335	290	248	204	170	142	71	34	11
2	0·015	9.0	2	7	4	6	6	4	3	2	0
4	0·030	18·1	12	22	16	17	17	15	12	4	1
6	0·045	27·1	41	46	43	36	32	27	18	7	1
8	0·060	36·2	66	64	58	53	43	38	22	9	1
10	0·075	45·2	81	77	72	63	50	45	26	11	2
12	0·090	54·3	92	86	82	70	57	48	28	13	2
14	0·105	63·3	100	94	90	75	63	54	30	15	3
16	0·120	72·4	109	101	95	80	67	57	34	16	4
18	0·135	81·4	112	105	100	83	72	60	36	18	4
20	0·150	90·5	118	110	104	88	76	63	38	20	6

(b) *Oscillatory Changes.*

The first experiments which were undertaken with a view to investigating the harmonic changes of resistance of the grid made use of a telephone receiver which was coupled inductively with the grid heating circuit. In addition to the fundamental the octave could be heard distinctly, and there was also evidence of higher harmonics. A vibration galvanometer was afterwards introduced in place of the telephone, and the presence of these harmonics was confirmed.

The instrument used was a Tinsley Moving Coil Vibration Galvanometer with a bifilar suspension. The suspended system had three adjustments, which could be varied to alter its natural frequency :

(1) The length of the suspension.
(2) The tension of the wires.
(3) The distance apart of the two wires.

When these were adjusted to make the natural frequency of the system equal to the frequency of the alternating current passing through the galvanometer, the latter was said to be "tuned." In this state resonance occurred, and the spot of light broadened out into a wide band. During these experiments the distance apart of the two wires remained fixed, and the tension and length adjustments gave a range from about 85 to 500 cycles per second. Scales had been engraved on the torsion head and on the side of the case near the sliding bridge, so that it was possible to record definite positions for the tension and length of suspension respectively. Thus any particular condition could be repeated at will. The galvanometer had been calibrated for frequency by passing alternating currents of known frequencies through it and noting the positions of the bridge reading and torsion head.

The grid heating current, which was known to have a complex wave form, was passed through the vibration galvanometer, and the adjustments were made throughout the whole of the above range. The harmonics present in the current could then be picked out at once, because when the galvanometer became tuned to any one component, resonance was observed. The frequency of the component was then found from the calibration curves.

The results of this analysis showed that, denoting the frequency of the tuning fork by n, the grid heating current had a series of harmonic constituents whose frequencies were given by $2n$, $3n$, $4n$, and in one case for a very low fork $5n$, in addition to the fundamental. For these experiments on the oscillatory changes several forks were used, of frequencies varying from 68 to 167 vibrations per second, but in most cases the fork of frequency 96 vibrations per second was used as in the experiments on the steady drop. The experiments were repeated for a straight platinum wire of diameter ·001 cm. mounted horizontally on the fork, and similar results were obtained, the harmonics being found as before.

A distinction must be made between the two cases, when the wire is vibrating (*a*) vertically, *i. e.* in its own convection current, and (*b*) horizontally. In (*a*) the fundamental and the octave appeared to be of approximately the same magnitude, but in (*b*) the octave was by far the most predominant harmonic present. This distinction is important on theoretical grounds, and is discussed in detail in section 4. The higher components of frequency $3n$, $4n$, etc. were observed to have considerably smaller amplitudes than the

fundamental and octave, although it proved impossible to measure any of these amplitudes with a great degree of accuracy. Attempts to make such measurements were made both directly and by means of photographing the wave form with the help of a rotating mirror, but they proved unsuccessful because the galvanometer could not be tuned sufficiently far away from the several resonance points to give a faithful reproduction of the wave form of the current, unless it was made too insensitive.

Photographs were taken of the vibrations of the prong of the fork to see whether the motion was accurately sinusoidal. Light from an arc was passed through a small diaphragm reflected from a mirror attached to the prong of the fork and from a rotating mirror, and finally was focussed on to the photographic plate. Several photographs were taken, and these showed that the prong was moving with simple harmonic motion, as was to be expected.

3. Theoretical Considerations.

(a) *General.*

The rate of loss of heat from a thin oscillating hot wire depends on several factors.

Heat Supplied.—If the wire is heated electrically, then the rate of heat supplied is E^2/R, where E is the e.m.f. in the heating circuit, and R is the resistance of the wire. If E is measured in volts, and R in ohms, then the rate of heat supplied will be measured in watts.

As the resistance of the wire is large compared with any other resistances in the circuit, the potential drop across the ends of the wire may be regarded as constant, and will not be affected by the oscillation.

Radiation.—In the treatment which follows, the loss of heat due to radiation will be ignored because Langmuir * has shown that for fine wires such as those used in the experimental work it is negligibly small.

Thermal Capacity of the Wire.—The thermal capacity (ϵ) is defined as the mass of the wire (m) multiplied by its specific heat (c).

Then $\epsilon\, d\theta$ represents the amount of heat added to or taken away from the wire for a change of temperature $d\theta$.

In the analysis given below the convention is adopted that

* Langmuir, Phys. Rev. xxxiv. pp. 401–422 (1912).

θ is reckoned positive for a lowering of temperature, and therefore

$\epsilon\, d\theta$ = amount of heat taken away from the wire for a drop in temperatnre of $d\theta$.

Hence $\epsilon \frac{d\theta}{dt}$ = rate at which heat is taken away from the wire.

Free Convection.—If the wire is *at rest*, and is heated electrically, then it will take up a certain definite equilibrium temperature when the rate of heat lost by free convection is exactly equal to the rate of heat supplied by the electric current.

Let θ_1 = excess temperature of the wire above that of the surrounding atmosphere ;

E = e.m.f. in the heating circuit ;

R_1 = resistance of the wire at temperature θ_1.

Then
$$\frac{E^2}{R_1} = H\theta_1, \quad . \quad . \quad . \quad . \quad . \quad (3)$$

where H is the free convection constant.

Forced Convection.—When the wire is cooled by being placed in a current of air, the phenomenon is called forced convection, and the escape of heat from the wire is dependent upon the velocity of the imposed draught. This may be treated as completely equivalent to the case when the wire is caused to move through still air with a definite velocity.

King * has derived two formulæ which give the heat-loss per cm. (W) from a wire of diameter d in a *steady* air-current of velocity V :

$$W = A'\theta_1 + B'V^{\frac{1}{2}}d^{\frac{1}{2}}\theta_1, \quad . \quad . \quad . \quad . \quad . \quad (4)$$

$$W = a'\theta_1/\log\frac{b'}{Vd}, \quad . \quad . \quad . \quad . \quad . \quad . \quad . \quad (5)$$

where A′, B′, a', and b' are constants, and θ_1 is the excess temperature of the wire above that of the surrounding air.

He found a critical value $Vd = 0{\cdot}0187$, where V is measured in cm./sec. and d in cm.

When $Vd > 0{\cdot}0187$, *i. e.* for high velocities or thick wires, equation (4) must be used.

When $Vd < 0{\cdot}0187$, *i. e.* for low velocities or thin wires, equation (5) is applicable.

The critical velocity for any wire is denoted by V_c.

* King, Phil. Trans. Roy. Soc. A, ccxiv. pp. 312–432 (1914).

An attempt has been made here to see whether King's formulæ can be adapted to the case when the wire is subjected to an oscillating draught, or, what is equivalent, to the case where the wire itself vibrates when mounted on a tuning-fork.

Let y = displacement of the prong of the tuning-fork, and consequently of the wire.

By experiment the motion is found to be simple harmonic, say $y = y_0 \sin pt$, where p is the pulsatance of the imposed vibration $= 2\pi$ times the frequency.

The velocity (v) of the wire at any time is given by

$$v = \frac{dy}{dt} = py_0 \cos pt,$$

but as the cooling of the wire is assumed to be independent of the direction of motion, the speed of the wire through the air at any moment can be written $py_0 |\cos pt|$ *, or $V|\cos pt|$, where V is the maximum value of the velocity, *i.e.* $V = py_0$.

For generality the escape of heat due to forced convection may be written $h(\theta_1, V|\cos pt|)$, and the appropriate formulæ (4) or (5) can be applied in special cases.

Differential Equation.—The general differential equation governing the escape of heat from the hot wire when it is oscillating can now be written down.

As before, let θ_1 = temperature excess of the wire above that of the surrounding atmosphere.

When the wire is set in vibration it is cooled by forced convection, and its temperature drops.

Let θ equal the divergence of the temperature from θ_1 at any time t, and let θ be regarded as positive when measured in a downward direction.

Then

$$\epsilon\frac{d\theta}{dt} = H(\theta_1 - \theta) + h((\theta_1 - \theta), V|\cos pt|) - \frac{E^2}{R_1(1-\alpha\theta)}, \quad \ldots\ldots (6)$$

where α is the temperature coefficient of resistance of the material of the wire.

Since θ is small, equation (6) may be written

$$\epsilon\frac{d\theta}{dt} = H(\theta_1 - \theta) + h((\theta_1 - \theta), V|\cos pt|) - \frac{E^2}{R_1}(1+\alpha\theta) \quad \ldots\ldots (7)$$

* The expression $|\cos pt|$ is used to signify the numerical value of $\cos pt$ without regard to sign. The function $|\cos pt|$ is thus always positive.

In the following sections the applications of this equation will be considered.

(b) *High Velocities.*

In this case King's formula for the rate of loss of heat due to forced convection may be written

$$W = (\beta V^{\frac{1}{2}} + \gamma)(\theta_1 - \theta),$$

where β and γ are constants having the same meaning as in King's paper.

Equation (4) now becomes

$$\epsilon \frac{d\theta}{dt} = H(\theta_1 - \theta) + (\beta V^{\frac{1}{2}} |\cos pt|^{\frac{1}{2}} + \gamma)(\theta_1 - \theta) - \frac{E^2}{R_1}(1 + \alpha\theta)$$

$$= -\left((H + \gamma) + \frac{E^2}{R_1}\alpha\right)\theta + \left((H + \gamma)\theta_1 - \frac{E^2}{R_1}\right)$$

$$+ \beta V^{\frac{1}{2}} |\cos pt|^{\frac{1}{2}} \theta_1 - \beta V^{\frac{1}{2}} |\cos pt|^{\frac{1}{2}} \theta. \quad . \quad (8)$$

The last term is of a smaller order than the other terms, and to a first approximation it may be omitted. When an approximate value for the temperature θ has thus been obtained, it may be substituted in this small term, and the equation can then be solved to a higher degree of accuracy.

The equation may now be written in the simple form :

$$\frac{d\theta}{dt} = -a\theta + b + c\{|\cos pt|\}^{\frac{1}{2}}, \quad . \quad . \quad . \quad . \quad (9)$$

where

$$a = \frac{1}{\epsilon}\left[(H + \gamma) + \frac{E^2}{R_1}\alpha\right],$$

$$b = \frac{1}{\epsilon}\left[(H + \gamma)\theta_1 - \frac{E^2}{R_1}\right],$$

and

$$c = \frac{1}{\epsilon}\beta V^{\frac{1}{2}}\theta_1.$$

The function $\{|\cos pt|\}$ is not in a form suitable for integration. It may, however, be expressed as a Fourier Series, and the numerical values of the different coefficients can be found by graphical integration.

If T is the periodic time of the oscillation, then the required limits of the function must be $t=0$ and $t=T$, because after this everything will be repeated.

For brevity let x be written in place of pt ; then, when $t=0$, $x=0$, and when $t=T$, $x=2\pi n T=2\pi$, and the limits now become 0 and 2π.

The Fourier Series may be written down :

$$\{|\cos x|\}^{\frac{1}{2}} = a_0 + a_1 \cos x + a_2 \cos 2x + \ldots a_n \cos nx$$

$$+ b_1 \sin x + b_2 \sin 2x + \ldots b_n \sin nx.$$

It is known that

$$a_0 = \frac{1}{2\pi}\int_0^{2\pi} \{|\cos x|\}^{\frac{1}{2}} dx,$$

$$a_n = \frac{1}{\pi}\int_0^{2\pi} \{|\cos x|\}^{\frac{1}{2}} \cos nx\, dx,$$

and

$$b_n = \frac{1}{\pi}\int_0^{2\pi} \{|\cos x|\}^{\frac{1}{2}} \sin nx\, dx.$$

The numerical values of these coefficients were determined by plotting the graph of the function within the integral sign for different values of x between the required limits, and finding the area enclosed between the curve and x-axis.

It was found that

$$\begin{aligned} a_1 = a_3 = a_5 = \ldots a_{2n-1} &= 0, \\ b_1 = b_2 = b_3 = \ldots b_n &= 0, \\ a_0 &= 0{\cdot}757, \\ a_2 &= 0{\cdot}330, \\ a_4 &= -0{\cdot}111, \\ a_6 &= 0{\cdot}080, \\ a_8 &= -0{\cdot}006. \end{aligned}$$

Therefore

$$\{|\cos x|\}^{\frac{1}{2}} = 0{\cdot}757 + 0{\cdot}330\cos 2x - 0{\cdot}111\cos 4x + 0{\cdot}080\cos 6x - 0{\cdot}006\cos 8x + \ldots\ldots$$

Equation (9) now becomes

$$\frac{d\theta}{dt} = -a\theta + b + c\{0{\cdot}757 + 0{\cdot}330\cos 2pt - 0{\cdot}111\cos 4pt + 0{\cdot}080\cos 6pt - 0{\cdot}006\cos 8pt + \ldots\}. \quad (10)$$

The solution of (10) is

$$\theta = \frac{b}{a} + c\left\{\frac{0{\cdot}757}{a} + \frac{0{\cdot}330}{\sqrt{4p^2+a^2}}\cos(2pt-\phi_2) - \frac{0{\cdot}111}{\sqrt{16p^2+a^2}}\cos(4pt-\phi_4) + \frac{0{\cdot}080}{\sqrt{36p^2+a^2}}\cos(6pt-\phi_6) - \frac{0{\cdot}006}{\sqrt{64p^2+a^2}}\cos(8pt-\phi_8)\right\} + Ae^{-at}. \quad (11)$$

The last term dies out as t becomes large, and may be ignored so far as periodic solutions are concerned.

The mathematical analysis shows :

(1) A steady drop in temperature (Δ), given by

$$\Delta = \frac{b + ca_0}{a},$$

and (2) a series of harmonics of frequency $2n$, $4n$ ....., of which the octave is the most predominant.

If this value of θ is substituted in the last term of equation (8), no new terms are introduced, but there is a small change in the values of the constants.

(c) *Low Velocities.*

For low velocities it is necessary to use the form of King's formula given in equation (5), and when applied to an oscillatory draught equation (7) becomes

$$\epsilon \frac{d\theta}{dt} = \mathrm{H}(\theta_1 - \theta) + \frac{a'}{\log \frac{b'}{\mathrm{V}|\cos pt|\, d}}(\theta_1 - \theta) - \frac{\mathrm{E}^2}{\mathrm{R}_1}(1 + \alpha\theta) \quad . \quad . \quad . \quad . \quad . \quad (12)$$

The solution of this equation shows temperature changes of just the same form as those given by equation (11).

(d) *Critical Velocity.*

It is important to calculate the critical velocity (V_c) corresponding to King's value $\mathrm{V}d = 1{\cdot}87 \times 10^{-2}$ for the actual wire used in the experimental work.

In this case $d = 6 \times 10^{-4}$ cm.

$$\therefore \quad \mathrm{V}_c = \frac{1{\cdot}87 \times 10^{-2}}{6 \times 10^{-4}}$$

$$= 31{\cdot}2 \text{ cm. sec.}^{-1}.$$

This velocity marks the boundary between the high and low velocity formulæ, and this must be kept in mind during the succeeding sections.

4. Comparison of Theory with Experiment.

(a) *Steady Drop.*

It is possible to calculate values of the steady drop Δ by means of equation (11), using the appropriate values of β and γ as given by King * in his paper. The values thus found are not in sufficient agreement with those obtained experimentally to be given in detail in this paper, but they are of the same order of magnitude. Furthermore, in both cases

* *Loc. cit.* pp. 420 and 422.

the steady drop is found to increase with temperature and with velocity.

It must be remembered, however, that the experimental conditions were by no means the ideal conditions demanded by the theory. For one thing, instead of a straight wire stretched between two fixed supports, the crumpled wire of a microphone grid was used. There are three loops in such a grid, and as the grid was clamped in a vertical position, it is quite possible that the convection current from one part of the wire impinged upon another part, thus lowering the resistance of the grid as a whole*. Again, since the wire was not straight, it was very difficult to measure its length with any degree of accuracy. The value adopted —0·7 cm.— was found by observing the grid with a microscope and measuring those portions of the wire which would be effective in contributing freely to the convection current. But since the calculated value of Δ increases with increase of length of wire, this uncertainty is bound to introduce a small error.

The wires used in this experiment were very much smaller than any used by King in his experiments on forced convection with steady draughts, and it may be that his formulæ will not bear extrapolation to such fine wires. For example, the term depending upon the velocity does not appear to have a sufficiently great coefficient to cause the theoretical value of the steady drop to increase sufficiently for the greater velocities, and it is possible that other formulæ could be devised which would fit the experimental curves better; but it does not seem worth while pursuing this line until the theoretical conditions are more accurately realized.

There is yet another factor affecting the cooling of the wire which should be noticed. It has been shown above (p. 957) that the critical velocity below which the high velocity formula given by equation (8) will not hold is given by $V_c = 31{\cdot}2$ cm. sec.$^{-1}$. Now, in the analysis put forward the actual velocity of $v = V \cos pt$ has been replaced by a mean velocity $a_0 V$, where $a_0 = 0{\cdot}757$. Actually, however, the velocity varies between the limits $v = V$ and $v = 0$, the velocity falling to zero twice during each complete vibration of the fork. Thus, even if V is considerably greater than V_c, the actual velocity v must be less than V_c during certain portions of the cycle, and it cannot be expected, on this ground alone, that the theoretical equation would show exact agreement with the experimental results.

* *Cf.* Tucker & Paris, p. 396.

The last error which must be considered is that arising from neglecting the term $\beta V^{\frac{5}{2}} \mid \cos pt \mid^{\frac{5}{2}}\theta$. If this term is worked out numerically, using the values of θ already obtained, it is found that, for the case where it could have the greatest possible effect, the error is less than 10 per cent., which is smaller than some of the other errors which have been considered above.

(b) *Oscillatory Changes.*

Effect due to the heating-up of the surrounding air :—

The mathematical analysis given in Section 3 does not indicate the presence of the fundamental, or the odd harmonics. This is because the theoretical treatment is concerned entirely with the free and forced convection from a hot wire vibrating in cool air, and no account has been taken of the general heating-up of the air in the neighbourhood of the wire. As in King's analysis, it has been assumed that the wire is always moving into air of atmospheric temperature. In this case, if the wire is vibrating with frequency $n=p/2\pi$ there are two positions, one at each end of the swing, in every complete vibration, when the wire is at rest. The cooling is thus identical in the two halves of the cycle, and is periodic with a frequency $2n$. Hence it follows that on this theory the *octave* is the most important term.

In practice, however, it is essential to take into account the heating-up of the surrounding air ; and this depends upon the general convection current of the heated air which rises from the hot wire. There are two quite distinct cases :—

(a) *Hot wire vibrating vertically.*—As the wire moves upwards it travels with the convection current ; as it moves downwards it travels against it. Thus it is quite clear that the escape of heat from the wire to the air is different for the two motions ; consequently, any term arising from this convection effect will be periodic with the frequency of the fork, and the *fundamental* note occurs.

(b) *Hot wire vibrating horizontally.*—The motion of the wire is at right angles to the convection current ; the heated air escapes upwards, and so does not affect the cooling of the wire further. This case approximates more to the simple theory, and the *octave* predominates.

The effect of considering this heating-up of the air near the wire is to introduce a periodic term of the same frequency as that of the driving-fork. There is no evidence

available concerning the physical nature of this term, but since it is periodic, it should be possible to represent it as a Fourier series containing all the harmonics. In any case, the fundamental is probably the predominating term, and without in any way being dogmatic in the matter, it is of interest to see the effect of introducing a term $d\cos pt$ to be added on to (9), which then becomes

$$\frac{d\theta}{dt} = -a\theta + b + c\{|\cos pt|\}^{\frac{4}{3}} + d\cos pt. \quad . \quad . \quad . \quad . \quad (13)$$

$$\therefore \quad \theta = \frac{b}{a} + c\left\{\frac{0{\cdot}757}{a} + \frac{0{\cdot}330}{\sqrt{4p^2+a^2}}\cos(2pt-\phi_2)\right.$$
$$\left. - \frac{0{\cdot}111}{\sqrt{16p^2+a^2}}\cos(4pt-\phi_4) + \ldots\ldots\right\}$$
$$+ \frac{d}{\sqrt{p^2+a^2}}\cos(pt-\phi_1), \quad . \quad . \quad . \quad . \quad . \quad . \quad (14)$$

the decaying exponentials being ignored as before.

If, now, this value of θ is substituted in the last term of (8), terms of the type

$$\cos(pt-\phi_1)\cos 2\mathrm{K}pt$$
$$= \tfrac{1}{2}\cos(\overline{2\mathrm{K}+1}-\phi_1) + \tfrac{1}{2}\cos(\overline{2\mathrm{K}-1}+\phi_1)$$

arise for all integral values of K. Thus the complete equation becomes

$$\theta = \gamma_0 + \gamma_1\cos(pt-\chi_1) + \gamma_2\cos(2pt-\chi_2)$$
$$+ \gamma_3\cos(3pt-\chi_3) + \ldots\ldots, \quad . \quad . \quad . \quad (15)$$

which agrees with the experimental results in indicating the presence of a steady drop and the full series of harmonics.

5. Wire cooled by a Steady Draught of Very Low Velocity.

It appears permissible in conclusion to discuss briefly some of the difficulties which occur in dealing with King's formula for loss of heat when the velocity of the cooling draught is small.

The experimental curves found for the cases when the draught is steady, and when it is oscillatory, are very similar in character, and the difficulties which underlie their interpretation are more or less the same in both cases ; so it is convenient merely to consider the simpler case, namely that in which a hot wire is subjected to a small steady cooling draught.

Thomas *, in his researches on the hot-wire anemometer, obtained a series of curves of the type shown in fig. 3 for a straight wire cooled by a steady draught. Richards †, using a microphone grid, and E. G. Richardson ‡, using a grid constructed of thicker wire, have both obtained curves of the same type. This curve should be compared with those shown in fig. 2, which were obtained by the writer for oscillating draughts. The curve is concave to the V axis for very small velocities ; indeed, it is approximately parabolic near the R axis. but it becomes convex to the V axis

Fig. 3.

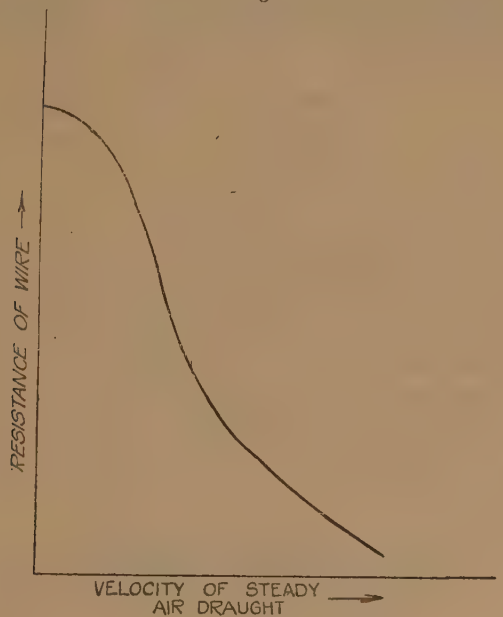

as the velocity increases. Tucker and Paris § obtained only the parabolic portion of the curve. using a microphone grid, but their velocities never exceeded 5 cm. per sec.

In every case the point of inflexion occurred when the velocity was far below the critical velocity V_c for the wire in question ; therefore it appears that the experimental curve for low velocities is made up of two distinct parts.

* Thomas, Phil. Mag. xxxix. pp. 505–534 (1920). See fig. 8.
† *Loc. cit.* p. 927. See fig. 1.
‡ Proc. Roy. Soc. A, cxii. pp. 552–541. See fig. 2.
§ *Loc. cit.* p. 408. See fig. 7.

Thomas also found that "the velocity at which the change of curvature of the respective graphs occurs is greater the larger the heating current employed." This statement is also true for oscillatory draughts, as may be seen on examination of the graphs given in fig. 2.

Turning now to King's formula, given in equation (5),

$$W = \frac{a'\theta_1}{\log \frac{b'}{Vd}}, \quad \ldots\ldots\ldots \quad (5)$$

it will be of interest to work it out numerically for a given temperature and for a series of velocities.

Preserving the notation, used by King, the constants a' and b' may be written

$$a' = 2\pi\kappa,$$
$$b' = 2bV,$$

where $$b = \frac{\kappa e^{(1-\gamma)}}{s\sigma V}$$

and κ = thermal conductivity of air
$= 5{\cdot}2 \times 10^{-5}$ calories (cm.)$^{-1}$(sec.)$^{-1}$ (° C.)$^{-1}$,

σ = density of air $= 1{\cdot}3 \times 10^{-3}$ (grm.) (cm.)$^{-3}$,

s = specific heat per unit mass of air
$= 1{\cdot}71 \times 10^{-1}$ calories (grm.)$^{-1}$ (° C.)$^{-1}$,

γ = Euler's Constant $= 0{\cdot}57721$.

$\therefore\ e^{(1-\gamma)} = 1{\cdot}52.$

$\therefore$ Numerically

$$b' = \frac{2 \times 5{\cdot}2 \times 10^{-5} \times 1{\cdot}52}{1{\cdot}3 \times 10^{-3} \times 1{\cdot}71 \times 10^{-1}}$$
$$= 7{\cdot}15 \times 10^{-1}\ *.$$

For the wire in the microphone grid $d = 6 \times 10^{-4}$.

$$\therefore\ \frac{b'}{d} = 1{\cdot}19 \times 10^{3}.$$

Now consider a particular temperature excess above atmospheric temperature, say $\theta_1 = 335°$ C. The heat-loss (W) will be given in watts per cm. of wire.

* This constant b' will be unaffected by a change of units from calories per second into watts, as long as κ and s are both measured in the same units. It is of the dimensions of a length.

In this case κ must be expressed in watt units, *i. e.*

$$\kappa = 2{\cdot}37 \times 10^{-4} \text{ watts (cm.)}^{-1} (^{\circ}\text{C.})^{-1}$$

and $$a'\theta_1 = 2\pi \times 2{\cdot}37 \times 10^{-4} \times 3{\cdot}35 \times 10^{2}$$
$$= 4{\cdot}96 \times 10^{-1}.$$

$$\therefore \quad W = \frac{a'\theta_1}{\log_e \frac{b'}{\sqrt{d}}} = \frac{4{\cdot}96 \times 10^{-1}}{\log_e \frac{1{\cdot}19 \times 10^{3}}{V}} \text{ watts cm.}^{-1}.$$

The resulting graph is shown in fig. 4.

Fig. 4.

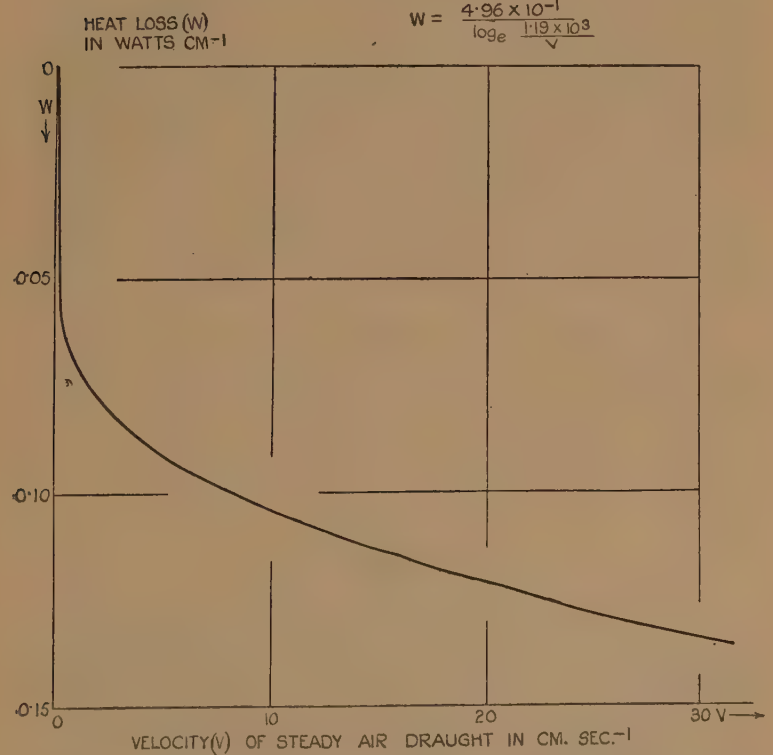

It can be seen from equation (5) that a graph plotted for a wire at a different temperature would be of exactly the same shape, because the only difference would be in the value of θ_1. Hence the graph of fig. 4 must be regarded as typical of the theoretical values predicted by King.

The question which must be faced is how to reconcile the theoretical curve shown in fig. 4 with the experimental

curve in fig. 3, for very small velocities, *i. e.* to explain the "parabolic" portion of the experimental curve. No attempt at a quantitative analysis is here put forward, but perhaps the following qualitative suggestions may throw some light on this rather complicated phenomenon.

Consider a hot wire at rest in absolutely still air. Then any heat which is lost must be lost by free convection. Let a very slowly moving air-stream pass across the wire. If the velocity of this stream is sufficiently slow, the wire will still lose heat almost entirely by free convection, and any loss due to forced convection must be extremely small. As the velocity increases, the loss of heat due to forced convection will also increase, and for a time such an increase will be fairly rapid. Such a state of affairs would be represented by the "parabolic" portion of the curve which has been found by all observers. When the velocity is increased still further, the forced convection would have become an appreciable factor in the cooling of the wire, and would increase less rapidly. This would correspond to the point of inflexion in the graph of fig. 3. For velocities higher than this and below V_c, King's low-velocity formula would hold, as shown in fig. 4.

The weakness in the above argument is that it differentiates so clearly between free and forced convection at these very low velocities. It is probably impossible to separate these two phenomena in practice, because they are both so intimately connected with the loss of heat from the wire.

Very little seems to be known about this portion of the subject, which appears to offer a field for further research.

6. Summary.

An electrically-heated platinum wire was mounted upon the prong of an electrically-maintained tuning-fork of frequency n. The hot wire was cooled, owing to the periodic motion through the air, and superimposed upon the steady fall in resistance ; there was also a periodic change, with a corresponding periodic change in current. This current was analysed by means of a vibration galvanometer, and was found to contain harmonics of frequency $2n$, $3n$, and $4n$ in addition to the fundamental.

The escape of heat from the wire is due to the following factors :—

(1) The Free Convection effect, which is the same whether the wire is at rest or in motion, except in so far as it depends

on the temperature of the wire, which is, of course, lowered when the wire is vibrating.

(2) The Forced Convection effect which depends upon the velocity of the wire through the air, and which gives rise to

(*a*) The steady drop in resistance.

(*b*) Periodic changes of resistance of frequencies $2n$, $4n$, $6n$.

The magnitudes of (*a*) and (*b*) depend upon the temperature and diameter of the wire and the velocity of the cooling draught.

(3) The effect due to the heating-up of the surrounding air, which causes the fundamental and probably all the rest of the harmonics to be present.

A mathematical theory is developed which is found to account qualitatively for the observed results.

The writer's thanks are due to Mr. R. C. Richards for some very helpful criticism, and to Prof. A. W. Porter, F.R.S., for his assistance and general direction throughout this research.

Carey Foster Laboratory,
University College, London.
July 1927.

XCV. *The Electrical Conductivity of Metals as a Function of Pressure according to the Sommerfeld Electron Theory.* *By* A. T. Waterman, *Ph.D., Assistant Professor of Physics, Yale University, U.S. National Research Fellow at King's College, London* *.

In a recent paper Houston † has made a noteworthy contribution to Sommerfeld's ‡ theory of electrical conductivity in metals by working out the dependence of the mean free path upon temperature, pressure, and other variables. This is done by recognizing the wave nature of the electron, and thus treating the problem after the method used by Debye § for the interference of X-rays.

* Communicated by O. W. Richardson, F.R.S.
† *Zeits. f. Phys.* xlviii. p. 449 (1928).
‡ *Zeits. f. Phys.* xlvii. p. 1 (1928).
§ *Ann. d. Phys.* xliii. p. 19 (1914).

The result shows very fair agreement with observation for the temperature gradient of the conductivity, qualitative agreement for the pressure gradient, and the correct order of magnitude for the conductivity itself, as well as several other interesting applications.

In the case of the effect of hydrostatic pressure upon the electrical conductivity of metals, Houston has merely given an approximate formula, and has briefly pointed out that its application is qualitatively correct. When subjected to quantitative calculation, this formula is found only to give the right order of magnitude for the pressure coefficient of resistance, as seen in Table I. (p. 969.). The accuracy of Bridgman's data * for the pressure coefficients of metals, however, warrants a more exact formula, which may be deduced as shown below.

The formula given by Houston † for the specific resistance of a metal is

$$\rho = 9\left(\frac{8\pi}{3}\right)^{4/3} \frac{e^2 m^2 \mathrm{L}^{2/3} \mathrm{Z}^{2/3} \phi(x) \mathrm{H}(c)}{hk\theta d^{1/3} \mathrm{A}^{2/3}}, \quad . \quad . \quad . \quad (1)$$

where L = Loschmidt number,

Z = number of free electrons per atom,

θ = characteristic temperature,

d = density,

$$\phi(x) = \text{Debye function } 1/x \int_0^x \xi d\xi/(e^\xi - 1),$$

$$\mathrm{H}(c) = (1+2c)/(1+c) - 2c \log (1+c)/c, \quad c = \lambda^2/(4\pi b)^2$$

(λ = electronic wave-length, b = constant determining the range of the ionic field).

Houston's approximation for the pressure effect lies in the assumptions: first, that the Poisson ratio is independent of pressure, so that $\theta = \text{const.}\ d^{-1.6}\kappa^{-1/2}$, where κ = compressibility; and secondly, that the temperature is high enough, so that $\phi(x)$ may be replaced by T/θ. Then $\rho = \text{const.}\ \mathrm{H}\kappa$, writing H for H($c$), and for the pressure coefficient

$$1/\rho\ d\rho/dp = \partial \log \kappa/\partial p - \partial \log \mathrm{H}/\partial p. \quad . \quad . \quad . \quad (2)$$

The first term on the right may be evaluated from the experimental data for the fractional change in volume

* Proc. Amer. Acad. lii. p. 571 (1917).

† *Loc. cit.* eq. (29).

$\Delta V/V_0$ under pressure, given in the form $\Delta V/V_0 = Ap + Bp^2$. From this we readily derive

$$\frac{\partial \log \kappa}{\partial p} = \frac{2B}{A+2Bp} - \frac{A+2Bp}{1+Ap+Bp^2},$$

or, at zero pressure,

$$(\partial \log \kappa/\partial p)_0 = 2B/A - A.$$

The remaining term, $\partial \log H/\partial p$, is evaluated in the derivation given below.

The approximations underlying eq. (2) may be avoided by adopting Gruneisen's * method, as applied by him to Wien's conductivity theory †, for the derivation of the pressure coefficient of resistance. The feature of this method consists in distinguishing between the adiabatic and the isothermal pressure variation. Since the derivative at constant entropy of any function of θ/T vanishes,

$$(\partial \phi(x)/\partial p)_s = 0,$$

so that, taking the logarithmic derivative of eq. (1) at constant entropy, we have

$$(\partial \log \rho/\partial p)_s = (\partial \log H/\partial p)_s - (\partial \log \theta/\partial p)_s - \tfrac{1}{3}(\partial \log d/\partial p)_s, \quad . \quad (3)$$

assuming $\partial Z/\partial p = 0$.

In order to transform from adiabatic to isothermal conditions, we use the relation

$$\left(\frac{\partial}{\partial p}\right)_s = \left(\frac{\partial}{\partial p}\right)_T + \left(\frac{\partial}{\partial T}\right)_p \left(\frac{\partial T}{\partial p}\right)_s.$$

Also $(\partial \log \theta/\partial p)_s = 1/T(\partial T/\partial p)_s$, $d(\log d) = -d(\log V)$;

and, since measurements involve the actual resistance R instead of the specific resistance,

$$(\partial \log R/\partial p)_T = (\partial \log \rho/\partial p)_T - \tfrac{1}{3}(\partial \log V/\partial p)_T.$$

Hence

$$\left(\frac{\partial \log R}{\partial p}\right)_T = \left(\frac{\partial \log H}{\partial p}\right)_T + \left(\frac{\partial T}{\partial p}\right)_s \left[\left(\frac{\partial \log H}{\partial T}\right)_p - \frac{1}{T} - \left(\frac{\partial \log R}{\partial T}\right)\right].$$

But

$$(\partial T/\partial p)_s = T/C_p(\partial V/\partial T)_p.$$

* *Verh. d. deutsche Phys. ges.* xv. p. 186 (1913).
† Columbia Univ. Lectures, 1913.

Hence, finally :

$$\left(\frac{\partial \log R}{\partial p}\right)_T = \left(\frac{\partial \log H}{\partial p}\right)_T + \frac{1}{C_p}\left(\frac{\partial V}{\partial T}\right)_p\left[T\left(\frac{\partial \log H}{\partial T}\right)_p - 1 - T\left(\frac{\partial \log R}{\partial T}\right)_p\right].$$

Writing $\alpha = (\partial \log R/\partial T)_p$, $\beta = (\partial \log V/\partial T)_p$, $c' =$ specific heat per gram, the pressure coefficient of resistance becomes

$$\frac{1}{R}\left(\frac{\partial R}{\partial p}\right)_T = \left(\frac{\partial \log H}{\partial p}\right)_T - \frac{\beta}{c'd}\left[1 + T\left(\alpha - \frac{\partial \log H}{\partial T}\right)\right]. \quad (4)$$

For the two derivatives of $\log H$:

$$(\partial \log H/\partial p)_T = B/H(\partial c/\partial p)_T,$$

where

$$B = 1 + 2/(1+c) - 2\log(1+c)/c,$$

$$c = 1/(4\pi b)^2(8\pi/3m)^{\frac{1}{3}},$$

where $n =$ number of free electrons per cubic centimetre.

Then

$$\left(\frac{\partial c}{\partial p}\right)_T = -\left(\frac{8\pi}{3}\right)^{\frac{1}{3}}\frac{1}{8\pi^2 b^2 n^{\frac{2}{3}}}\left[\frac{1}{3}\left(\frac{\partial \log n}{\partial p}\right)_T + \left(\frac{\partial \log b}{\partial p}\right)_T\right].$$

Taking n equal to the number of atoms per c.c., as done by Sommerfeld, if b varies under pressure directly as the mean atomic separation, or $b \propto n^{-\frac{1}{3}}$, then

$$(\partial \log b/\partial p)_T = -\tfrac{1}{3}(\partial \log n/\partial p)_T \quad \text{and} \quad (\partial c/\partial p)_T = 0,$$

so that

$$(\partial \log H/\partial p)_T = 0.$$

If b remains constant under pressure, say $b = a\delta_0$, where $\delta_0 =$ mean atomic separation at zero pressure, then

$$\left(\frac{\partial \log H}{\partial p}\right)_T = -\left(\frac{8\pi}{3}\right)^{\frac{1}{3}}\frac{B}{H}\frac{K}{24\pi^2 a^2 \delta_0^2 n^{\frac{2}{3}}}, \quad . \quad . \quad (5)$$

where $K = -1/V(\partial V/\partial p)_T =$ compressibility.

Similarly for $(\partial \log H/\partial T)_p$; if $b \propto n^{-\frac{1}{3}}$, $(\partial \log H/\partial T_p = 0$; if $a = a\delta_0 =$ constant, then

$$\left(\frac{\partial \log H}{\partial T}\right)_p = \left(\frac{8\pi}{3}\right)^{\frac{2}{3}}\frac{B}{H}\frac{\beta}{24\pi^2 a^2 \delta_0^2 n^{\frac{2}{3}}}, \quad . \quad . \quad (6)$$

where $\beta = 1/V(\partial V/\partial T)_p =$ thermal expansion coefficient.

Taking $a = \frac{1}{6}$, i. e. $b = \frac{1}{6}\delta$, with Houston, Table I. gives the observed pressure coefficients, $1/R(\partial R/\partial p)_T$, and the

values computed by eq. (4), both for b=constant and for $b \propto n^{-\frac{1}{3}}$. The last column shows the values of the pressure coefficient as computed from Houston's formula, eq. (2), which uses $b = \frac{1}{6}\delta_0$ = constant.

TABLE I.

$$\frac{1}{R}\left(\frac{\partial R}{\partial p}\right)_T \times 10^{-12} \text{ (C.G.S.)}.$$

(All values negative unless otherwise indicated.)

Element.	Calc. ($b \propto n^{-1/3}$).	Calc. (b=const.).	Obs.	Calc. (Houston).
Li	−23	− 38	+ 6·9	+12
Na	43	68·0	− 68	+ 7·0
K	72·5	128	200	+10
Cu	3·2	4·2	2·05	− 5·6
Ag.....	4·8	6·2	3·7	6·7
Au.....	3·5	4·4	3·2	9·5
Mo	0·88	1·52	1·36	4·5
W	0·76	1·32	1·31	9·5
Ni	2·40	3·0	1·61	7·0
Pd	2·32	3·0	2·02	6·9
Pt	1·92	2·40	2·02	9·4
Al	6·0	7·9	4·25	2·1
Cd	7·5	11·6	10·8	5·3
Fe	2·30	3·4	2·5	—
Pb	12·2	15·7	14·7	5·1

The general agreement is best for the values calculated by the formula here developed, eq. (4), for the case b=constant, *i. e.* the range of the ionic field practically unaffected by pressure. The agreement may be considered fairly satisfactory, considering the necessarily approximate treatment of the field of an ion involved in Houston's theory. The present method apparently does not account for the positive pressure coefficient of Li, unless the value of b as a fraction of δ_0 differs markedly from that of other substances. If $b \propto n^{-\frac{1}{3}}$, there is on this theory (and also in Houston's formula) no possibility of a positive pressure coefficient. Houston's formula gives positive pressure coefficient for Li, Na, and K ; for the other elements the pressure coefficient

is negative and in most cases considerably higher than the observed values.

I wish to express my indebtedness to the United States National Research Council and to the International Education Board for the opportunity of study at King's College, London, and my sincere thanks to Prof. O. W. Richardson for his continued interest and encouragement.

King's College, London.
August 24th, 1928.

XCVI. *The Variation of Velocity Amplitude close to the Surface of a Cylinder moving through a Viscous Fluid.* *By* N. A. V. Piercy, *D.Sc., and* E. G. Richardson, *B.A., D.Sc., Ph.D.**

1. *Introductory.*

IT has been tentatively suggested † that the discrete eddies appearing in the wake of a body moving through a viscous fluid beyond the range for streamline flow, may grow into being from the coalescence of neighbouring vortices during their passage over the surface of the body. Experiments directed towards investigating the matter in the case of an ogival wedge ‡ in a stream, showed comparatively steady motion near to the surface through the vortex sheet cast off from it. The counter suggestion was therefore made that the periodic motion in the wake was due to the rolling up of the vortex sheets some distance behind the body.

An exploration of the fluctuation of velocity adjacent to the surface of a circular cylinder, placed with its axis across the stream, has recently been carried out in the aerodynamics laboratory at East London College. The results differ from Messrs. Fage and Johansen's experiments at the back of a wedge and tend rather in support of Prof. Levy's view, with the proviso that the cumulative process is limited to a small area of the surface.

2. *Nature of Investigation.*

A quantity that is roughly proportional to the amplitude of the velocity fluctuation was observed at short intervals round twelve circles, concentric with the cylinder and

* Communicated by the Authors.
† Levy, Phil. Mag. ii. p. 844 (1926).
‡ Fage and Johansen, Phil. Mag. v. p. 417 (1928).

separated from its surface by distances ranging from 0·0025 cylinder diameters to one hundred times that amount. The readings were found to be sufficiently consistent to permit of the construction of contours, and the results to which these pointed were in part checked by an alternative method. The second method, in which the periodicity was made audible, it is thought may prove of general use in experiments of this nature.

3. *Apparatus and Methods.*

The smooth aluminium cylinder, turned to 4 inches diameter, reached from wall to wall of a 4-foot wind-channel. It was supported in bearings at the walls so as to permit of orientation about its long axis without interrupting the air-stream. The hot wire was of platinum, 0·001 inch diameter and 1·0 inch long, and was fastened between the ends of two thin brass rods, which were threaded through insulating bushes fitted along parallel diameters of the cylinder and projected an adjustable distance from its surface. These rods served as leads for a current of about 0·5 amp.

The quasi-periodic variation in resistance of the hot wire due to its heating and cooling in the fluctuating stream, induced oscillatory e.m.f.'s in the secondary coil of a step-up transformer connected with a vibration galvanometer of unifilar type. The instrument was set considerably out of tune with the frequency of the motion and thus acted as a string galvanometer which was not critically damped. Various tests, reported elsewhere *, confirmed that in this use of the instrument the amplitude of the oscillation of the string could be regarded as roughly proportional to the amplitude of the velocity fluctuation, assuming nearly constant frequency and speed. The refinement of allowing for the variation of mean velocity was not attempted.

In the alternative method, the oscillatory e.m.f.'s induced in the secondary of the transformer were amplified until they were capable of producing an audible note of corrresponding frequency in a telephone receiver. We used a three-valve resistance-capacity coupled amplifier in which the secondary of the transformer with its oscillating e.m.f. formed the "grid-bias" of the first valve (fig. 1).

To illustrate the use of this method, some estimates were

* In a paper submitted by us to the Aero. Res. Comm. See also Relf and Simmons, Phil. Mag. xlix. p. 509 (1925); and Tyler, Phil. Mag. v. p. 449 (1928).

made of the frequency in the wakes of a few thin rods, as follows :—

Velocity, V.	Diameter, D.	Frequency, n.	$\frac{V}{nD}$.
400	0·12	600	5·55
562	0·51	215	5·10
400	0·24	315	5·83
562	0·24	413	5·68
400	0·40	186	5·40
562	0·40	265	5·20

The above values of n were determined by comparing the note heard with a note in the sonometer. The results are in agreement with those obtained by other means *. The path

Fig. 1.

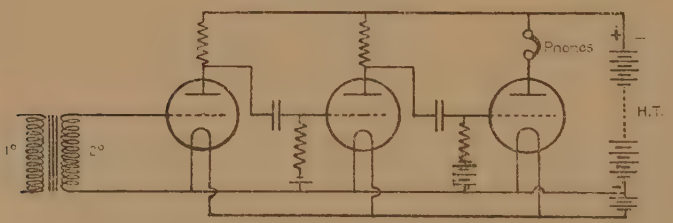

Arrangement of Audible Method.

of the vortices was traceable downstream by means of the 'phones, while a diminishing intensity of sound showed a damping out. By choosing suitable cylinders the critical value of Reynolds's number could be found, the channel speed being gradually increased until a note became audible.

4. *The Results.*

The readings obtained with the vibration galvanometer are given in fig. 2, plotted in cylindrical coordinates. The numbers attached to the curves give the distance of the wire from the boundary—constant for each curve—expressed in terms of the diameter of the cylinder. From these curves and those of fig. 3, contours of equal galvanometer amplitude have been prepared and are shown in fig. 4. The

* Richardson, Proc. Phys. Soc. xxxvii. p. 178 (1925).

numbers attached to the contours are proportional to the width of the band of light thrown upon the scale less its static width. The peculiar form of the contours near the front of the cylinder led to the more detailed exploration in this region recorded in fig. 3.

Fig. 2.

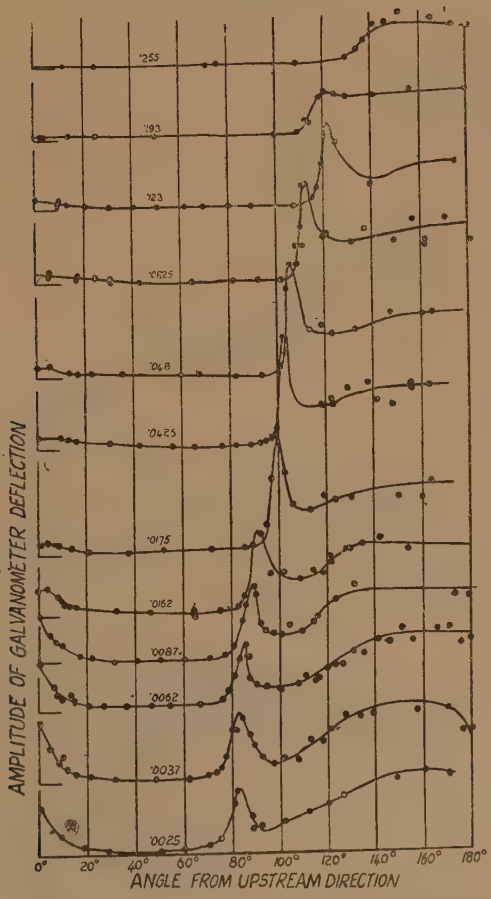

Amplitude of deflexion of vibration galvanometer with the hot wire at various constant distances from the surface, as marked on the curves in cylinder diameters.

It will be seen that the front stagnation point is a centre of disturbance, which, however, is damped out in the air as

Fig. 3.

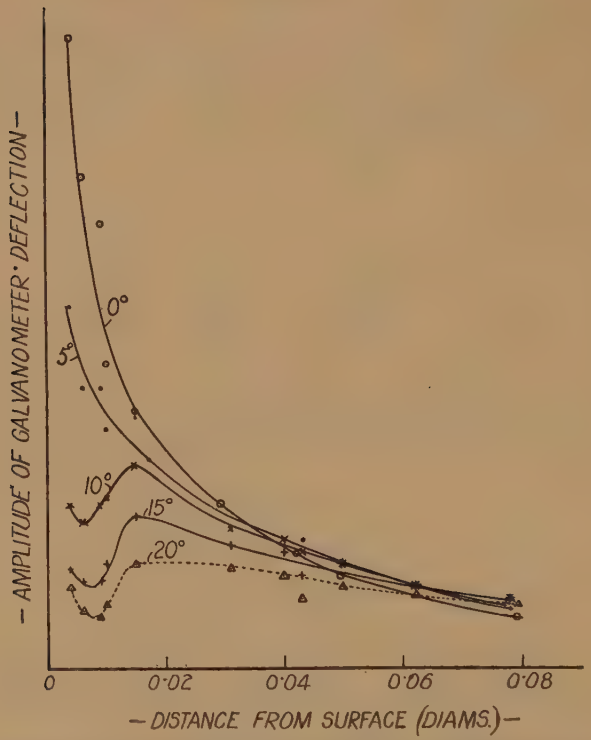

Exploration by vibration galvanometer near front stagnation point. The angles are measured from the upstream direction.

Fig. 4.

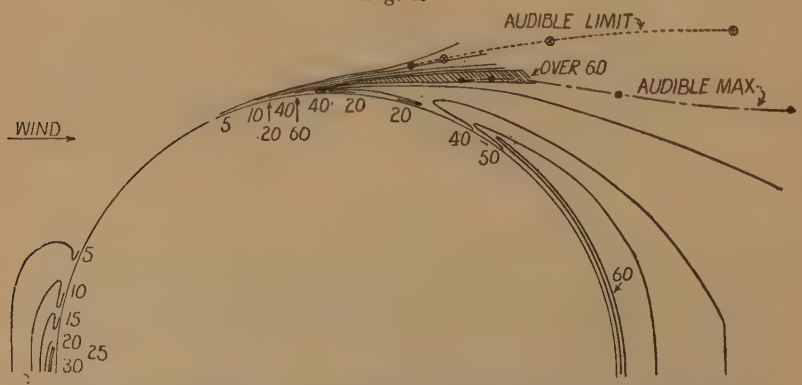

Contours of equal deflexion amplitude of vibration galvanometer. The numbers are proportional to the width of the band of light observed on the scale. Curves are added showing where the eddying produced an audible note and maximum intensity of sound.

it flows out of the region. The reading close to the surface again begins to have an appreciable amplitude at an angle of 60° with the upstream direction. From there, the amplitude rapidly increases, reaching a maximum at an angle of about 80°. After this sharp peak, it as rapidly decreases, and is then built up more gradually to a large value that extends round the back of the cylinder. These features are

Fig. 5.

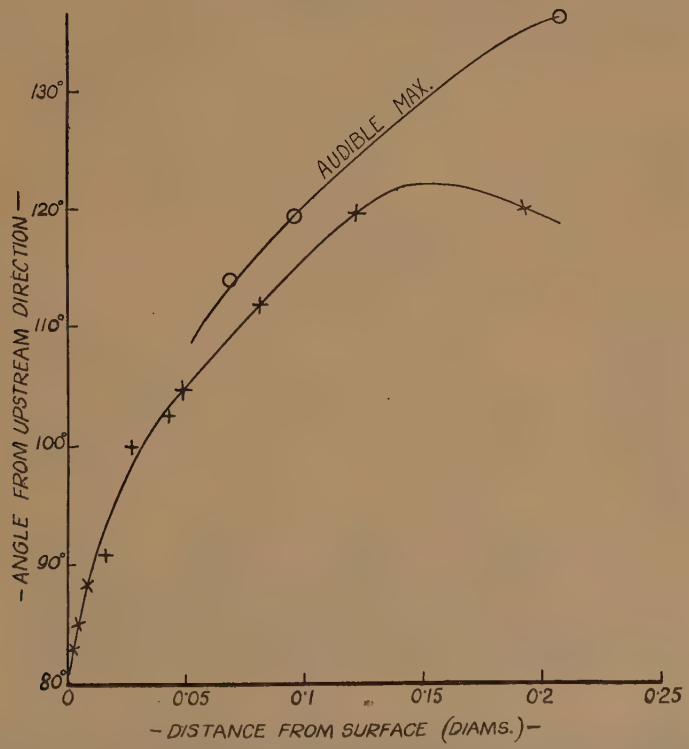

Locus of peak values of velocity amplitude, as determined by the vibration galvanometer method (crosses) and the audible method (circles).

similar in many ways to those that we have found close to the upper surface of an aerofoil *, so that it is likely that they apply to cylinders differing widely in section.

The peaks of fig. 2 mark the position of a wedge of large velocity amplitude, which is shaded in fig. 4. Within this

* *Loc. cit.* Aero. Res. Comm.

wedge the low frequency rumble discernible in the telephone receivers, using the second method of experiment, attained maximum intensity. In fig. 4 is also drawn a contour along which the periodic motion became audible.

Fig. 5 gives the position of maximum amplitude found by the vibration galvanometer and for comparison includes that indicated by the other, or telephone, method. Fig. 6 shows the variation of maximum amplitude with distance from the surface of the cylinder. From the latter figure it will be observed that at a very short distance from the surface the

Fig. 6.

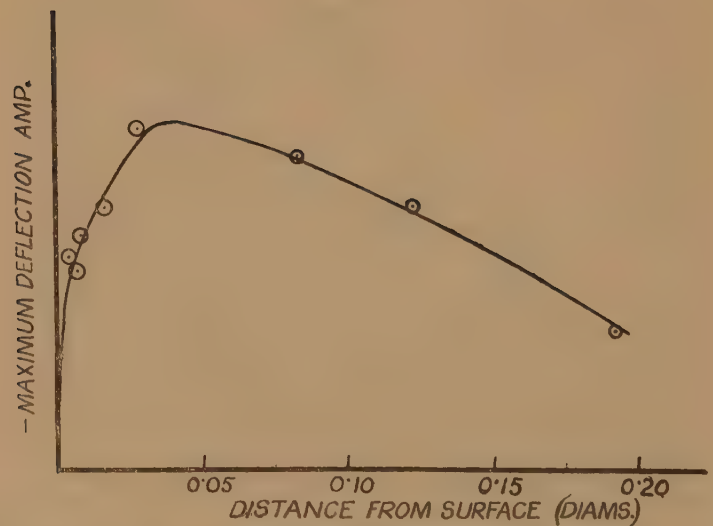

Variation of maximum velocity amplitude with distance from surface, as determined by the vibration galvanometer method.

amplitude reaches half-way towards a maximum, which itself occurs, according to this method, at no greater distance from the surface than 0·04 cylinder diameter.

5. *Conclusions.*

These experiments show that the turbulence in the region of the front stagnation point of a circular cylinder is not carried by the fluid round the surface. The velocity appears steady over about one-third of the surface facing the wind. Well before the shoulder of the section is reached, however, turbulence sets in anew, and rapidly increases to a maximum,

or peak, value. A wedge-shaped funnel of high velocity amplitude almost abuts on the surface here. This may possibly form a species of exhaust duct for coalesced vortices, such as Prof. Levy envisages, but in that case the vortices are collected from only a small area on the neighbouring surface. The experiments might well be developed at some time to take account of variation of mean velocity.

Dr. Piercy has pleasure in acknowledging assistance from the Keddey Fletcher-Warr Studentship Fund, and from the Dixon Fund, both of the University of London, which enabled this investigation to be carried out.

XCVII. *On the Dynamics of an Electron.* *By* D. Meksyn *.

I. Space and Time in Physics.

§ 1. *The General Principle of Relativity and Motion of Electrons.*

An attempt to apply the General Principle of Relativity to the motion of Electrons is met at the outset with insurmountable difficulties. It appears as if the problem is inherently self-contradictory. As a matter of fact, the track of an electron in an electromagnetic field is a curvilinear one ; on the other hand the space, as follows from the law of motion of an electron, is not curved (unless a gravitational field exists) ; hence the motion cannot be a free one, as it should be according to the General Principle of Relativity.

It seems that this contradiction is intimately connected with the conception of Space and Time in the Principle of Relativity.

§ 2. *Space and Time in Geometry and in the Special Theory of Relativity.*

Space and Time are considered in the Special Theory of Relativity and in Geometry to be a physical Entity *sui generis*, which imposes its metrical laws upon solid bodies located in it. So, for instance, we could conceive two spaces (and times) which are similar in every respect, except that the dimensions of the first are, say, only half of the second

* Communicated by H. T. Flint, D.Sc.]

one. If we transfer a solid body from the second space into the first one, the latter will cause the body to shrink and take only half the size that it had previously. Such a change in dimensions of Space can be brought about, according to the Special Theory of Relativity, if we set a body in motion.

Until the appearance of the Principle of Relativity it was usually held that space had three dimensions, and its metric was given by Laws of Geometry. The Special Principle of Relativity has discarded the conception of a three-dimensional space and one-dimensional time, but has accepted the idea of Geometry that space is a kind of objective physical Entity which imposes its metrical laws upon solid bodies ; therefore the Theory of Relativity has drawn the conclusion that, because it follows from Lorentz's transformations that the space dimensions of a fourfold system decrease if the latter is set in motion, a solid physical body which belongs to a moving system will shrink in its space dimensions.

§ 3. *Geometrical or Rigid Space.*

What, however, is meant by Space in Geometry is as follows :—There exist solid physical bodies which possess some metrical properties ; they have finite dimensions (length, surface, volume) ; they do not change their dimensions if transferred from one part of space into another.

Now, it appears that it is possible to account by deduction for all metrical properties of solid bodies, if we construct an appropriate system of reference, a "space," in such a way that all metrical properties of solid bodies (length, surface, volume) are properties of the space itself, and every element of length is expressed by some definite (quadratic) function of three appropriately chosen directions in space.

Hence, rigid bodies do not change their size if transferred from one part of Geometrical Space into another, not because the latter is homogeneous, but conversely the Geometrical Space is homogeneous for bodies which do not change their dimensions by such transfer.

It does, of course, not follow that there is no objective space, or that this space has no metrical properties of its own. (We do not touch upon this question here ; what it is necessary to notice is that the Geometrical Space, which gives us the metrical properties of solid bodies, is something quite different from the objective space (if we admit its existence).)

§ 4. *Four-dimensional or Kinematical Space.*

The idea of Space in Geometry will become clearer if we turn our attention to classical kinematics. It was built up upon different lines than Geometry.

In Geometry, as we have seen, all metrical properties of solid bodies are properties of the space itself.

In classical kinematics, side by side with metrical properties of Space, it was necessary to introduce some quantities which do not belong to the space (velocity and acceleration). The classical kinematics has lacked the unity of design which characterized Geometry.

The achievement of the Special Principle of Relativity was to restore this unity. The four-dimensional space is constructed in such a way that all kinematical elements of motion appear as metrical forms of the space itself; so velocity is the tangent of the angle between time axes, and acceleration is the radius of curvature of the four-track.

§ 5. *Dynamical Space.*

If we turn our attention to the dynamics of the Theory of Relativity we notice that here again the above-mentioned unity is not maintained; the fundamental quantities of dynamics, momentum, and Energy appear not as metrical properties of the Space itself, but, so to say, as properties brought into the space.

It is clear, therefore, that the natural generalization of the Special Theory of Relativity is to construct a dynamical space in which momentum and energy would be properties belonging to the Space itself.

§ 6. *Electricity and Gravitation.*

Before proceeding further we must bear in mind the divergence between an Electromagnetic field and a field of Gravitation. An isolated mass-point possesses a field of Gravitation, and it is usually held that an isolated charged mass-point has also an Electromagnetic field. We think, however, that the latter appears only if there are at least two electrons at a finite distance.

Hence, in the corresponding fundamental form this must be brought out by appearance of cross-terms of different spaces rather than by a change in the fundamental form of every space separately.

II. The Fundamental Form of Dynamical Space.

§ 7. *Lagrange's Equations in the Special Theory of Relativity.*

The idea of a dynamical space is not a new one. Such space is used in Lagrange's equations. Lagrange's space, however, is built up in conformity with the old kinematics, *i. e.* in it the time coordinate is separated from Space. This ought to be modified in such a way that time shall appear symmetrically with Space; this is necessary to bring it into agreement with the Special Theory of Relativity.

Lagrange's equations are:

$$\frac{d}{dt}\frac{\partial \mathrm{T}}{\partial \dot{x}_k} - \frac{\partial \mathrm{T}}{\partial x_k} = \mathrm{Q}_k. \quad . \quad . \quad . \quad . \quad . \quad (1)$$

In the classical Mechanics T is the kinetic Energy; but in the Theory of Relativity T is the so-called kinetic Potential, a quantity which has neither a dynamical nor a metrical meaning.

The first step to be made is to bring Lagrange's equations in the Special Theory of Relativity into such a form that it shall contain only metrical quantities.

For one material point this is easily done. If the fundamental form is

$$ds^2 = dt^2 - dx^2 - dy^2 - dz^2, \quad . \quad . \quad . \quad . \quad (2)$$

where t is chosen in light seconds. Lagrange's equations become in a variational form

$$\delta \int_{\tau_0}^{\tau_1} (m\,ds + \mathrm{V}\,d\tau) = 0, \quad . \quad . \quad . \quad . \quad . \quad (3)$$

where V is the potential Energy. The Geometrical interpretation of (3) is that the four-track is a geodesic line on some surface $\mathrm{V} = 0$. If V disappears the track is a geodesic line of a free space.

In the case of several material points we consider the fundamental form

$$ds^2 = \sum_{k=1}^{k=n} m_k (dt_k^2 - dx_k^2 - dy_k^2 - dz_k^2), \quad . \quad . \quad . \quad (4)$$

which has $4n$ dimensions. It is easily seen that Lagrange's equations become

$$\delta \int_{\tau_0}^{\tau_1} \left(ds + \frac{1}{\sqrt{\sum_k m_k}} \mathrm{V}\,d\tau \right) = 0; \quad . \quad . \quad . \quad (5)$$

as a matter of fact, from (5) we obtain

$$m_k \frac{d}{d\tau}\left(\frac{dx_k}{ds}\right) + \frac{1}{\sqrt{\sum_k m_k}} \frac{\partial V}{\partial x_k} = 0. \quad . \quad . \quad . \quad (6)$$

There are in all $4n-1$ independent equations and only $3n$ given space projections of force, so that we are left with $n-1$ time projections which we can dispose.

We define them from the following $n-1$ equations:

$$dt_k^2 - dx_k^2 - dy_k^2 - dz_k^2 = dt_l^2 - dx_l^2 - dy_l^2 - dz_l^2 \; ; \quad . \quad . \quad (7)$$

they are evidently equivalent to

$$X_k\, dx_k + Y_k\, dy_k + Z_k\, dz_k - T_k\, dt_k = 0, \quad . \quad . \quad (7\,a)$$

where $X_k\, Y_k\, Z_k\, T_k$ are the projections of the force.

From (7) the denominator in (6) becomes

$$ds = \sqrt{\sum_{l=1}^{l=n} m_l \,.\, (dt_k^2 - dx_k^2 - dy_k^2 - dz_k^2)},$$

or inserting (ds) in (6) we obtain

$$m_k \frac{d}{d\tau}\left(\frac{dx_k}{\sqrt{dt_k^2 - dx_k^2 - dy_k^2 - dz_k^2}}\right) + \frac{\partial V}{\partial x_k} = 0,$$

which is the law of motion.

The expression $\sqrt{\sum m_k}$ in (6) appears to be rather disappointing, as it has had hitherto no dynamical meaning; it need not, however, trouble us, because it will later disappear in the rigorous laws of motion.

What we have to notice is, that for several material points the law of motion is a geodesic line of a $4n$ dimensional space.

§ 8. *The Electromagnetic Field and the Form of Space.*

We turn our attention to the case of an Electromagnetic Force. Lagrange's equations for an electron are

$$\frac{d}{dt}\frac{\partial}{\partial \dot{x}_k}(T-M) - \frac{\partial}{\partial x_k}(T-M) = 0, \quad . \quad . \quad . \quad (8)$$

where T is the kinetic Energy,

$$M = e_1(\phi - u_1 F - v_1 G - w_1 H), \quad . \quad . \quad . \quad (9)$$

$-\phi$ is the scalar, F, G, H the vector potential of Force, e_1 the charge, and $u_1\, v_1\, w_1$ the velocity of the electron.

To find now the fundamental form of space, we must bear in mind two points:

(1) In (8) the kinetic and potential Energies appear perfectly symmetrically.

(2) Lagrange's expression (1) for the equations of Motion becomes a geodesic if T is a quadratic function of $\dot{x}_k$.

Hence our task will be achieved if we transform (9) into a quadratic expression.

Suppose that the external field is produced by one moving electron whose coordinates, charge, and velocity are

$$x_2\, y_2\, z_2\, t_2,\quad e_2,\quad u_2,\, v_2,\, w_2.$$

Then (9) becomes

$$\mathrm{M}=\frac{e_1 e_2}{r}(1-u_1u_2-v_1v_2-w_1w_2),\quad .\quad .\quad .\quad (10)$$

where

$$r=\sqrt{(x_1-x_2)^2+(y_1-y_2)^2+(z_1-z_2)^2}.$$

This expression for M suggests at once the expression for the fundamental form of space in this case. It is

$$\begin{aligned} ds^2 &= m(dx_4^2-dx_1^2-dx_2^2-dx_3^2) \\ &\quad +\frac{e_1 e_2}{r}(dx_4\,dx_8-dx_1\,dx_5-dx_2\,dx_6-dx_3\,dx_7) \\ &\quad +\mathrm{M}(dx_8^2-dx_5^2-dx_6^2-dx_7^2).\quad .\quad .\quad .\quad .\quad (11) \end{aligned}$$

In the general case where the external force is produced by $n-1$ electrons, *i. e.* in the case of the n electron problem, if we denote the mass, charge, and coordinates of the kth electron respectively by

$$m_k,\ e_k,\ x_{k+1}\, x_{k+2}\, x_{k+3}\, x_{k+4},\quad .\quad .\quad .\quad .\quad (12)$$

we obtain the following expression for the fundamental form

$$\begin{aligned} ds^2 &= g_{\mu\nu}\,dx_\mu\,dx_\nu \\ &= \sum_{k=1}^{k=n} m_k(dx^2{}_{k+4}-dx^2{}_{k+1}-dx^2{}_{k+2}-dx^2{}_{k+3}) \\ &\quad +\sum_{k,\,l=1}^{k,\,l=n}\phi_{kl}(dx_{k+4}\,dx_{l+4} \\ &\quad -dx_{k+1}\,dx_{l+1}-dx_{k+2}\,dx_{l+2}-dx_{k+3}\,dx_{l+3}),\quad .\quad (13) \end{aligned}$$

where

$$\left.\begin{aligned} k \neq l \text{ and } \phi_{kl} &= \frac{e_k e_l}{r_{kl}} \\ r_{kl} &= \sqrt{(x_{k+1}-x_{l+1})^2+(x_{k+2}-x_{l+2})^2+(x_{k+3}-x_{l+3})^2} \end{aligned}\right\}, \quad (14)$$

or

$$\phi_{kl} = \frac{e_k e_l}{c^2 r_{kl}}$$

if c is the velocity of light.

The Equation of Motion will be

$$\delta \int ds = 0, \quad \ldots\ldots \quad (15)$$

or a geodesic line in $4n$ dimensional space, which we proceed to discuss.

III. The Two-Electron Problem.

§ 9. *The Form of Space.*

We consider the problem of 2 electrons. The fundamental form for this particular case is

$$\begin{aligned} ds^2 = m(dx_4^2 - dx_1^2 - dx_2^2 - dx_3^2) \\ + \frac{e\mathrm{E}}{r}(dx_4\,dx_8 - dx_1\,dx_5 - dx_2\,dx_6 - dx_3\,dx_7) \\ + \mathrm{M}(dx_8^2 - dx_5^2 - dx_6^2 - dx_7^2) \ldots\ldots \quad (16) \end{aligned}$$

A glance at this expression shows us that it satisfies the physical conditions of an electromagnetic Field. The eight-dimensional space is split up into two four-dimensional spaces which are Euclidean, but taken as a whole this space is not Euclidean because of the cross terms. Hence an electron will not move in a straight line.

§ 10. *The Fundamental Tensor.*

The discriminant g is equal to

$$g = \begin{vmatrix} g_{11} & \cdot & \cdot & \cdot & g_{15} & \cdot & \cdot & \cdot \\ \cdot & g_{22} & \cdot & \cdot & \cdot & g_{26} & \cdot & \cdot \\ \cdot & \cdot & g_{33} & \cdot & \cdot & \cdot & g_{37} & \cdot \\ \cdot & \cdot & \cdot & g_{44} & \cdot & \cdot & \cdot & g_{48} \\ g_{51} & \cdot & \cdot & \cdot & g_{55} & \cdot & \cdot & \cdot \\ \cdot & g_{62} & \cdot & \cdot & \cdot & g_{66} & \cdot & \cdot \\ \cdot & \cdot & g_{73} & \cdot & \cdot & \cdot & g_{77} & \cdot \\ \cdot & \cdot & \cdot & g_{84} & \cdot & \cdot & \cdot & g_{88} \end{vmatrix} \quad (17)$$

and is split up into four separate determinants.

Or

$$g=(g_{11}g_{55}-g_{15}^2)(g_{22}g_{66}-g_{26}^2)(g_{33}g_{77}-g_{37}^2)(g_{44}g_{88}-g_{48}^2), \quad (18)$$

and the contravariant tensor $g^{\mu\nu}$ is equal to

$$\left.\begin{aligned} g^{11}&=\frac{g_{55}}{g_{11}g_{55}-g_{15}^2}\ldots, \quad g^{55}=\frac{g_{11}}{g_{11}g_{55}-g_{15}^2},\\ g^{15}&=\frac{-g_{15}}{g_{11}g_{55}-g_{15}^2}\ldots, \quad g^{48}=\frac{-g_{48}}{g_{44}g_{88}-g_{48}^2}, \end{aligned}\right\} \quad (19)$$

in our particular case

$$\left.\begin{aligned} g_{11}&=g_{22}=g_{33}=-g_{44}=-m,\\ g_{55}&=g_{66}=g_{77}=-g_{88}=-\mathrm{M},\\ g_{15}&=g_{26}=g_{37}=-g_{48}=-\frac{e\mathrm{E}}{r}, \end{aligned}\right\} \quad (20)$$

where

$$m,\ e,\ x_1\,x_2\,x_3\,x_4, \quad \text{and} \quad \mathrm{M},\ \mathrm{E},\ x_5\,x_6\,x_7\,x_8$$

relate respectively to the Electron and Proton.

§ 11. *The Equation of Motion* is, as we have seen, a geodesic line of this space, or

$$\frac{d^2x_\alpha}{ds^2}+\{\mu\nu\alpha\}\frac{dx_\mu}{ds}\frac{dx_\nu}{ds}=0. \quad (21)$$

In the general case of an eight-dimensional space, there are 288 three-index symbols, but in our case the number reduces to 136, and, if $g_{\mu\nu}$ does not depend upon time, to 102.

The only symbols which do not vanish are

$$\left.\begin{aligned} \{\alpha\alpha,\alpha\} &= g^{\alpha\alpha'}\frac{\partial g_{\alpha\alpha'}}{\partial x_\alpha},\\ \{\alpha\nu,\alpha\} &= \tfrac{1}{2}g^{\alpha\alpha'}\frac{\partial g_{\alpha\alpha'}}{\partial x_\nu} \quad (\text{but } \{\alpha\alpha',\alpha\}=0),\\ \{\mu\mu',\alpha\} &= -\tfrac{1}{2}g^{\alpha\alpha}\frac{\partial g_{\mu\mu'}}{\partial x_\alpha}-\tfrac{1}{2}g^{\alpha'\alpha'}\frac{\partial g_{\mu\mu'}}{\partial x_{\alpha'}},\\ \{\mu\alpha',\alpha\} &= \tfrac{1}{2}g^{\alpha\alpha}\frac{\partial g_{\alpha'\alpha}}{\partial x_\mu}, \end{aligned}\right\} \quad (22)$$

where $(\alpha'-\alpha)=4$.

There are in all 8 equations; the first four give us the motion of the electron; the last four, of the proton.

If we write out the equations (21) and insert the values of the 3-index terms, we obtain the following expressions:—

$$\left.\begin{aligned}
&\frac{d^2x_1}{ds^2}+g^{11}\left(\frac{\partial g_{51}}{\partial x_2}V_5-\frac{\partial g_{26}}{\partial x_1}V_6\right)V_2+g^{11}\left(\frac{\partial g_{51}}{\partial x_3}V_5-\frac{\partial g_{37}}{\partial x_1}V_7\right)V_3\\
&\quad+g^{11}\left(\frac{\partial g_{51}}{\partial x_4}V_5-\frac{\partial g_{48}}{\partial x_1}V_8\right)V_4+g^{15}\left(\frac{\partial g_{51}}{\partial x_7}V_1-\frac{\partial g_{37}}{\partial x_5}V_3\right)V_7\\
&\quad+g^{15}\left(\frac{\partial g_{15}}{\partial x_6}V_1-\frac{\partial g_{26}}{\partial x_5}V_2\right)V_6+g^{15}\left(\frac{\partial g_{15}}{\partial x_8}V_1-\frac{\partial g_{48}}{\partial x_5}V_4\right)V_8\\
&\quad+g^{15}\left(\frac{\partial g_{15}}{\partial x_1}V_1+\frac{\partial g_{15}}{\partial x_2}V_2+\frac{\partial g_{15}}{\partial x_3}V_3+\frac{\partial g_{15}}{\partial x_4}V_4\right)V_1\\
&\quad+g^{11}\left(\frac{\partial g_{15}}{\partial x_5}V_5+\frac{\partial g_{15}}{\partial x_6}V_6+\frac{\partial g_{15}}{\partial x_7}V_7+\frac{\partial g_{15}}{\partial x_8}V_8\right)V_5=0,\\
&\qquad\qquad\qquad

From the values of g_{15}, g_{26}, we see that (except for a constant factor)

$$\left.\begin{aligned} g_{15}V_5 &= -eF_p, \quad g_{26}V_6 = -eG_p, \quad g_{37}V_7 = -eH_p, \\ & \qquad\qquad\qquad\qquad g_{48}V_7 = +e\phi_p, \\ g_{51}V_1 &= -EF_e, \quad g_{62}V_2 = -EG_e, \quad g_{73}V_3 = -EH_e, \\ & \qquad\qquad\qquad\qquad g_{84}V_4 = +E\phi_e, \end{aligned}\right\} \quad . \quad . \quad . \quad (25)$$

where the subscripts p and e denote that it is the vector-potential due to the proton (and, hence, acting on the electron) and the electron respectively.

We also denote the velocity of the electron and proton :

$$V_1V_2V_3V_4 = V_e, \quad V_5V_6V_7V_8 = V_p. \quad . \quad . \quad (26)$$

If we make use of (24) and (25), the equations (23) become

$$\left.\begin{aligned} \frac{d^2x_1}{ds^2} = & -g^{11}e\,[X_pV_4 + Y_pV_2 - \beta_pV_3] \\ & -g^{15}E\,[X_eV_8 + Y_eV_6 - \beta_eV_7] \\ & -g^{11}\left(\frac{\partial g_{15}}{\partial x_5}V_5 + \frac{\partial g_{15}}{\partial x_6}V_6 + \frac{\partial g_{15}}{\partial x_7}V_7 + \frac{\partial g_{15}}{\partial x_8}V_8\right)V_5 \\ & -g^{15}\left(\frac{\partial g_{15}}{\partial x_1}V_1 + \frac{\partial g_{15}}{\partial x_2}V_2 + \frac{\partial g_{15}}{\partial x_3}V_3 + \frac{\partial g_{15}}{\partial x_4}V_4\right)V_1, \\ \frac{d^2x_4}{ds^2} = & \; g^{44}e\,[X_pV_1 + Y_pV_2 + Z_pV_3] \\ & +g^{48}E\,[X_eV_5 + Y_eV_6 + Z_eV_7] \\ & -g^{44}\left(\frac{\partial g_{84}}{\partial x_5}V_5 + \frac{\partial g_{84}}{\partial x_6}V_6 + \frac{\partial g_{84}}{\partial x_7}V_7 + \frac{\partial g_{84}}{\partial x_8}V_8\right)V_8 \\ & -g^{48}\left(\frac{\partial g_{48}}{\partial x_1}V_1 + \frac{\partial g_{48}}{\partial x_2}V_2 + \frac{\partial g_{48}}{\partial x_3}V_3 + \frac{\partial g_{48}}{\partial x_4}V_4\right)V_4. \end{aligned}\right\} \quad (27)$$

1. Let us consider the case of a steady electromagnetic field. Or we assume that $M \to \infty$ and the velocity of the proton is

$$V_5, V_6, V_7 \to 0.$$

Then

$$g^{11} = -\frac{1}{m}, \quad g^{44} = +\frac{1}{m}, \quad g^{15} = g^{26} = g^{37} = g^{48} = 0,$$

and (27) becomes:

$$\left.\begin{aligned} m\frac{d^2x_1}{ds^2} &= e\,[X_pV_4+Y_pV_2-\beta_pV_3],\\ m\frac{d^2x_4}{ds^2} &= e\,[X_pV_1+Y_pV_2+Z_pV_3], \end{aligned}\right\} \quad . \quad . \quad (28)$$

Now the four-velocity can be transformed as follows:—

$$ds^2 = m(dx_4^2-dx_1^2-dx_2^2-dx_3^2)+M(dx_8^2-dx_5^2-dx_6^2-dx_7)^2 + \frac{eE}{r}(dx_4dx_8-dx_1dx_5-dx_2dx_6-dx_3dx_7)\ ;$$

to the first order of approximation the last term may be omitted because $\frac{eE}{r}$ $\left(\text{or } \frac{eE}{rc^2}, \text{ if } c \text{ is the velocity of light}\right)$ is small in comparison with the mass of an electron; also, the force acting on the electron satisfies to the first approximation the equation (7 *a*); hence we have

$$dx_4^2-dx_1^2-dx_2^2-dx_3^2 = dx_8^2-dx_5^2-dx_6^2-dx_7^2, \quad (29)$$

as this does not impose new conditions on the variables.

Whence

$$ds^2 = (m+M)(dx_4^2-dx_1^2-dx_2^2-dx_3^2) = (m+M)(dx_8^2-dx_5^2-dx_6^2-dx_7^2).$$

The factor $\sqrt{M+m}$ appears twice in the denominator of the left and the right side of (28) (in the electric force through the vector potential, and in the velocity); hence it drops out from the equation of Motion, and they become, if we divide both sides by V_4,

$$\left.\begin{aligned} m\frac{d}{dx_4}\frac{dx_1}{d\tau} &= e[X_p+(Y_pv-\beta_pw)],\\ &\cdots\cdots\cdots\\ m\frac{d}{dx_4}\frac{dx_4}{d\tau} &= e[X_pu+Y_pv+Z_pw], \end{aligned}\right\} \quad . \quad . \quad (30)$$

where u, v, w is the three-velocity, and

$$d\tau^2 = dx_4^2-dx_1^2-dx_2^2-dx_3^2.$$

These are the usual equations of motion for the electron.

2. In the general case, as is seen from (27), the force consists of four parts. Two of them are due to the direct action of the proton, and the other two forces to the reaction on the proton, due to the electromagnetic force of the electron.

The first one is the usual Lorentz's force, the second one is some new force ; it is equal to

$$-g^{11}(\underset{5-8}{\text{grad}}\, g_{15} \cdot V_p)V_5 - g^{15}(\underset{1-4}{\text{grad}}\, g_{15} \cdot Ve)V_1.$$

3. From the equations of motion (21) a remarkable consequence follows concerning the number of degrees of freedom of an electron.

As is known,

$$\frac{dx_\alpha}{ds}\left\{\frac{d^2x^\alpha}{ds} + \{\mu\nu\alpha\}\frac{dx^\mu}{ds}\frac{dx^\nu}{ds}\right\} = 0, \quad . \quad . \quad (31)$$

or there are only $4n-1$ independent equations for n electrons. If we assume that the proton has three degrees of freedom, then we are left with $4n-4$ equations for $n-1$ electrons; or an electron has four degrees of freedom.

The fourth degree of freedom is in the direction of time, or, better, it is the kinetic energy, which is not equal to $m\frac{dt}{d\tau}$, as the Special Theory of Relativity gives, but has to be found from the equations of Motion.

Our assumption (29) about the connexion between different times is only an approximate one. We must choose one time (of the proton) as an independent variable, and find all others from the equations of motion.

4. The so-called vector potential of Electrodynamics is the covariant velocity in the dynamical space.

For instance,

$$\frac{dx_5}{ds} = -m\frac{dx^5}{ds} - g_{15}\frac{dx'}{ds},$$

which, for the particular case where the proton is at rest, is proportional to the vector potential of the electron

$$\frac{dx_5}{ds} = \mathrm{E}F_e.$$

§ 13. *The Wave Equation*

$$g^{\mu\nu}\phi_{\mu\nu} = g^{\mu\nu}\left(\frac{\partial^2\phi}{\partial x_\mu \partial x_\nu} + \{\mu\nu, \alpha\}\frac{\partial\phi}{\partial x_\alpha}\right) = 0 \quad . \quad (32)$$

is rather complicated. We consider here the simple instance, when $g_{15} = g_{26} = g_{37} = 0$, or of a purely electric field. For this case $\phi_{\mu\nu} = \dfrac{\partial^2\phi}{\partial x_\mu \partial x_\nu}$, except for the expression

$$\phi_{48} = \frac{\partial^2\phi}{\partial x_4 \partial x_8} + \frac{1}{2}\Big[g^{11}\frac{\partial g_{48}}{\partial x_1}\frac{\partial\phi}{\partial x_1} + g^{22}\frac{\partial g_{48}}{\partial x_2}\frac{\partial\phi}{\partial x_2} + g^{33}\frac{\partial g_{48}}{\partial x_3}\frac{\partial\phi}{\partial x_3} + g^{55}\frac{\partial g_{48}}{\partial x_5}\frac{\partial\phi}{\partial x_5} + g^{66}\frac{\partial g_{48}}{\partial x_6}\frac{\partial\phi}{\partial x_6} + g^{77}\frac{\partial g_{48}}{\partial x_7}\frac{\partial\phi}{\partial x_7}\Big]. \quad (33)$$

We neglect, however, the cross terms in (33), because from the expression of ϕ, which we shall take, the second term for the Hydrogen Atom is only $\sim 10^{-10}$ of the first one.

So that the wave equation becomes

$$g^{11}\frac{\partial^2\phi}{\partial x_1^2} + \ldots + g^{44}\frac{\partial^2\phi}{\partial x_4^2} + g^{55}\frac{\partial^2\phi}{\partial x_5^2} + \ldots + g^{88}\frac{\partial^2\phi}{\partial x_8^2} + 2g^{84}\frac{\partial^2\phi}{\partial x_4 \partial x_8} = 0. \quad (34)$$

Inserting in (34) the values of the tensor $g^{\mu\nu}$, we obtain after easy transformations

$$\frac{1}{m}\Big(\frac{\partial^2\phi}{\partial x_1^2} + \frac{\partial^2\phi}{\partial x_2^2} + \frac{\partial^2\phi}{\partial x_3^2}\Big) + \frac{1}{\mathrm{M}}\Big(\frac{\partial^2\phi}{\partial x_5^2} + \frac{\partial^2\phi}{\partial x_6^2} + \frac{\partial^2\phi}{\partial x_7^2}\Big) + \Big\{-\frac{1}{m}\frac{\partial^2\phi}{\partial x_4^2} - \frac{1}{\mathrm{M}}\frac{\partial^2\phi}{\partial x_8^2} + \frac{2\mathrm{V}}{\mathrm{M}m}\frac{\partial^2\phi}{\partial x_4 \partial x_8}\Big\} = 0, \quad (35)$$

where $\mathrm{V} = -\dfrac{\mathrm{E}e}{r}$ is the electrostatic potential.

This can be brought (under special assumptions) to Schrödinger's wave equations. Let us take for ϕ the expression

$$\phi \eqsim \psi \cdot e^{\frac{2\pi}{h}\{(m+\mathrm{E}_1)x_4 + (\mathrm{M}+\mathrm{E}_2)x_8\}i}, \quad (36)$$

or we assume in conformity with de Broglie's ideas that *not only Energy due to motion of an electron passes a frequency* $\dfrac{\mathrm{E}}{h}$, *but also Energy due to the rest-mass has a frequency.*

For the Hydrogen Atom $\dfrac{\mathrm{E}_1}{m} = \mathrm{V}^2 \eqsim 10^{-5}$; hence E_1^2, E_2^2 could be neglected in comparison with $m\mathrm{E}_1$, ME_2, and E_1,

E_2 in comparison with m and M. Under such approximation we easily obtain from (35) (36) the equation for ψ:

$$\frac{1}{m}\left(\frac{\partial^2\psi}{\partial x_1^2}+\frac{\partial^2\psi}{\partial x_2^2}+\frac{\partial^2\psi}{\partial x_3^2}\right)+\frac{1}{M}\left(\frac{\partial^2\psi}{\partial x_5^2}+\frac{\partial^2\psi}{\partial x_6^2}+\frac{\partial^2\psi}{\partial x_7^2}\right)$$
$$+\frac{8\pi^2}{h^2}\left[\frac{M+m}{2}+(E_1+E_2)-V\right]\psi=0. \quad (37)$$

We can now transform (37) as follows :—Let us change the variables :

$$\left.\begin{aligned} x &= x_1-x_5 \quad (m+M)\xi = mx_1+Mx_5,\\ y &= x_2-x_6 \quad (m+M)\eta = mx_2+Mx_6,\\ z &= x_3-x_3 \quad (m+M)\zeta = mx_3+Mx_7. \end{aligned}\right\} \quad (38)$$

Using (38), we obtain from (37) :

$$\frac{1}{m}\left(\frac{\partial^2\psi}{\partial x^2}+\frac{\partial^2\psi}{\partial y^2}+\frac{\partial^2\psi}{\partial z^2}\right)+\frac{1}{m+M}\left(\frac{\partial^2\psi}{\partial\xi^2}+\frac{\partial^2\psi}{\partial\eta^2}+\frac{\partial^2\psi}{\partial S^2}\right)$$
$$+\frac{8\pi^2}{h^2}\left[\frac{M+m}{2}+(E_1+E_2)-V\right]\psi=0,$$

$$\mu=\frac{mM}{m+M}. \quad (39)$$

Let us assume for ψ :

$$\psi=f(x,y,z)\,g(\xi,\eta,\zeta); \quad (40)$$

hence

$$\frac{1}{\mu}g\nabla^2_{xyz}f+\frac{1}{M+m}f\nabla^2_{\xi,\eta,\zeta}g+\frac{8\pi^2}{h^2}$$
$$\times\left[\frac{M+m}{2}+(E_1+E_2)-V\right]g=0. \quad (41)$$

Let
$$\frac{1}{m+M}\nabla^2 g=-\frac{4\pi^2}{h^2}g. \quad (42)$$

From (41) and (42) we obtain

$$\frac{1}{\mu}\nabla^2 f+\frac{8\pi^2}{h^2}[(E_1+E_2)-V]f=0, \quad (43)$$

which is Schrödinger's equation.

The radiation function is

$$\psi=\psi e^{\frac{2\pi}{h}(M+m+E_1+E_2)it}, \quad (44)$$

because to the first order of approximation

$$x_4 = x_8 = t,$$

the rest time.

§ 14. *The Metric of Space.*

The bearing of the fundamental Form of Space to Einstein's gravitational tensor $G_{\mu\nu}$ and G is as follows :—

To the first order of approximation (or neglecting the squares of $g_{\alpha\alpha'}$ and $g^{\alpha\alpha'}$ in comparison with $g^{\alpha\alpha}$) we obtain

$$G_{\mu\nu} = \tfrac{1}{2} g^{\sigma\rho}\left(\frac{\partial^2 g_{\sigma\rho}}{\partial x_\mu \partial x_\nu} + \frac{\partial^2 g_{\mu\nu}}{\partial x_\rho \partial x_\sigma} - \frac{\partial^2 g_{\mu\sigma}}{\partial x_\rho \partial x_\nu} - \frac{\partial^2 g_{\rho\nu}}{\partial x_\mu \partial x_\sigma}\right). \quad (45)$$

We have to take for our approximation only $\sigma = \rho$; hence

$$G_{\mu\nu} = \tfrac{1}{2} g^{\sigma\sigma}\left(\frac{\partial^2 g_{\mu\nu}}{\partial x_\sigma^2} - \frac{\partial^2 g_{\mu\sigma}}{\partial x_\nu \partial x_\sigma} - \frac{\partial^2 g_{\nu\sigma}}{\partial x_\mu \partial x_\sigma}\right), \quad (46)$$

and we obtain

$$\left.\begin{aligned} G_{11} &= -g^{55}\frac{\partial^2 g_{15}}{\partial x_1 \partial x_5}, \\ G_{12} &= -\tfrac{1}{2} g^{55}\frac{\partial^2 g_{15}}{\partial x_1 \partial x_5} - \tfrac{1}{2} g^{66}\frac{\partial^2 g_{26}}{\partial x_2 \partial x_6}, \\ &\cdots\cdots\cdots\cdots\cdots\cdots \\ G_{15} &= \tfrac{1}{2}\left\{ g^{11}\frac{\partial^2 g_{15}}{\partial x_1^2} + g^{22}\frac{\partial^2 g_{15}}{\partial x_2^2} + \ldots + g^{88}\frac{\partial^2 g_{15}}{\partial x_8^2}\right\} \\ &\qquad - \tfrac{1}{2} g^{11}\frac{\partial^2 g_{15}}{\partial x_1^2} - \tfrac{1}{2} g^{55}\frac{\partial^2 g_{15}}{\partial x_5^2}. \end{aligned}\right\} \quad (47)$$

From (47) it is easily seen that $G_{\mu\nu} = 0$ only if $G_{\mu\nu} = \text{const.}$, or if there is no electromagnetic connexion between the electrons.

The gravitational invariant G is equal to

$$\begin{aligned} G &= g^{\mu\nu} G_{\mu\nu} \\ &= -2 g^{11} g^{55}\left(\frac{\partial^2 g_{16}}{\partial x_1 \partial x_5} + \frac{\partial^2 g_{25}}{\partial x_2 \partial x_6} + \frac{\partial^2 g_{35}}{\partial x_3 \partial x_7} - \frac{\partial^2 g_{45}}{\partial x_4 \partial x_8}\right). \end{aligned}$$

Hence $\zeta = 0$ for our fundamental Form.

My thanks are due to Dr. H. T. Flint, for his criticism and help in the writing of this paper.

Wheatstone Laboratory,
King's College, London.

XCVIII. *An Example of Operational Methods.*

To the Editors of the Philosophical Magazine.

GENTLEMEN,—

SINCE the publication of Dr. Jeffreys's Tract * on Heaviside's operational methods, several enquiries have reached me, from which it would seem that a few additional easy examples may be found of interest to students of these methods. One such has suggested itself from reading a leader in 'The Times' (of the 8th June) on the effect of the *deep-earth-temperature*: it seems that, roughly speaking, when this temperature is below 47° Fahr. pulmonary diseases are prevalent; and above 57° Fahr., infantile diarrhœa is to be feared. The mathematical problem suggested is the following:—*Suppose the air outside a conductor (having a plane face) to be kept at temperature v_0, and the deep-temperature in the conductor to be v_1. Find the temperature at the surface, allowing for radiation.*

Take the face of the conductor as $x=0$, and the positive direction of x to be inside the conductor: then, using the notation explained in my paper †, we have (inside the conductor)

$$v=v_1+(v_2-v_1)e^{-qx},$$

where v_2 is the temperature at $x=0$ and $q^2=p/k$, $p=\partial/\partial t$. The correct form of the surface-condition is uncertain, but we may use an equation similar to that which holds at a metal surface, namely

$$\frac{\partial v}{\partial x}=h(v_2-v_0).$$

Thus
$$q(v_1-v_2)=h(v_2-v_0),$$

or
$$v_2=\frac{hv_0+qv_1}{h+q}.$$

An exact calculation of v_2 can be made in terms of error-functions (by means of the formulæ on p. 96 of Dr. Jeffreys's Tract): but in problems of this kind, as remarked by

* 'Operational Methods in Mathematical Physics' (No. 23 of the Cambridge Tracts), 1927.

† Proc. Camb. Phil. Soc. vol. xx. p. 411 (1921).

Heaviside ('Electromagnetic Theory,' vol. ii. pp. 14–16), there are two easy series which may be found, the first being suitable when t/τ is small, the second when t/τ is large, where τ is the time-interval given by $1/\tau = h^2k$.

In the present problem exact values of the constants h, k are not available, but if we make estimates on the lines of Lord Kelvin's article * on "Conduction of Heat" (Encyclopædia Britannica, 9th ed., vol. xi. pp. 580, 586), it seems not unreasonable to take τ to be from 40 to 50 hours. Thus the solution to be aimed at corresponds to the hypothesis that t/τ is small; or, in the symbolic calculations, we may treat h/q as small. This gives the result

$$v_2 = v_1 + (v_0 - v_1)\left(\frac{h}{q} - \frac{h^2}{q^2} + \frac{h^2}{q^3} - \ldots\right)$$

$$= v_1 + (v_0 - v_1)\left\{\frac{2}{1}\sqrt{\frac{t}{\pi\tau}} - \frac{t}{\tau} + \frac{2.2}{1.3}\frac{1}{\sqrt{\pi}}\left(\frac{t}{\tau}\right)^{3/2} - \frac{1}{2!}\left(\frac{t}{\tau}\right)^2 + \frac{2.2.2}{1.3.5}\frac{1}{\sqrt{\pi}}\left(\frac{t}{\tau}\right)^{5/2} - \frac{1}{3!}\left(\frac{t}{\tau}\right)^3 + \ldots\right\}.$$

The series converges for all values of t, but is convenient for calculation only if $t/\tau \leqq \frac{1}{2}$ (as a rough guide).

However, in the application suggested, the interval t i not likely to exceed 7 hours, and t/τ may be taken as abou $\frac{1}{7}$; this gives roughly $\frac{1}{3}$ as the value of the series in the brackets. This shows, for instance, that if the maximum outside temperature is 90°, and the deep-temperature is 54°, the surface-temperature would not be likely to rise above 66°. These numbers make no pretensions to great accuracy; but they do seem to confirm the conclusions of the 'Times' that *the deep-earth-temperature is of more importance than the air-temperature in determining conditions of health at the surface of the earth.*

I am, Gentlemen,

Your obedient servant,

T. J. I'A. Bromwich.

Cambridge,
8th June, 1928.

* Reprinted in volume ii. of Kelvin's 'Mathematical and Physical Papers.'

XCIX. *The Potential Function due to certain Plane Boundary Distributions.* *By* C. Fox, *M.A.(Camb.), D.Sc.(Lond.)* *.

§ 1. *Introduction.*

THE object of this paper is to give the potential function throughout space when either the potential or (in an electrical problem) the charge is known over (i.) a plane and (ii.) two parallel planes. The method is illustrated by application to several problems : for example, the guard-ring, the freely-charged elliptic disk, and the problem of the potential field arising from an infinite conductor bounded by two parallel planes with two elliptical disk electrodes, applied so that the join of their centres is perpendicular to the bounding planes. When the two axes of the elliptical disks are equal, so that they become circular, the last problem becomes identical with that of Nobili's † rings, first solved by Riemann.

The method consists in applying a theorem, due to Neumann, as follows :

$$2\pi f(r, \phi) = \int_0^\infty u\,du \int_{-\pi}^{\pi} \int_0^\infty f(\mathrm{R}, \Phi) \times \mathrm{J}_0[u\sqrt{\{\mathrm{R}^2 + r^2 - 2\mathrm{R}r\cos(\Phi - \phi)\}}]\,\mathrm{R}d\mathrm{R}d\Phi, \quad (1.1)$$

provided that the following conditions ‡ are satisfied :—

(i.) $f(\mathrm{R}, \Phi)$ *is a bounded function of the real variables* R *and* Φ *whenever* $-\pi \leqq \Phi \leqq \pi$ *and* $0 \leqq \mathrm{R}$, *and is such that*

$$\int_{-\pi}^{\pi} \int_0^\infty f(\mathrm{R}, \Phi)\,\mathrm{R}^{\frac{1}{2}}d\mathrm{R}d\Phi$$

exists and is absolutely convergent.

(ii.) $f(\mathrm{R}, \Phi)$ *as a function of* R *is of bounded variation in the interval* $(0, \infty)$ *for every value of* Φ *lying between* $\pm\pi$, *this variation being an integrable function of* Φ.

(iii.) *If* $\Omega(\mathrm{R}, \Phi)$ *denote the total variation of* $\mathrm{F}(\mathrm{R}, \Phi)$ *in the interval* (r, R), let $\Omega(\mathrm{R}, \Phi)$ *tend uniformly to zero with*

* Communicated by the Author.

† The solution of this problem with references is given in Gray, Matthews, and MacRobert's 'Bessel Functions,' p. 144, § 3, 1922 ed.

‡ Since writing this paper I have discovered that condition (ii.) is superfluous, whilst condition (i.) can be replaced by another which is satisfied by all the functions that occur here. The proofs have not yet been published.

respect to Φ *as* $R \to r$ *throughout the whole interval* $(-\pi, \pi)$, *with the exception of values of* Φ *in a number of sectors the sum of whose angles may be assumed arbitrarily small.*

(iv.) *If* (r, ϕ) *is a point of discontinuity of* $f(R, \Phi)$, *then* $f(r, \phi)$ *on the left-hand side of* (1.1) *must be replaced by the mean value of* $f(R, \Phi)$ *taken round a small circle with the point* (r, ϕ) *as centre. We assume that this mean value is finite.*

This theorem is proved in Watson's 'Bessel Functions' *, where it is also shown that the order of the integrations on the right-hand side of (1.1) with respect to R and Φ may be interchanged.

Thus (1.1) can be written

$$2\pi f(r, \phi) = \int_0^\infty u\,du \int_0^\infty \int_{-\pi}^{\pi} f(R, \Phi) \times J_0[u\sqrt{\{R^2+r^2-2Rr\cos(\Phi-\phi)\}}]R\,d\Phi\,dR. \quad (1.2)$$

The conditions above are too narrow †, as we shall show by an example later on. We shall also make use of the fact that in cylindrical coordinates

$$e^{\pm uz}J_0(ur) \quad . \quad . \quad . \quad . \quad . \quad . \quad (1.3)$$

is a solution of Laplace's equation. On changing the origin in the plane $z=0$ to the point (R, Φ), it follows from (1.3) that

$$e^{\pm uz}J_0[u\sqrt{\{R^2+r^2-2Rr\cos(\Phi-\phi)\}}]. \quad . \quad (1.4)$$

is also a solution of Laplace's equation.

§ 2. *The Potential Field arising from a Known Plane Distribution.*

2.1. If the value of the potential ‡ over the plane $z=0$ is given by $f(r, \phi)$, which satisfies the conditions of § 1, then the potential function V throughout space is given by

$$2\pi V = \int_0^\infty e^{\mp uz}u\,du \int_{-\pi}^{\pi} \int_0^\infty f(R, \Phi) \times J_0[u\sqrt{\{R^2+r^2-2Rr\cos(\Phi-\phi)\}}]R\,dR\,d\Phi, \quad (2.11)$$

* P. 470.

† See footnote ‡, p. 994.

‡ Cylindrical coordinates are used throughout the paper.

or by

$$2\pi V = \int_0^\infty e^{\mp uz} u\, du \int_0^\infty \int_{-\pi}^{\pi} f(R, \Phi) \times J_0[u\sqrt{\{R^2 + r^2 - 2Rr\cos(\Phi - \phi)\}}]\, R\, d\Phi\, dR, \quad (2.12)$$

whichever is more convenient, the upper or lower sign being taken according as z is positive or negative. These formulæ follow immediately from (1.1) and (1.2) on putting $z=0$.

As an illustration, consider the case of a unit point charge at the origin for which

$$f(r, \phi) = r^{-1}.$$

Conditions (i.) and (ii.) of § 1 are both violated ; nevertheless, on substituting in (2.12) we get the correct result, showing, I think, that the conditions of § 1 are too narrow. The calculations are as follows :—

We have

$$2\pi V = \int_0^\infty e_{\mp u z} u\, du \int_0^\infty \int_{-\pi}^{\pi} \times J_0[u\sqrt{\{R^2 + r^2 - 2Rr\cos(\Phi - \phi)\}}]\, d\Phi\, dR. \quad . \quad (2.13)$$

Also it is known that *

$$J_0[u\sqrt{\{R^2 + r^2 - 2Rr\cos(\Phi - \phi)\}}] = J_0(uR)J_0(ur) + 2\sum_{m=1}^{\infty} J_m(uR)J_m(ur)\cos m(\Phi - \phi), \quad (2.14)$$

and that we may integrate term by term with respect to Φ. Hence (2.13) becomes

$$V = \int_0^\infty e^{\mp uz} u\, du \int_0^\infty J_0(uR)J_0(ur)\, dR. \quad . \quad (2.15)$$

Now †

$$\int_0^\infty J_0(uR)\, dR = u^{-1}$$

and ‡

$$\int_0^\infty e^{-uz} J_0(ur)\, du = (r^2 + z^2)^{-\frac{1}{2}} \quad . \quad . \quad . \quad (2.16)$$

if $z \geq 0$. Hence (2·15) reduces to

$$V = (r^2 + z^2)^{-\frac{1}{2}}$$

* Watson, 'Bessel Functions,' pp. 127–128.
† Watson, *loc. cit.* p. 391 (1).
‡ Watson, *loc. cit.* p. 384 (1). For the case $z=0$ we use (1), p. 391.

for all values of r and z. This, it is well known, is the potential due to a unit charge at the origin.

2.2. If the charge at the point (r, ϕ) in the plane $z=0$ is given by $f(r, \phi)$, which satisfies the conditions of § 1, then the potential at the point (r, ϕ, z) is given by

$$V = \int_0^\infty e^{\mp uz} du \int_{-\pi}^{\pi} \int_0^\infty f(R, \Phi) \times J_0[u\sqrt{\{R^2+r^2-2Rr\cos(\Phi-\phi)\}}]\, R\,dR\,d\Phi, \quad (2.21)$$

the upper or lower sign being taken according as z is positive or negative. The order of the integrations with respect to R and Φ may be interchanged.

To prove this from Neumann's theorem, § 1,

$$\int_0^\infty u\,du \int_{-\pi}^{\pi} \int_0^\infty f(R, \Phi) \times J_0[u\sqrt{\{R^2+r^2-2Rr\cos(\Phi-\phi)\}}]\, R\,dR\,d\Phi$$

converges when considered as an integral with respect to u. Hence

$$\int_0^\infty e^{\pm uz} u\,du \int_{-\pi}^{\pi} \int_0^\infty f(R, \Phi) \times J_0[u\sqrt{\{R^2+r^2-2Rr\cos(\Phi-\phi)\}}]\, R\,dR\,d\Phi$$

converges uniformly with respect to z. We may then differentiate the right-hand side of (2.21) under the integral sign, and so

$$\left(\frac{\partial V}{\partial z}\right)_{z=0} = -2\pi f(r, \phi)$$

on using Neumann's theorem once again. But for a plane distribution

$$\left(\frac{\partial V}{\partial z}\right)_{z=0} = -2\pi\sigma,$$

where σ is the intensity of charge per unit area. Also there is only one potential function which gives rise to a given charge distribution. Hence this potential must be given by (2.21).

As an illustration, consider the elliptic disk whose semi-axes are a and b. The charge * at (R, Φ) is proportional to

$$\left\{1-\frac{R^2\cos^2\Phi}{a^2}-\frac{R^2\sin^2\Phi}{b^2}\right\}^{-\frac{1}{2}},$$

* Jeans, ' Electricity and Magnetism,' § 287, pp. 248–249.

where R varies from 0 to the positive root of

$$1-\frac{R^2\cos^2\Phi}{a^2}-\frac{R^2\sin^2\Phi}{b^2}=0,$$

and Φ varies from $-\pi$ to π. For other values of R the charge is zero. If we let

$$\Psi^2=\frac{a^2b^2}{b^2\cos^2\Phi+a^2\sin^2\Phi}, \quad . \quad . \quad . \quad (2.22)$$

then

$$f(R,\Phi)=K\left\{1-\frac{R^2}{\Psi^2}\right\}^{-\frac{1}{2}},$$

where K is a constant. From (2.21) the potential function * throughout space is

$$V=\int_0^\infty e^{\mp uz}du\int_{-\pi}^{\pi}\int_0^{\Psi}\left\{1-\frac{R^2}{\Psi^2}\right\}^{-\frac{1}{2}}$$
$$\times J_0[u\sqrt{\{R^2+r^2-2Rr\cos(\Phi-\phi)\}}]RdRd\Phi, \quad (2.23)$$

the upper or lower sign being taken according as z is positive or negative.

The integral on the right of (2.23) with respect to R can be evaluated in terms of hypergeometric functions defined by

$${}_pf_q(\alpha_1,\alpha_2,\dots\alpha_p\,;\,\rho_1,\rho_2,\dots\rho_q\,;\,x)$$
$$=\sum_{n=1}^{\infty}\frac{\Gamma(\alpha_1+n)\Gamma(\alpha_2+n)\dots\Gamma(\alpha_p+n)}{\Gamma(\rho_1+n)\Gamma(\rho_2+n)\dots\Gamma(\rho_q+n)}\frac{x^n}{n!}.$$

On using the power series for the Bessel function and integrating term by term, a process which is known to be permissible for a power series, we have

$$\int_0^{\Psi}\left\{1-\frac{R^2}{\Psi^2}\right\}^{-\frac{1}{2}}J_m(uR)RdR$$
$$=\tfrac{1}{2}\sqrt{\pi}\Psi^2(\tfrac{1}{2}u\Psi)^m,\ {}_1f_2(\tfrac{1}{2}m+1\,;\ m+1,\tfrac{1}{2}m+\tfrac{3}{2}\,;\ -\tfrac{1}{4}u^2\Psi^2).$$
$$. \quad . \quad . \quad (2.24)$$

* $f(R,\Phi)$ is not of bounded variation in an interval which includes the value $R=\Psi$, thus violating (ii.), § 1. This difficulty is easily overcome by taking the range of integration with respect to R in (2.23) to be $(0,\Psi-\epsilon)$, and then letting $\epsilon\to 0$. There is no difficulty in showing that this limit is given by the right-hand side of (2.23). But see the footnote ‡ on p. 994.

Now substitute (2.14) in (2.23). The series in (2.14) being uniformly convergent with respect to R, we may interchange the order of summation and integration. On using (2.24) and simplifying the first term, (2.23) becomes

$$V = K\int_0^\infty e^{\mp uz}du\int_{-\pi}^{\pi}\Psi\frac{\sin u\Psi}{u}J_0(ur)d\Phi$$

$$+\sqrt{\pi}K\int_0^\infty e^{\mp uz}du\int_{-\pi}^{\pi}\Psi^2\sum_{m=1}^{\infty}(\tfrac{1}{2}u\Psi)^m,$$

$$\times {}_1f_2(\tfrac{1}{2}m+1\,;\ m+1\,;\ \tfrac{1}{2}m+\tfrac{3}{2}\,;\ -\tfrac{1}{4}u^2\Psi^2)$$

$$\times J_m(ur)\cos m(\Phi-\phi)d\Phi. \quad . \quad . \quad . \quad . \quad . \quad (2.25)$$

It is not difficult to show that this series converges with the same rapidity as $\sum_{m=1}^{\infty} m^{-2}$.

When $a=b$ the disk is circular. We then have from (2.22) $\Psi^2=a^2$, and it can be seen that all the integrals with respect to Φ vanish except the first, giving us

$$V = 2\pi Ka\int_0^\infty e^{\mp uz}\sin au J_0(ur)\frac{du}{u},$$

which, it is well known *, is the formula for the potential field due to a freely-charged circular disk of radius a.

To obtain the potential of the elliptic disk itself it is sufficient to find the potential of the origin, *i.e.* we make $r=z=0$ in (2.25). We then get

$$V = K\int_0^\infty du\int_{-\pi}^{\pi}\Psi\frac{\sin u\Psi}{u}d\Phi$$

$$= 2K\int_0^\infty du\int_0^{\pi}\Psi\frac{\sin u\Psi}{u}d\Phi, \quad . \quad . \quad (2.26)$$

since Ψ is always positive.

Again, since

$$\int_0^\infty \frac{\sin u\Psi}{u}du$$

* Gray, Matthews, and MacRobert's 'Bessel Functions,' pp. 141–142.

is uniformly convergent with respect to $\Psi(>0)$, we may interchange the order of integration of (2.26), when we get

$$\begin{aligned} V &= 2K\int_0^{\pi} \Psi d\Phi \int_0^{\infty} \frac{\sin u\Psi}{u} du \\ &= K\pi \int_0^{\pi} \Psi d\Phi \\ &= K\pi ab \int_0^{\pi} \frac{d\Phi}{\{b^2\cos^2\Phi + a^2\sin^2\Phi\}^{\frac{1}{2}}}, \end{aligned}$$

an integral well known in the theory of elliptic functions.

§ 3. *The Potential Function due to two Parallel Plane Distributions.*

3.1. If we are given that in the plane $z=-c$ the potential at the point (R, Φ) is $f(R, \Phi)$, whilst at the same time in the plane $z=c$ the potential at the point (R, Φ) is $F(R, \Phi)$ both of these functions satisfying the conditions of § 1, then the potential V in between the two planes $z=\pm c$ is given by

$$\begin{aligned} 2\pi V = &\int_0^{\infty} u \frac{\sinh u(c-z)}{\sinh 2uc} du \int_{-\pi}^{\pi} \int_0^{\infty} f(R, \Phi) \\ &\times J_0[u\sqrt{\{R^2+r^2-2Rr\cos(\Phi-\phi)\}}]RdRd\Phi \\ &+ \int_0^{\infty} u \frac{\sinh u(c+z)}{\sinh 2uc} du \int_{-\pi}^{\pi} \int_0^{\infty} F(R, \Phi) \\ &\times J_0[u\sqrt{\{R^2+r^2-2Rr\cos(\Phi-\phi)\}}]RdRd\Phi. \end{aligned} \quad . \ . \ . \quad (3.11)$$

We may change the order of integration with respect to R and Φ.

As an illustration consider the problem of the guard-ring. In this problem $V=0$ over the whole plane $z=c$, and $V=$ a constant, K say, over a circular disk in the plane $z=-c$ of radius a and centre on the z axis, whilst $V=0$ over the rest of the plane $z=-c$. Thus $F(R, \Phi)=0$, whilst $f(R, \Phi)=K$ when $R<a$, and $f(R, \Phi)=0$ when $R>a$. Hence

$$\begin{aligned} 2\pi V = &\int_0^{\infty} u \frac{\sinh u(c-z)}{\sinh 2uc} du \int_0^{a} \int_{-\pi}^{\pi} K \\ &\times J_0[u\sqrt{\{R^2+r^2-2Rr\cos(\Phi-\phi)\}}]RdRd\Phi \\ = &\ 2\pi K \int_0^{\infty} u \frac{\sinh u(c-z)}{\sinh 2uc} du \int_0^{a} J_0(ur)J_0(uR)RdR \end{aligned}$$

on using (2.14) and integrating with respect to Φ. But on using the Taylor's series for $J_0(uR)$ and integrating term by term, we get

$$\int_0^a RJ_0(uR)dR = \frac{a}{u}J_1(au).$$

The potential function between the two planes $z = \pm c$ then reduces to

$$V = aK\int_0^\infty \frac{\sinh u(c-z)}{\sinh 2uc} J_1(au)\, J_0(ur)\, du.$$

3·2. If we are given that the intensity of charge at the point (R, Φ) on the side of the plane $z=-c$ facing $z=+c$ is $f(R, \Phi)$ per unit area, and that the intensity of charge at the point (R, Φ) on the side of the plane $z=c$ facing $z=-c$ is $F(R, \Phi)$ per unit area, then the potential function between the two planes $z=\pm c$, corresponding to this distribution, is given by

$$V = 2\int_0^\infty \frac{\cosh u(c-z)}{\sinh 2uc} du \int_{-\pi}^{\pi}\int_0^\infty f(R, \Phi) \times J_0[u\sqrt{\{R^2+r^2-2Rr\cos(\Phi-\phi)\}}]\, RdRd\Phi$$
$$+2\int_0^\infty \frac{\cosh u(c+z)}{\sinh 2uc} du \int_{-\pi}^{\pi}\int_0^\infty F(R, \Phi) \times J_0[u\sqrt{\{R^2+r^2-2Rr\cos(\Phi-\phi)\}}]\, RdRd\Phi. \quad . \quad . \quad . \quad . \quad . \quad (3.21)$$

Formulæ of this type can also be used to solve the following problem. An infinite conductor is bounded by two parallel planes $z=\pm c$, and two elliptical electrodes are applied to these planes. To simplify the analysis we shall assume that the centres of the disks lie on the axis of z, that both the ellipses have semi-axes a and b $(a>b)$, that both the major axes are in the plane $\Phi=0$, and that the potential of the plane $z=0$ is zero. The last assumption does not entail any loss of generality.

The disks being at constant potential, the charge at a point (R, Φ) on one of them at any instant is proportional to

$$\left\{1-\frac{R^2\cos^2\Phi}{a^2}-\frac{R^2\sin^2\Phi}{b^2}\right\}^{-\frac{1}{2}},$$

whilst at other points on the planes $z=\pm c$ the charge is zero.

Again, if V is the potential function of the system (V must, of course, be a solution of Laplace's equation), the rate of flow from the upper disk, say, to the medium is $-k\dfrac{\partial V}{\partial z}$ with $z=c$.

We must therefore have

$$k\frac{\partial V}{\partial z}=0, \quad \text{for } z=\pm c \text{ and } (R,\Phi) \text{ a point outside either of the elliptical electrodes,}$$

$$k\frac{\partial V}{\partial z}=K\left\{1-\frac{R^2\cos^2\Phi}{a^2}-\frac{R^2\sin^2\Phi}{b^2}\right\}^{-\frac{1}{2}}, \quad \text{for } z=\pm c$$

and (R,Φ) a point inside either of the electrodes,

where K is a constant. If we assume that the disk in the plane $z=c$ is at positive potential whilst that in the plane $z=-c$ is at a negative potential (*i. e.* the flow of the electricity is in the negative direction of the z axis), then the total flow S, say, from the upper disk to the medium is given by

$$S=K\iint\left\{1-\frac{R^2\cos^2\Phi}{a^2}-\frac{R^2\sin^2\Phi}{b^2}\right\}^{-\frac{1}{2}}R\,dR\,d\Phi,$$

taken over the area of the upper disk. Putting

$$R\cos\Phi=ar\cos\phi \quad \text{and} \quad R\sin\Phi=br\sin\phi,$$

the integral on the right-hand side is easily evaluated when we get

$$S=K\,.\,2\pi ab.$$

Hence we may write, with the notation of (2.22) :

$$\frac{\partial V}{\partial z}=\frac{S}{2\pi abk}\cdot\left\{1-\frac{R^2}{\Psi^2}\right\}^{-\frac{1}{2}}, \quad \text{for } z=\pm c$$

and (R,Φ) a point inside either of the electrodes.

The potential function is then given by

$$2\pi V=\frac{S}{2\pi abk}\int_0^\infty\frac{\cosh u(c-z)}{\sinh 2uc}\,du\int_{-\pi}^{\pi}\int_0^{\Psi}\left\{1-\frac{R^2}{\Psi^2}\right\}^{-\frac{1}{2}}\times J_0[u\sqrt{\{R^2+r^2-2Rr\cos(\Phi-\phi)\}}]\,R\,dR\,d\Phi$$

$$+\frac{S}{2\pi abk}\int_0^\infty\frac{\cosh u(c+z)}{\sinh 2uc}\,du\int_{-\pi}^{\pi}\int_0^{\Psi}\left\{1-\frac{R^2}{\Psi^2}\right\}^{-\frac{1}{2}}\times J_0[u\sqrt{\{R^2+r^2-2Rr\cos(\Phi-\phi)\}}]\,R\,dR\,d\Phi,$$

which, after simplification, becomes

$$2\pi V = \frac{S}{2\pi abk}\int_0^\infty \frac{\sinh uz}{\cosh ac}du \int_{-\pi}^{\pi}\int_0^{\Psi}\left\{1-\frac{R^2}{\Psi^2}\right\}^{-\frac{1}{2}} \times J_0[u\surd\{R^2+r^2-2Rr\cos(\Phi-\phi)\}]\,R\,dR\,d\Phi. \quad (3.22)$$

When $a=b$ this becomes identical with the problem of Nobili's rings. In this case $\Psi=a$, and the integrals with respect to Φ and R can be evaluated just as for (2.23). The result is

$$V = \frac{S}{2\pi a^2 k}\int_0^\infty \frac{\sinh uz}{\cosh uc}\sin au\, J_0(ur)\frac{du}{u},$$

agreeing with Riemann's solution *.

In (3.22) put $R^2=\Psi^2 v$, when we get

$$2\pi V = \frac{S}{2\pi abk}\int_0^\infty \frac{\sinh uz}{\cosh uc}du \int_{-\pi}^{\pi}\int_0^{1}(1-v)^{-\frac{1}{2}} \times J_0[u\surd\{\Psi^2 v+r^2-2\Psi v^{\frac{1}{2}} r\cos(\Phi-\phi)\}]\tfrac{1}{2}\Psi^2\,dv\,d\Phi. \quad . \quad . \quad . \quad (3.23)$$

By making a and b tend to zero, we can find the potential field when the electrodes become very small. We have

$$\Psi^2 = \frac{a^2b^2}{a^2\cos^2\Phi+b^2\sin^2\Phi}\to 0, \quad \text{as } a, b\to 0,$$

and it is not difficult to show when $-c<z<c$, that the limit of the right-hand side of (3.23) is the same as

$$\frac{S}{4\pi k}\int_0^\infty \frac{\sinh uz}{\cosh uc}du \lim_{\substack{a\to 0\\ b\to 0}}\int_{-\pi}^{\pi}\frac{ab\,d\Phi}{a^2\cos^2\Phi+b^2\sin^2\Phi}\int_0^1(1-v)^{-\frac{1}{2}} \times J_0(ur)\,dv.$$

But

$$\int_{-\pi}^{\pi}\frac{ab\,d\Phi}{a^2\cos^2\Phi+b^2\sin^2\Phi} = 4\int_0^{\pi/2}\frac{\frac{b}{a}\sec^2\Phi}{1+\frac{b^2}{a^2}\tan^2\Phi}d\Phi$$

$$= 4\tan^{-1}\left(\frac{b}{a}\tan\Phi\right)\Big|_0^{\pi/2} = 2\pi$$

* Gray, Mathews & MacRobert, *loc. cit.* pp. 144–146.

if b/a is neither zero nor infinite. Hence

$$\lim_{\substack{a\to 0\\ b\to 0}} \int_{-\pi}^{\pi} \frac{ab\, d\Phi}{a^2\cos^2\Phi + b^2\sin^2\Phi} = 2\pi,$$

and so (3.23) becomes in the limit:

$$V = \frac{S}{2\pi k}\int_0^\infty \frac{\sinh uz}{\cosh uc} J_0(ur)\, du, \quad . \quad . \quad (3.24)$$

provided that a and b tend to zero in such a way that $\lim b/a$ is neither zero nor infinite and $-c<z<c$.

The case $z=\pm c$ presents considerable analytical difficulty, but if we use the fact that the potential function is continuous, then the potential on the plane $z=c$ is given by

$$\lim_{z\to c} \frac{S}{2\pi k}\int_0^\infty \frac{\sinh uz}{\cosh uc} J_0(ur)\, du,$$

and, with the help of the asymptotic expansion of the Bessel Function, it is not difficult to show that this is equal to

$$\frac{S}{2\pi k}\int_0^\infty \frac{\sinh uc}{\cosh uc} J_0(ur)\, du.$$

Similarly for the case $z=-c$. Hence (3.24) is the potential function for $-c\leq z\leq c$.

It is interesting to note that the result is independent of the shape of the electrodes * as they shrink to zero, provided lim a/b is neither zero nor infinite, that is, provided that the ellipses do not shrink into straight lines.

§ 4. *The Introduction of a Unit Point Charge.*

4.1. When the planes in the preceding problems are all occupied by conducting matter, the potential functions can also be found if a point charge is introduced. We shall assume that this charge is positive, of strength unity, and situated at the point (z', r', ϕ').

To find the field due to a point charge situated in the presence of a plane of conducting material at $z=0$ charged to the potential $f(R, \Phi)$ at the point (R, Φ), we add the expression

$$\{(z-z')^2+r^2-r'^2-2rr'\cos(\phi-\phi')\}^{-\frac{1}{2}} - \{(z+z')^2+r^2+r'^2-2rr'\cos(\phi-\phi')\}^{-\frac{1}{2}} \quad (4.11)$$

* (3.24) is the same as the solution of the similar problem for circular electrodes (see Gray, Mathews, and MacRobert, *loc. cit.* p. 146).

to (2.11), using the upper or lower sign in (2.11) according as z' is positive or negative. If z' is positive, the potential throughout the space $z<0$ is zero, whilst if z' is negative, the potential throughout the space $z>0$ is zero.

To prove this, (4.11) is evidently a potential function which vanishes at $z=0$ and which has an infinity at $z=z'$, $r=r'$, $\phi=\phi'$, due to a unit point charge.

4.2. To find the field due to a unit charge at (z', r', ϕ') in the presence of a plane of conducting matter at $z=0$ charged to intensity $\frac{1}{2}f(R, \Phi)$ per unit area at the point (R, Φ), we add the expression

$$\{z-z')^2+r^2+r'^2-2rr'\cos(\phi-\phi')\}^{-\frac{1}{2}} + \{(z+z')^2+r^2+r'^2-2rr'\cos(\phi-\phi')\}^{-\frac{1}{2}}. \quad (4.21)$$

to (2.21), using the upper or lower sign in (2.21) according as z is positive or negative. If z' is positive, the potential throughout the space $z<0$ is zero, whilst if z' is negative the potential throughout the space $z>0$ is zero.

To prove this, it is easy to see that (4.21) is a potential function whose differential coefficient with respect to z vanishes when $z=0$.

4.3. To find the field due to a point charge situated at (z', r', ϕ') between two planes $z=\pm c$, the upper of which is charged at the point (R, Φ) to potential $F(R, \Phi)$ and the lower to potential $F(R, \Phi)$, we add to (3.11) the expression

$$\left.\begin{aligned} V &= 2\int_0^\infty \frac{\sinh u(c-z)\sinh u(c+z')}{\sinh 2uc} \\ &\qquad \times J_0[u\sqrt{\{r^2+r'^2-2rr'\cos(\phi-\phi')\}}]\,du \\ &\qquad\qquad \text{when } z' \leqq z \leqq c, \\ V &= 2\int_0^\infty \frac{\sinh u(c-z')\sinh u(c+z)}{\sinh 2uc} \\ &\qquad \times J_0[u\sqrt{\{r^2+r'^2-2rr'\cos(\phi-\phi')\}}]\,du \\ &\qquad\qquad \text{when } -c \leqq z \leqq z'. \end{aligned}\right\} \quad (4.31)$$

To prove this, we must show that the above expressions for V, which are evidently potential functions, vanish when $z=\pm c$, which is obvious, are continuous as z passes through z', which is also obvious, since both integrals converge and are equal when $z=z'$; and finally we must also show that $\dfrac{\partial V}{\partial z}$ is continuous as z passes through z'.

The formulæ of (4.31) are given by Gray, Mathews, and MacRobert* in their treatise, but they omit to prove that $\frac{\partial V}{\partial z}$ is continuous. As this is not at all obvious, I take the opportunity of proving it here. If we differentiate either of the integrals of (4.31) under the integral sign with respect to z, we find that the resultant integrals converge uniformly only if $z \neq z'$, and, in fact, when $z=z'$ they diverge. This shows, I think, that the continuity of $\frac{\partial V}{\partial z}$ at $z=z'$ cannot be taken for granted. The proof proceeds as follows. Using the usual exponential formulæ for the hyperbolic sine and cosine, it is easy to show that

$$\frac{2\sinh u(c-z)\sinh u(c+z')}{\sinh 2uc} = e^{-u(z-z')} + \frac{e^{-2uc}\cosh u(z-z') - \cosh u(z+z')}{\sinh 2uc}.$$

With the help of (2.16) it then follows that the upper formula for V in (4.31) is equivalent to

$$V = \{(z-z')^2 + r^2 + r'^2 - 2rr'\cos(\phi-\phi')\}^{-\frac{1}{2}} + \int_0^\infty \frac{e^{-2uc}\cosh u(z-z') - \cosh u(z-z')}{\sinh 2uc} \times J_0[u\sqrt{\{r^2+r'^2-2rr'\cos(\phi-\phi')\}}]\,du, \quad (4.32)$$

whilst the lower formula for V in (4.31) is equivalent to (4.32) with z and z' interchanged. On differentiating with respect to z under the integral sign in (4.32), we find that the resulting integral is uniformly convergent with respect to z and z' for all values of z and z' lying between $\pm c$, including $z=z'$. Hence, from the upper formula of (4.31), if $r \neq r'$ and $\phi \neq \phi'$, then

$$\left(\frac{\partial V}{\partial z}\right)_{z=z'} = -\int_0^\infty \frac{\sinh 2uz'}{\sinh 2uc}\, u \times J_0[u\sqrt{\{r^2+r'^2-2rr'\cos(\phi-\phi')\}}]\,du.$$

We find the same value of $\left(\frac{\partial V}{\partial z}\right)_{z=z'}$ by this method from the lower formula of (4.31). This shows that $\frac{\partial V}{\partial z}$ is con-

* 'Bessel Functions,' p. 193 (20).

tinuous as z passes through z' and completes the proof of the statement at the beginning of § 4.3.

4.4. To find the field due to a point charge situated at (z', r', ϕ') between two planes $z=\pm c$, the upper of which is charged at the point (R, Φ) to an intensity $F(R, \Phi)$ per unit area on its lower surface and the lower of which is charged to an intensity $f(R, \Phi)$ on its upper surface, we add to (3.21) the expression

$$\left.\begin{aligned} V &= 2\int_0^\infty \frac{\cosh u(c-z)\cosh u(c+z')}{\sinh 2uc} \\ &\qquad \times J_0[u\sqrt{\{r^2+r'^2-2rr'\cos(\phi-\phi')\}}]\,du \\ &\qquad\qquad \text{when } z' \leqq z \leqq c, \\ V &= 2\int_0^\infty \frac{\cosh u(c-z')\cosh u(c+z)}{\sinh 2uc} \\ &\qquad \times J_0[u\sqrt{\{r^2+r'^2-2rr'\cos(\phi-\phi')\}}]\,du \\ &\qquad\qquad \text{when } -c \leqq z \leqq z'. \end{aligned}\right\} \quad (4.41)$$

To prove this, we write

$$\frac{2\cosh u(c-z)\cosh u(c+z')}{\sinh 2uc} = e^{-u(z-z')} + \frac{e^{-2uc}\cosh u(z-z') + \cosh u(z+z')}{\sinh 2uc}$$

in the upper formula of (4.41), and, proceeding as in § 4.3, we can show that this formula is equivalent to

$$\begin{aligned} V &= \{(z-z')^2+r^2+r'^2-2rr'\cos(\phi-\phi')\}]^{-\frac{1}{2}} \\ &\quad + \int_0^\infty \frac{e^{-2uc}\cosh u(z+z') + \cosh u(z+z')}{\sinh 2uc} \\ &\qquad \times J_0[u\sqrt{\{r^2+r'^2-2rr'\cos(\phi-\phi')\}}]\,du, \quad (4.42) \end{aligned}$$

whilst the lower formula of (4.41) is equivalent to (4·42) with z and z' interchanged. We may differentiate the integral of (4.42) with respect to z underneath the integral sign, and we obtain

$$\begin{aligned} \left(\frac{\partial V}{\partial z}\right)_{z=z'} &= \int_0^\infty \frac{\sinh 2uz'}{\sinh 2uc}\,u \\ &\qquad \times J_0[u\sqrt{\{r^2+r'^2-2rr'\cos(\phi-\phi')\}}]\,du, \end{aligned}$$

whilst the same value for $\left(\frac{\partial V}{\partial z}\right)_{z=z'}$ is obtained if we start

with the lower formula for V in (4.41). Hence we see that V is a potential function having an infinity at $z=z'$, $r=r'$, $\phi=\phi'$ due to a unit point charge, is continuous at all other points of the plane $z=z'$, and that $\dfrac{\partial V}{\partial z}$ is also continuous as z passes through z'.

Again, if $z \neq z'$, we may differentiate the integrals of (4.41) with respect to z underneath the integral sign, from which it easily follows that

$$\left(\frac{\partial V}{\partial z}\right)_{z=\pm c} = 0.$$

Hence this system gives rise to no charge on either of the planes $z=\pm c$.

This completes the proof of the statement at the beginning of § 4.4.

C. *The Intensity Distribution of the General and Characteristic X-Radiation from Molybdenum.* *By* L. R. G. Treloar, *B.Sc., Wantage Scholar, University of Reading* *.

Introduction.

THE experiments described in this paper were made with the object of determining more precisely the nature of the complete radiation emitted under working conditions from a Shearer tube fitted with a molybdenum target. The experiments were intended primarily to be of practical rather than of theoretical interest.

The chief measurements were as follows :—

1. The intensity distribution of the general radiation at various voltages.
2. The corresponding intensities of the Kα- and Kβ-line radiation.
3. The ratio of the homogeneous to the general radiation.

Apparatus.

Two methods of excitation of the tube were employed. Most of the experiments were carried out with an induction coil and mercury interrupter, but for purposes of comparison

* Communicated by Prof. J. A. Crowther, Sc.D.

some later experiments were made with a 2-kilowatt oil-immersed transformer. During operations the tube was continuously exhausted by a two-stage diffusion pump, backed by a rotary oil-pump, and was controlled by means of an air-leak. It was run at voltages ranging from 19·75 kv. to 48·4 kv., the current being maintained constant at 3 milliamps. in all readings. The molybdenum target was about 1 mm. thick, and was brazed on to the water-cooled end of the tube at an inclination of 45° to the axis of the tube, and the beam emerged from the tube through an aluminium window ·056 mm. thick.

The spectrometer was of the standard Bragg pattern, employing a calcite crystal whose surface was ground. The ionization chamber, which had a length of 15·8 cm. and was closed by an aluminium window ·056 mm. thick, was filled with methyl iodide. It was saturated by a potential of 300 volts, supplied by a storage battery, and the ionization was measured by means of a Wilson tilted electroscope. The incident beam of X-rays was limited by two slits, and the reflected beam by a third slit, placed immediately in front of the chamber window.

Method of taking Readings.

Preliminary tests were carried out, sometimes with the help of the photographic method, to see that the crystal was accurately centred, and that it focussed the radiation sharply and accurately into the ionization chamber.

Owing to a slow change in the intensity of the radiation emitted from the tube, due, presumably, to spreading of the cathode stream etc., all the readings for a particular voltage were taken on the same day, with a continuous running of the tube. The voltage was found afterwards from the high-frequency limit of the spectrum. It would have been desirable to have had a more accurate control of the voltage during the course of readings, but this was not found possible. A spark gap between spheres of 5 cm. diameter, for example, was found not to increase the accuracy of the experiments. By the method employed, readings taken during a day's running were consistent to 3 per cent.

In taking readings the integrated reflexion method, which has been fully discussed by Bragg, James, and Bosanquet *, was used throughout. The crystal table was rotated by hand by means of a tangent screw fitted with radial spokes. To take a reading the chamber was set at the desired angle, and

* Bragg, James, and Bosanquet, Phil. Mag. xli. p. 309 (1921).

the crystal table was turned through an angle of $3\frac{3}{4}$ minutes at intervals of $2\frac{1}{2}$ seconds. The total angle swept through by the crystal in each reading was $2\frac{1}{4}°$, the corresponding time taken being 90 seconds.

The electroscope was operated at a comparatively low sensitivity of about 75 scale divisions per volt, and it was adjusted so that its sensitivity was at a maximum (*i. e.*, the sensitivity was reduced either by increasing or diminishing the tilt). In this position the leaf was found to be particularly stable, and, in addition, the deflexion was proportional to its potential. The leaf was connected to a potentiometer for calibration purposes, and its sensitivity was checked at frequent intervals between readings. The charge collected on the leaf could thus be converted directly into volts, after allowance had been made for any leakage of charge or drift of the leaf due to other causes.

Deflexions were made of convenient magnitude by adjusting the widths of the slits limiting the beam, and also, in the case of the lines, by the addition of a small condenser to the electroscope system. A knowledge of the slit-widths and of the condenser factor enabled these various readings to be compared.

In the measurement of the intensity of the general radiation, readings were taken at successive $\frac{1}{2}°$, or (where this was sufficient) 1° intervals of the ionization chamber, except in the neighbourhood of the lines. It was possible, however, to obtain a point on the curve lying between the α- and β-lines. In the measurement of the line intensities the chamber slit was opened sufficiently wide to include all the components of the line, and readings were taken as the chamber was moved through the line by successive $7\frac{1}{2}$-minute steps. In this way the line was shown as a flat-topped curve on a flat background of general radiation, and the line intensity was obtained by subtracting this background intensity from the maximum intensity. In all measurements, both of the general and of the homogeneous radiation, the mean of the intensities on the left- and right-hand sides of the spectrometer was taken as the true intensity.

At the higher voltages a discontinuity occurred in the general radiation curves at the frequency of the K-absorption limit of iodine. This discontinuity was always near the short wave-length end of the spectrum, and for wave-lengths shorter than this critical wave-length no quantitative significance was attached to the readings obtained, but they were nevertheless necessary for the determination of the limit of the spectrum.

The following data were obtained :—

(a) *With coil and interrupter.*

1. Curves at voltages of 48·4 kv., 38·9 kv., and 26·0 kv., giving the intensity distribution of the general radiation for wave-lengths as far as 1·34 Å.U.
2. The intensities of the α-line at these voltages.
3. The ratio of the α- and β-lines.
4. The relative intensities of the α-line in the 1st, 2nd, and 3rd orders respectively.

(b) *With transformer.*

1. Curves of general radiation at voltages of 34·9 kv. and 19·75 kv.
2. The intensity of the α-line at 34·9 kv. (In the other case no K-lines were present.)

In the comparison of the α- and β-lines, the tube was run at about 38 kv., and by the insertion of the condenser (which reduced the sensitivity of the apparatus to about one-fifth), when measuring the α-line, the deflexions were made of the same order of magnitude, with a consequent gain in accuracy. From a large number of readings taken without this improvement, however, the ratio of the lines was found to be independent of the excitation voltage, and of the method of excitation. Consequently, only the α-line was measured in the final experiments, the β-line intensity being found from the known ratio.

Calculations and Corrections.

(1) Correction for presence of 2nd- and 3rd-order reflexion in the general radiation.

The relative intensities of the α-line in the first three orders respectively were as follows :—

1st order	100
2nd order.....	7·6
3rd order	4·05

The percentages of the 1st-order intensity which appear in the 2nd and 3rd orders respectively are therefore 7·6/2 and 4·05/3, since the dispersion of the general radiation is proportional to the order in which it appears. To apply the order correction, these fractions of the 1st-order intensity, as obtained from the curve, were subtracted from the

intensities at wave-lengths corresponding to the 1st- and 2nd-order reflexions respectively.

(2) Correction for partial absorption in the methyl iodide in the ionization chamber.

The fraction of the shorter wave-lengths absorbed by the vapour was only about one-tenth, whereas the longer wave-lengths were completely absorbed ; hence it was necessary to determine with considerable accuracy the quantity of gas actually present in the chamber at any time. The chamber was filled by evaporation of the liquid methyl iodide into a vacuum, to a pressure of about 240 mm. of mercury ; but a measurement of the absorption of the α-line in passing through the chamber showed that the vapour-pressure was not a true indication of the quantity of methyl iodide present. This was due, no doubt, to the presence of volatile impurities in the liquid employed, and to the absorption of the gas by the walls of the chamber subsequent to measuring its pressure. It was not found possible, however, to carry out this absorption measurement with the accuracy required by the experiment, so the following method of determining the iodine content of the chamber was devised.

The chamber, connected to a manometer, was filled to a convenient pressure with the vapour, and set to receive a narrow beam of the general radiation of mean wave-length ·894 Å.U. The integrated reflexion was found. The pressure was then successively reduced, and the operation repeated at each pressure, so that a curve could be plotted to show the relation between pressure and ionization. The chamber was then refilled and sealed, and the ionization again measured. It was then ready for use.

Let I_0, I be the intensities of the beam of radiation at the beginning and end of its path through the vapour respectively, and let p be the corresponding pressure of vapour. Then $I=I_0e^{-\mu p}$, where μ is a constant. Assuming that the ionization is proportional to the energy absorbed, and denoting by q the ionization produced in the vapour at pressure p, and by q_0 the ionization which would be produced by complete absorption, we have $q=k(I_0-I)$, hence combining these two equations,

$$\log (q_0-q) = -\mu p + \text{const.}$$

The curve obtained experimentally, relating q and p, was of logarithmic form, and it was always found possible to assign a value to q_0 such that the curve relating $\log (q_0-q)$ and p was a straight line. This value was therefore the ionization

which would have been produced if the rays had been completely absorbed, and the fractional absorption of the selected wave-length after refilling of the chamber was q_1/q_0, where q_1 was the corresponding ionization. Knowing the absorption for that particular wave-length, the absorption of the other wave-lengths was calculated from values of the absorption coefficients for iodine obtained from tables given by Compton *.

The measurements described above were made before and after sets of readings covering a period of four or five days, with the result that the absorption on any day was accurately known. It is estimated that the errors arising from the application of this large and rather difficult correction are certainly within 3 per cent.

(3) Correction for absorption by the aluminium windows of the tube and ionization chamber.

The thickness of aluminium in each of these windows was ·056 mm., and the requisite corrections for absorption of the various wave-lengths were calculated from tables of absorption coefficients †. This correction amounted to over 100 per cent. for the longer wave-lengths.

(4) Correction for absorption in air.

The total length of air-path traversed by the rays from the window of the tube to the window of the chamber was 28·5 cm. The amounts of absorption were again found from tables of absorption coefficients of the constituent elements ‡.

(5) Effects of slit-widths and dispersion.

The quantity measured in the experiments on the general radiation is $I_\lambda \Delta\lambda$, where I_λ is the intensity at the wave-length λ and $\Delta\lambda$ is the range of wave-lengths entering the ionization chamber. The beam, on emerging from the tube, passed through slits distant 12 cm. and 3 cm. respectively from the centre of the crystal, and, after reflexion, through a third slit also at a distance of 12 cm. from the centre of the crystal. In the following discussion these three slits will be denoted by A, B, and C respectively, and the corresponding slit-widths by a, b, and c. Since A and C are

* A. H. Compton, 'X-rays and Electrons.'
† A. H. Compton, *loc. cit.*
‡ A. H. Compton, *loc. cit.*

equidistant from the centre of the crystal, then, by a well-known geometrical property of this arrangement*, all the rays of a given wave-length emerging from a single point of the slit A will be focussed to a point in the plane of C. Let D be the distance of either A or C from the centre of the crystal, then the rays from a point in A which, after reflexion, enter C are all included within an angle equal to c/D. Similarly, the angular range of rays of a given wave-length emerging from the slit A, which, after reflexion, pass through a single point of the slit C, is a/D. Adding these two effects, it follows that all rays of wave-length λ emerging from A, and reflected through C, are deflected through angles lying between 2θ and $2(\theta+\Delta\theta)$, where θ is the angle of reflexion for that wave-length, and $2\Delta\theta=(a+c)/D$. If d is the grating space of calcite, and $\Delta\lambda$ the wave-length range included by the slits, then $\lambda=2d.\sin\theta$, and

$$\Delta\lambda = 2d.\cos\theta\,.\,\Delta\theta = 2d\,.\cos\theta\,.\frac{a+c}{2D}.$$

The quantity required for plotting is the intensity at wave-length λ, *i.e.* I_λ, and may be found by dividing the observed quantity $I_\lambda\Delta\lambda$ by the wave-length range $\Delta\lambda$. Thus

$$I = I_\lambda\Delta\lambda\,.\,\frac{D\,.\sec\theta}{(a+c)d}\,.$$

The total energy emitted is then represented by the area of the curve, *i.e.* $\int I_\lambda d\lambda$. The effect of dispersion is thus completely accounted for. There is, however, another quite distinct question which has to be considered in connexion with the widths of the slits, namely the relative amounts of energy incident upon the crystal for slits of different widths. For this purpose it was assumed that the energy of the beam was proportional to the product ab.

(6) It was assumed that the crystal reflected all wave-lengths equally. The available data do not fully justify this assumption, but the results of Davis and Terrill †, and Wagner and Kulenkampff ‡, show that it is, at any rate, approximately true.

* Bragg, 'X-Rays and Crystal Structure,' p. 31.
† Davis & Terrill, Phil. Mag. xlv. p. 463 (1923).
‡ Wagner & Kulenkampff, *Ann. der Phys.* lxviii. p. 369 (1922).

Results.

(a) *With coil and interrupter.*

1. Curves I., II., and III. (fig. 1) show the relative proportions of general radiation at voltages of 48·4 kv., 38·9 kv., and 26·0 kv. respectively The areas of these curves, *i. e.* the total energies in the spectrum, as far as a wave-

Fig. 1.

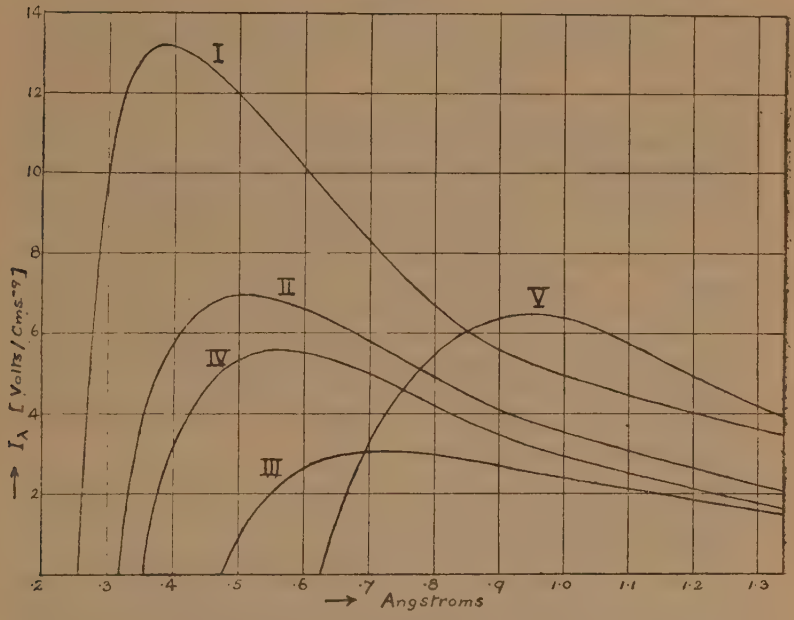

length of 1·34 Å.U., together with the measured α-line intensities, are shown in the following table :—

	Kv.	Area (volts).	α-line (volts).
I.	48·4	82·88	38·0
II.	38·9	47·44	16·5
III.	26·0	20·76	3·24

2. The value obtained for the ratio of the intensity of the α-line to that of the β-line (including the γ-line) was $\alpha/\beta = 4{\cdot}0$.

3. The ratios, obtained from these figures, of the energies of the α- and β-lines to the energy in the general radiation, and the fractions of the total emitted radiation which appear

as homogeneous K-radiation, are given below as percentages :—

	Kv.	α/General.	β/General.	$(\alpha+\beta)$/Total.
		%	%	%
I.	48·4	45·8	11·5	36·4
II.	38·9	34·8	8·7	30·3
III.	26·0	15·6	3·9	16·3

Discussion of Accuracy and Sources of Error.

(1) Errors due to gradual changes in the running of the tube.

There was a noticeable falling-off in intensity after several days' running of the tube, presumably due to changes in the cathode beam and in the position and size of the focal spot. In order to avoid, as far as possible, errors arising from these causes, the above readings were all taken within a period of three days, and all readings for a particular voltage were taken at a single running of the tube. Readings taken during the course of a day were consistent to 3 per cent. The effects become more important in connexion with the relative intensities at different voltages, and it is thought that these relative intensities can only be considered significant to an accuracy of about 10 per cent. These difficulties are inherent in the gas-tube.

(2) Errors due to inaccuracy in the estimation of the iodine content of the chamber.

The correction for partial absorption in the chamber was very carefully investigated, and has already been fully discussed. Errors arising from the application of this correction are probably nowhere greater than 2 per cent.

(3) Errors in the correction for absorption in the aluminium windows and air-path.

There is an element of doubt in the values of the absorpsorption coefficients for aluminium, and the inaccuracy introduced on this account may be as great as 5 per cent. in the case of the longest wave-lengths employed (1·34 Å.U.). For this reason the curves are not considered reliable beyond about 1·0 Å.U., but below this wave-length the error due to the above corrections is estimated at less than 2 per cent., and for the shorter wave-lengths (*i. e.* below ·5 Å.U.) it is quite negligible.

(4) Error in the measurement of voltage.

The difficulty of this measurement is increased by the proximity of the K-absorption limit of iodine to the limit of the spectrum in many cases. There is also the possibility of a slight variation of voltage during the course of readings, but the latter is included under heading (1). The voltage could be measured to an accuracy of 2 per cent.

(5) In general, taking account of the above considerations, the maximum error in the determination of the ratios of the characteristic radiations to the general radiation, and in the curves for a particular voltage, is estimated at 6 per cent. The ratio of the lines was more accurately determinable, the probable error here being 3 per cent. It was not the object of the work to determine the variation of absolute intensity with voltage, and the relative intensities of curves and lines of different voltages can only be considered as approximate, the error being of the order of 10 per cent.

The intensity of the general radiation is seen to vary approximately as the square of the excitation voltage, according to the following table :—

	V.	A.	A/V^2.
I.	48·4 kv.	82·88	351
II.	38·9 „	47·44	312
III.	26·0 „	20·76	306

The value of A/V^2 would be expected to diminish with decrease in voltage, since at the higher voltages a greater fraction of the total energy emitted occurs at wave-lengths below 1·34 Å.U.

Many observers have shown that the intensity of the lines is, in general, proportional to $(V-V_0)^n$, where V is the excitation voltage and V_0 is the critical excitation potential. The value of n is usually between 1·5 and 2·0. The results obtained for the α-line at these three voltages agree, to the accuracy obtainable, with this law if a value of about 1·6 is assigned to n.

The variation of the ratio of the energy in the α-line to that in the general radiation, with applied voltage, is shown graphically in fig. 2.

(b) *With transformer.*

(1) Curves IV. and V. give the intensity distribution of the general radiation at 34·9 and 19·75 kv. respectively (fig. 1). The absolute intensities are not significant, the

curves merely being drawn of convenient magnitude for illustration and comparison. Curve V. is interesting, since at this voltage there are no K-lines present. The following are the figures obtained for the energy in the general radiation and in the α-line, respectively, for curve IV.

	Kv.	Area (volts).	α-line (volts).
IV.	34·9	36·0	12·55

(2) The α-line and β-line were approximately in the same ratio as before.

Fig. 2.

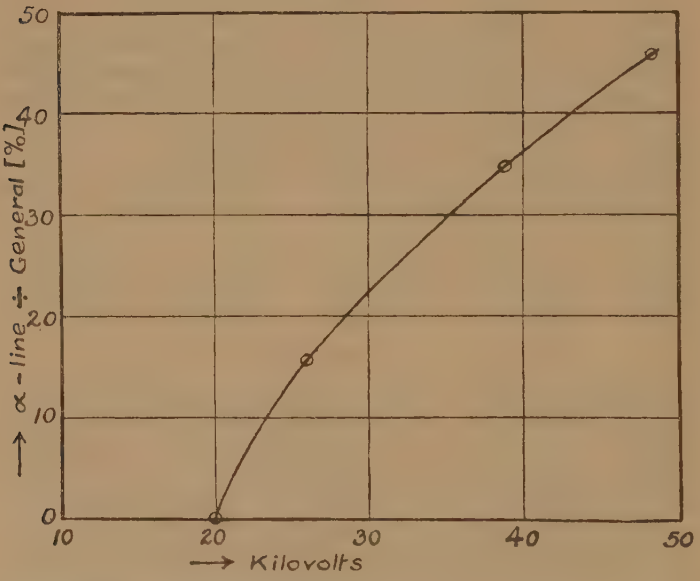

The corresponding figures for the relative proportions of characteristic and general radiation are as follows :—

	Kv.	α/General.	β/General.	$(\alpha+\beta)$/Total.
		%	%	%
IV.	34·9	34·8	8·7	30·4

Comparison of Results for both Methods of Excitation.

The corresponding value obtained for the ratio $(\alpha+\beta)$/Total in the case of the coil and interrupter is (by interpolation) 27·0 per cent., and differs from the above figure for the transformer by about 12 per cent. In view of the experimental

error of 6 per cent., it can only be said that these ratios are only slightly different, if at all.

The curves are all of the same form, and the method of excitation appears to have no marked effect on the intensity distribution. In particular, the wave-length of maximum energy is found to bear a constant ratio to the minimum wave-length, as shown below :—

	Kv.	$\lambda_{max.}$	λ_0.	$\lambda_{max.}/\lambda_0$.
I.	48·4	·385	·255	1·51
II.	38·9	·505	·317	1·59
III.	26·0	·73	·474	1·59
IV.	34·9	·56	·354	1·58
V.	19·75	·955	·626	1·53

The mean value of the ratio is 1·55.

In conclusion, I should like to express my great indebtedness to Professor J. A. Crowther for his valuable advice and for the energetic interest he has shown in the progress of this work.

Department of Physics,
The University,
Reading.

CI. *The Amount of Uniformly-diffused Light that will go in Series through Two Apertures Forming Opposite Faces of a Cube.* *By* Lewis F. Richardson, *D.Sc., F.R.S.* *

FOR example, the radiation might come out of a blackened enclosure at a uniform temperature through one aperture and thence across the cube and through the other aperture into a calorimeter; the problem being to find Stefan's constant.

We have to evaluate the integral †

$$\iint\iint \frac{\cos\zeta_1 \cdot dA_1 \cdot \cos\zeta_2 \cdot dA_2}{r^2}, \quad \ldots \quad (1)$$

in which dA_1, dA_2 are elements of area of the apertures, r is the distance between the centres of dA_1, dA_2, and ζ_1, ζ_2

* Communicated by the Author.

† Planck 'Vorlesungen ueber die Theorie der Wärmestralung' (Barth, 1913), p. 19.

are the angles which the normals to dA_1, dA_2 make with the line joining the centre of dA_1 to that of dA_2.

Let the edge of the cube be of length l. Take two systems of rectangular coordinates x_1, y_1 and x_2, y_2, one in the plane of each aperture, the origins being at the centres of the apertures and the two x-axes parallel to one another and to edges of the cube.

Then

$$\left.\begin{aligned} dA_1 = dx_1 dy_1\,; \quad dA_2 = dx_2 dy_2, \\ r^2 = l^2 + (x_1 - x_2)^2 + (y_1 - y_2)^2, \\ \cos\zeta_1 = \cos\zeta_2 = l/r, \end{aligned}\right\} \quad . \quad . \quad . \quad (2)$$

so that (1) becomes

$$l^2 \iiiint \frac{dx_1 dy_1 dx_2 dy_2}{r^4} = q l^2, \text{ say}, \quad . \quad . \quad . \quad (3)$$

each integration ranging from $-l/2$ to $+l/2$.

In order to make the calculation, consider instead of (3) a problem in finite differences. Regard each aperture as a window cut into n^2 panes, each pane being square. Take each pane in the first window in turn with each pane in the second, forming n^4 pairs of panes. Then $dx_1\,dy_1\,dx_2\,dy_2$ is analogous to (area of first pane) (area of second pane), and is the same for all pairs being l^4/n^4. So instead of (3) we calculate

$$\frac{l^6}{n^4} \sum^{n^4 \text{ pairs}} \frac{1}{(\text{separation of mid-points of panes})^4} = Q_n l^2, \text{ say}. \quad (4)$$

$Q l^2$ varies as l^2 because the distance of mid-points is proportional to l. Let us therefore make the calculation for $l = 1$.

First approximation. One pane in each window :

$$Q_1 = 1.$$

Second approximation, $n = 2$. Four panes in each window :

$$\begin{aligned} Q_2 &= \frac{1}{16}\left\{4 + \frac{8}{(1+\frac{1}{4})^2} + \frac{4}{(1+\frac{1}{4}+\frac{1}{4})^2}\right\} \\ &= 0{\cdot}681,111,1. \end{aligned}$$

Third approximation, $n = 3$. Nine panes in each window:

$$Q_3 = \frac{1}{81}\left\{\frac{9}{1} + \frac{12\times 2}{(1+1/9)^2} + \frac{6\times 2}{(1+4/9)^2} + \frac{8\times 2}{(1+1/9+1/9)^2} + \frac{4}{(1+4/9+4/9)^2} + \frac{16}{(1+4/9+1/9)^2}\right\}$$

$$= 0{\cdot}649,\,821,\,9.$$

Fourth approximation, $n = 4$. Sixteen panes to each window. To keep account of 256 pairs would be perplexing were it not that we can arrange them in a simple pattern.

Fig. 1.

						1 34
					4 24	2 29
				9 18	6 21	3 26
			16 16	12 17	8 20	4 25

The blank squares can be filled in because the distribution of numbers is symmetrical both about the diagonals of the large square and also about the lines joining the mid-points of its sides.

In fig. 1 let the central square represent *any* pane in one window. All possible relative positions of the panes in the other window are represented by the squares in fig. 1. In each square the upper number is the number of pairs of panes so situated, the lower number is the square of their distance apart multiplied by n^2. To form Q_4 we have to divide each upper number by the *square* of the lower number, and to sum the quotients. Presumably there is a

corresponding transformation from a fourfold to a double integral. However that may be, the result is

$$Q_4 = 0{\cdot}639,\ 910,\ 5.$$

To continue in this way until the accuracy of experiment were surpassed would be insufferably tedious. Instead, to make the "deferred approach to the limit*", it is assumed that, as there are neither discontinuities nor frills †, in (3)

$$Q_n = q + Bn^{-2} + Cn^{-4} + Dn^{-6}, \quad . \quad . \quad . \quad . \quad (5)$$
$$(n = 1, 2, 3, 4).$$

Fig. 2.

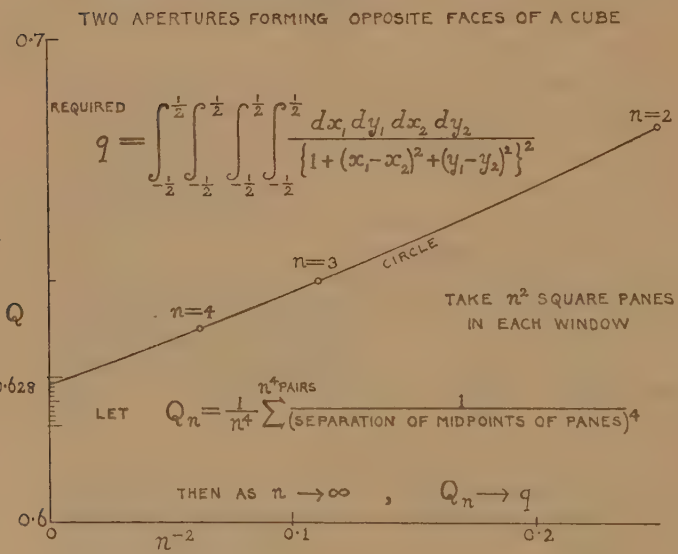

On eliminating B, C, D, from this set of four equations it is found that

$$2520\,q = 8192\,Q_4 - 6561\,Q_3 + 896\,Q_2 - 7\,Q_1, \quad . \quad (6)$$

the coefficients in which are useful in other problems.

Whence $$q = 0{\cdot}627,\ 75.$$

This may be called an h^6-extrapolation. As a rough check Q_2, Q_3, Q_4 are plotted against n^{-2} in fig. 2‡, and a circle drawn through the points is found to cut the axis, $n^{-2}=0$, at

* Phil. Trans. Roy. Soc. A. vol. ccxxvi. pp. 300, 311.
† *Loc. cit.* p. 315.
‡ Fig. 2 was shown at the British Association, Glasgow, 1928.

$Q = 0{\cdot}628$. To judge how many digits are reliable, we can neglect various parts of the four equations (5), retaining just enough of B, C, D to give a unique solution, B being retained first, then C, then D. Thus we form two sequences of extrapolations both leading to that already obtained :—

Q_4 ..... 0·639, 91	Q_1 ..... 1·000, 00
from Q_4, Q_3 ..... 0·627, 17	from Q_1, Q_2 ..... 0,574, 81
from Q_4, Q_3, Q_2... 0·627, 95	from Q_1, Q_2, Q_3... 0·631, 04

from Q_1, Q_2, Q_3, Q_4 ... 0·627, 75.

From these numbers it seems safe to conclude that 0·6278 is right to within $\pm 0\,001$. That accuracy is, however, barely enough. An estimate of the error could be obtained by the use of general formulæ expressing the difference between the integral and the sum as a series involving derivatives of the integrand. But it seems more profitable to compute Q_6 by the aid of a diagram like fig. 1. The law of these diagrams is found to be expressed by

$$Q_n = \sum_{s=1-n}^{s=n-1} \sum_{t=1-n}^{t=n-1} \frac{(n-|s|)(n-|t|)}{(n^2+s^2+t^2)^2}.$$

It is thus found that $Q_6 = 0{\cdot}633, 086, 28$.
Extrapolating, as above, from Q_4 and Q_6 gives 0·627, 63.
Extrapolating from Q_2, Q_4, Q_6 gives 0·627, 81.

Conclusion.—The amount of light, uniformly diffused with brightness I, that will go in series through two apertures forming opposite faces of a cube of edge l is

$$(0{\cdot}6278 \pm 0{\cdot}0001) l^2 \mathrm{I}.$$

The physical meaning of the above result may be understood by comparison with the statement of Stefan's constant. Instead of two squares we have one square of side l, drawn on a flat radiating solid of uniform brightness I. The second square is replaced by a hemisphere-at-infinity, drawn with its centre in the first square and its basal plane containing the radiating surface. The amount of light that will go through the square and hemisphere is known to be $\pi l^2 \mathrm{I}$, a result deducible from (1).

The method will obviously extend to parallel rectangular apertures.

The calculations were performed on a machine lent by the Government Grant Committee of the Royal Society.

CII. *Luminous Carborundum Detector and Detection Effect and Oscillations with Crystals.* *By* O. V. Lossev *.

[Plates XVII.–XX.]

Abstract.

In this paper are described further observations on the phenomenon of the luminescence produced at the contact of a carborundum detector in connexion with a view on luminescence as a consequence of the process in the contact which is very similar to cold electronic discharge.

Early observations were given by the author in the Russian language in 'Wireless Telegraphy and Telephony' (*Telegrafia i Telefonia bez provodov*, "*T. i T. b. p.*" no. 18, p. 61, 1923, and no. 26, p. 403, 1924 †).

Two types of luminescence are suggested—"I." and "II."

The luminescence II. depends upon the fluorescence of the crystal under the effect of electronic process at the contact.

The luminescence II. is more comparable than I. with cathodo-luminescence of carborundum in a discharge tube. The colour of luminescence II. changes considerably on altering the potential difference between the detector terminals, as may likewise be changed the colour of cathodo-luminescence. The spectrum of detector luminescence appears to be nearly identical with the spectrum of cathodo-luminescence.

The luminescence of a carborundum detector is closely connected with its rectifying action, which cannot be explained by a thermoelectric effect.

Increased conductivity of the contact at luminescence II., and the possibility of obtaining on the same carborundum crystal points with different direction of unilateral conductivity, are explained by the imposition of increased conductivity effect of the fluorescent layer upon the effect of electronic discharge properties at the contact.

A luminous detector may be used as a light relay, owing to the very small inertia of both the commencement and cessation of luminescence.

* Communicated by the Author.

† Also Lossev, 'Wireless World and Radio Review,' no. 271, p. 93 (1924); and *Zeit. f. Fernmeldetechnik*, no. 7, p. 97 (1926).

There are also several observations on the behaviour of oscillating crystals (zincite).

EXCEPT for some cases, at the contact of carborundum (SiC) * and metallic wire detector, more intense luminescence takes place when the metallic wire has a negative potential. In the case of current in the opposite direction (at the given luminous point), sometimes the luminescence is not observed at all (see figs. 2 and 3).

Fig. 2.

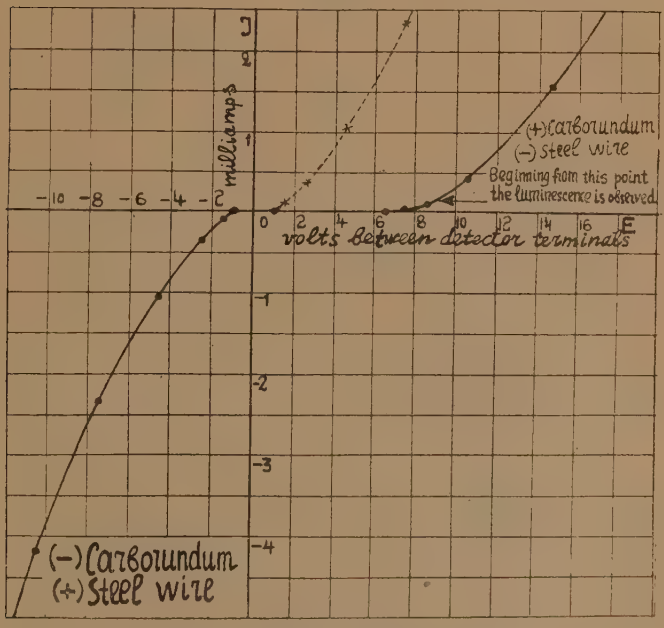

By the dotted line (in the first quadrant) is shown the branch of third quadrant. Luminescence I.

§1. *Two Types of Carborundum-Contact Luminescence. The Change of Luminescence II. Colour.*

From many observations it was found that two types of luminescence at carborundum contact may be distinguished.

* Silicon carbide.

"*Luminescence I.*"—Luminescence I. has a greenish-bluish colour. It is a bright little point (sometimes several little points) which is surrounded by diffuse luminescence with small brightness. The diffuse luminescence is due to reflected light from the nearest facets of the crystal (see Pl. XVII. fig. 1). The colour of luminescence I. does not perceptibly change with change of the potential difference between detector terminals.

On passing a current in the direction which produces the more intense luminescence I., the detector shows a lower

Fig. 3.

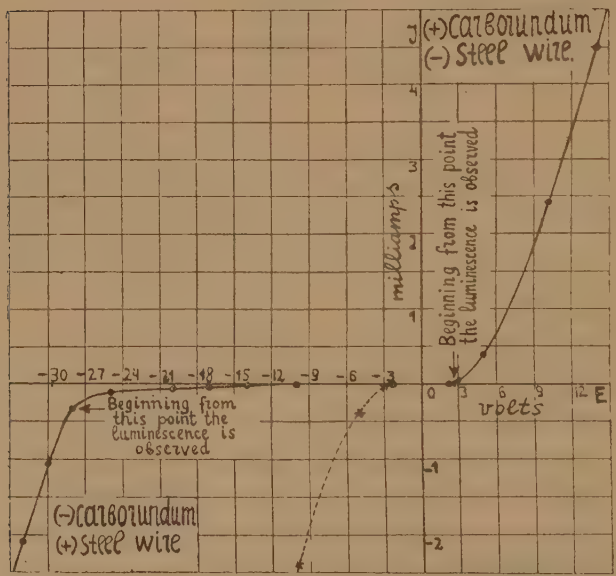
(+)carborundum
(-) steel wire
milliamps
Beginning from this point the luminescence is observed
-30 -27 -24 -21 -18 -15 -12 -9 -6 -3
0 3 6 9 12 E
volts
Beginning from this point the luminescence is observed
(-)carborundum
(+)steel wire

By the dotted line (in the third quadrant) is shown the branch of first quadrant. Luminescence II.

conductivity (see the static characteristic curve on fig. 2). The rectification of high-frequency current occurs in a corresponding direction (unless a continuous displacing of the potential difference is impressed: "polarizing voltage").

In early observations (*T. i T. b. p.*) only the luminescence I. was described *.

"*Luminescence II.*"—When a current is passing in a direction such that the luminescence II. is less intense, the

* Also 'Wireless World and Radio Review,' no. 271, p. 93 (1924); and *Zeit. für Fernmeldetechnik*, no. 7, p. 97 (1926).

contact shows less conductivity (fig. 3); *i. e.*, unilateral conductivity is in the opposite direction to that of luminescence I. (*cf.* figs. 2 and 3).

With luminescence II. strong fluorescence takes place upon a large surface of the crystal. Sometimes that fluorescent surface spreads beyond the limit of touch of the point of the contact wire (see Pl. XVII. fig. 4).

The colour of luminescence II. changes with change of the potential difference between detector terminals from orange to violet, as, for example, is shown in the following table:—

Orange	6 volts	(between	detector	terminals).
Yellow	10 „	„	„	
Light yellow	20 „	„	„	
Greenish	26 „	„	„	
Violet	28 „	„	„	

The change of the colour is somewhat different for different points, even on the same crystal. These results were obtained with a current in the direction which gives the more intense luminescence, *i. e.* (+) carborundum and (−) contact wire.

It must be mentioned that a direct cause for the change of colour is probably to be found in the temperature of the fluorescent surface of the crystal* depending upon the Joule effect at the contact. This suggestion is strengthened by the fact that external heating produced by a special heater changed considerably the colour of luminescence II. at the luminous detector.

All carborundum crystals used for observations were of four kinds. With the first and second kinds can be obtained only luminescence I. With the third and fourth kinds can be obtained (on the same crystal) both luminescences I. and II. The crystals were mounted by stannous in metallic cups. As a contact wire, a steel wire, tantalum, nickelin, and silver were used. The properties of these metals as a contact wire were nearly identical.

Under the microscope it may be seen that both luminescences I. and II. appeared if the contact wire was touched to the sharp edge of the crystal, or when a sharp point of contact wire was touched to the crystal surface.

Sometimes might be observed the cases of imposition of both luminescences I. and II. one upon the other.

* *Cf.* the cases of change of luminescence colour depending on the temperature which are known in photo-luminescence (H. Becquerel, *C. R.* cxlvi. p. 440, 1908; cli. p. 981, 1910).

Some typical features of both luminescences will be described later on.

§ 2. *Supposed Cold Electronic Discharge at the Contact of Carborundum Detector.*

(1) The character and intensity of the luminescence depends to a great degree on the direction of the current (even if the same current (abs. value) is taken in both directions with characteristic of type fig. 3, or same tension with characteristic of type fig. 2 ; see § 1).

(2) Unilateral conductivity of carborundum contact is closely connected with its luminescence (see § 1 & § 3 and *cf.* also § 4).

(3) As may be clearly seen under the microscope, the luminous surface is not incandescent. For example, a drop of benzene put on the luminous surface is not vaporized for a long time. Of course, when a strong current (of order more than 20 milliamps) is flowing through the detector, the part of the crystal near to the contact, in addition to showing the cold luminescence, will be slowly brought to a red heat (see § 5 ; *cf.* also item 2, § 4).

(4) The substance of carborundum does not produce thermo-luminescence. Hence the cause of luminescence is not due to a Joule effect at the contact (see § 1 and § 5—only the colour of fluorescence at luminescence II. depends on the temperature at the contact).

(5) The inertia of both the commencement and cessation of luminescence, even with possible strong currents through the contact (till the destruction of the contact), is very small (see § 5 and *cf.* also item 1, § 4).

It may be supposed, therefore, that the luminescence at a carborundum contact is a consequence of the process which is very similar to cold electronic discharge (*cf.* § 4).

The suggestion that unilateral conductivity of the contact with crystals can be explained by electronic process (electronic emission at the contact) has already been proposed by F. Braun *, G. Hoffmann †, and Pierce ‡.

Fig. 5 (Pl. XVII.) shows luminescence I., where the stratification of light is near the contact electrodes §. At

* F. Braun, Pogg. *Ann.* cliii. p. 556 (1874) ; Wied. *Ann.* i. p. 95 (1877), iv. p. 476 (1878), xix. p. 340 (1883). See also H. Lüke, *Phys. Zeit.* xxviii. p. 213 (1927).

† G. Hoffmann, *Phys. Zeit.* xxii. p. 422 (1921).

‡ *Cit.* A. C. James, Phil. Mag. xlix. p. 681 (1925).

§ See *T. i T. b. p.* no. 26; 'Wireless World and Radio Review,' no. 271.

the top is the point of contact wire (−) and at the bottom the crystal surface (+). Magnified 505 times; current through the contact = 18 milliamps. If the value of cross-section of the luminescence is counted as a diameter, from fig. 5 it is a simple matter to calculate "the area of luminescence," which is 700 sq. microns. The size of that order in comparison with the size of the fluorescent surface at luminescence II. is very small, and it is typical for luminescence I.

The question of whether the electronic process occurs in the layer of adsorbing gas or in the crystal lattice of the surface-layer of the crystal requires further investigation *. At any rate, the presence of apparent fluorescence of the crystal at luminescence II. (see § 1) shows that some process takes place also in the surface-layer of the crystal †.

Comparison of Detector Luminescence with Cathodo-Luminescence.

Luminescence II. is more comparable than I. with fluorescence of carborundum in a discharge-tube (see Pl. XVIII. fig. 6) under the cathode rays effect. It was found that the colour of carborundum cathodo-luminescence in an evacuated tube may be changed in a similar manner to the luminescence II. at the detector. With softening of the tube (*i. e.* with increase of pressure in it) the colour of cathodo-luminescence changes slowly from orange to violet.

First and third kinds of carborundum (SiC), two kinds of zincite (ZnO), and two kinds of iron glance (F_2O_3) were mounted in the tube as shown in fig. 6 (Pl. XVIII.). Strong cathodo-luminescence takes place only with carborundum (both kinds). With both the zincite and iron glance the cathodo-luminescence is very feeble.

The Spectrum of Detector Luminescence and Cathodo-Luminescence.

The spectrum obtained from carborundum contact luminescence (I. and II.) is continuous with a feebly-marked red portion. With increase of the potential difference between detector terminals, with luminescence II., the relative

* *Cf.* A. F. Joffe, Reports of V. Congress Russ. Phys. p. 11, 1926. It has been stated by A. F. Joffe that in the substance of *dielectric* crystals a process may occur similar to the production of ions at discharge in the gas. *Cf.* also A. C. James, Phil. Mag. xlix. p. 681 (1925).

† For the present consideration, it is of no importance whether the substance SiC fluoresce or some other admixture in the crystal.

brightness of the spectrum in the region of shorter wavelength is increased (*cf.* § 1).

The spectrum of carborundum cathodo-luminescence in a discharge-tube appears to be nearly identical with the spectrum of contact luminescence II.

In order to obtain some indications with respect to the essentials of the process at the contact, the luminescence of a carborundum detector was also observed in a magnetic field.

Sometimes the luminescence changed considerably as the luminous detector was transferred from air to another medium; for example, to benzene. The description of these observations is outside the scope of this paper.

§ 3. *Luminous Detector and Unilateral Conductivity of the Contact with Crystals. The Effect of Increased Conductivity of the Fluorescent Layer.*

The points of the crystal which were found at high frequency (without impressed "polarizing voltage") to give the rectified action were always non-equal as regards luminosity with direct current at a different direction of *d. c.* (and in meaning of item 1, § 2).

In order to explain the inverse directions of unilateral conductivity shown by characteristics of figs. 2 and 3 * (§ 1), it may be easily supposed that at luminescence II. occurs the increase of conductivity of the fluorescent layer (a very large surface of which is typical for luminescence II.; see fig. 4) under the effect of electronic process at the contact,—analogically to the known fact of increasing conductivity of cathodo-luminescent bodies in discharge-tubes †. (This suggestion was also made by Prof. B. A. Ostroumoff.)

The influence of increased conductivity effect of a layer near to the contact may be partly applied to the actions of some other (and non-luminous) contact detectors and impressed on the effect of properties of hypothetic electronic discharge itself.

In addition to the characteristics on figs. 2 and 3 (§ 1), on fig. 7 is shown the curve both positive and negative branches of which are crossed (when they are in the same quadrant). The presence of that cross can be explained by the imposition of these two effects. By examination of detector contact under the microscope, when the curve of fig. 7 was plotted, the case of imposition of both luminescences (I. and II.) can

* *Cf.* A. Schleede and H. Buggish, *Phys. Zeit.* xxviii. p. 174 (1927).
† E. Rupp, *Ann. d. Phys.* lxxiii. p. 127 (1924).

be observed. (The point of the crystal from which the curve of fig. 7 was taken was also tested for rectifying of high frequency (without impressed "polarizing voltage"). It was found that at low tension of H.F. the rectification occurred in one direction, but with increased tension of H.F. the direction was reversed).

Fig. 7.

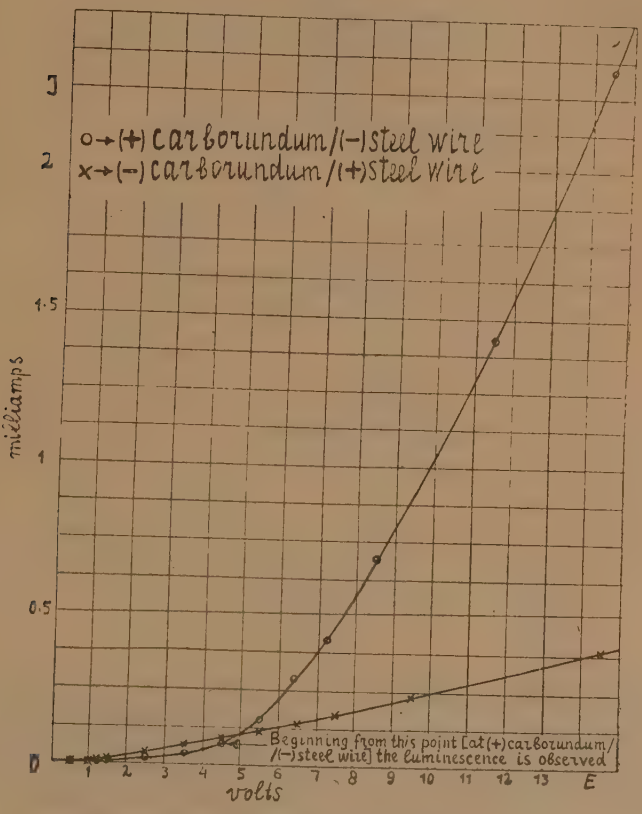

Both positive and negative branches of characteristic are shown in the same quadrant.

Unilateral conductivity of the carborundum detector cannot be explained by thermoelectric effect. In connexion with this an investigation was made *, the description of which is outside the scope of this paper. It was found that

* *T. i T. b. p.* no. 44, p. 485 (1927).

neither the value of the thermo-E.M.F. nor its direction agreed with the continuous component value of the E.M.F. of the rectified current, which at corresponding conditions can be easily obtained from the same detection point of the carborundum crystal *.

All characteristic curves given in this paper were plotted by means of the scheme shown in fig. 8 ($E = V - IR_b$).

Fig. 8.

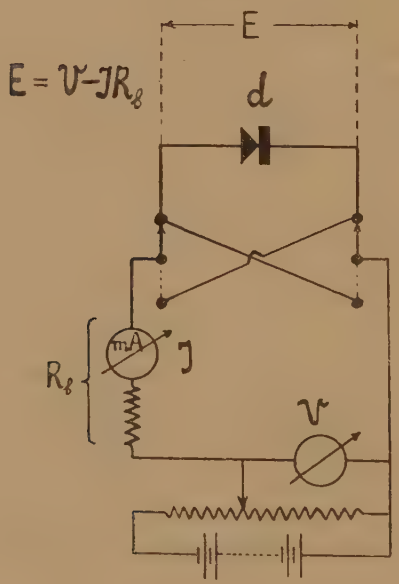

§ 4. *Luminous Detector and Oscillations with Crystals.*

The oscillation with crystal detector (galena) was discovered by W. Eccles in 1910 †. He formulated an interesting thermal theory of this phenomenon based on the

* *Cf.* F. Trey, *Phys. Zeit.* xxvi. p. 849 (1925). H. Lüke, *Phys. Zeit.* xxviii. p. 213 (1927).

† In May 1910 a communication was made by W. H. Eccles to the London Physical Society ('The Electrician,' p. 385, 1910); see G. W. Pickard, 'Radio News,' vi. p. 1166 (1925); H. J. Round and N. M. Rust, Wireless World and Radio Review,' xvii. p. 217 (1925); H. S. Pocock, Wireless World and Radio Review,' xiv. p. 299 (1924). See also G. Million, Jn., 'Radio News,' v. p. 714 (1923); R. Pennec, 'Radio Revue,' no. 28, p. 139 (1924).

fact that many detector minerals, having metallic conductivity, have a negative temperature resistance coefficient*.

A carborundum detector seldom gives the characteristics with negative slope $\left(\frac{dE}{dI} < 0\right)$, even on little space (*cf.* on fig. 9*a* the characteristic of oscillating point of zincite detector; on space $I_0 D$ $\frac{dE}{dI} < 0$). Sometimes in a zincite generating detector (zincite and steel wire) the luminescence can be

Fig. 9*a*.

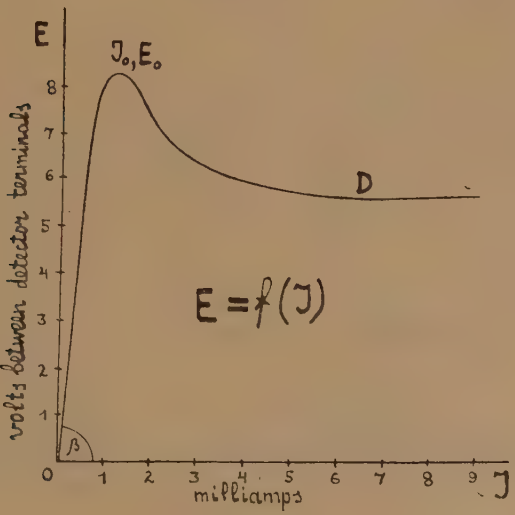

obtained, but it is very feeble (*cf.* § 2. The cathodo-luminescence of zincite is also very feeble in comparison with that of carborundum).

(1) The possibility of producing very steadily (continued for some hours), with a generating zincite detector, short waves to 24·3 metres ($1{\cdot}23 \times 10^7$ cycles per second) † shows

* W. H. Eccles, Phil. Mag. xix. p. 869 (1910). (*Cit.* by A. Petrowsky, *Morskoy Sbornic*, no. 10, 1911). For example, for specimens of zincite (ZnO), carborundum (SiC), and iron glance (F_2O_3) within 22° to 97° C. temperature resistance coefficients were correspondent to (1) −0·007; (2) −0·0027; (3) −0·0065 (*T. i. T. b. p.* no. 26, p. 403, 1924).

† *Cf.* R. Ettenreich, *Phys. Zeit.* xxi. p. 208 (1920). "It has been stated by R. Ettenreich that the time of reaction in crystal rectifiers is less than 10^{-6} second" (*cit.* A. C. James, Phil. Mag. xlix. p. 681, 1925).

that the inertia of the corresponding processes at the contact is very small (*cf.* § 5).

Fig. 10 represents the scheme used for receiving short waves*. The galvanometer μA was used as indicator; d = galena detector; G = zincite generating detector; L = seven turns in the diameter 11 cm.; wire in the diam. 2 mm.; L′ = one turn in the same diameter; wire in the diam. 2·2 mm.; R_b = ballast resistance 2300Ω; L″ and L‴ = choke-coils—single-layer coils (without iron core); wire in the diam. 0·1 mm.; C″ = blocking condenser 370 cm.; B = battery 12 volt. (Besides the fundamental frequency $1{\cdot}23 \times 10^7$ the second harmonic was also found.)

Fig. 10.

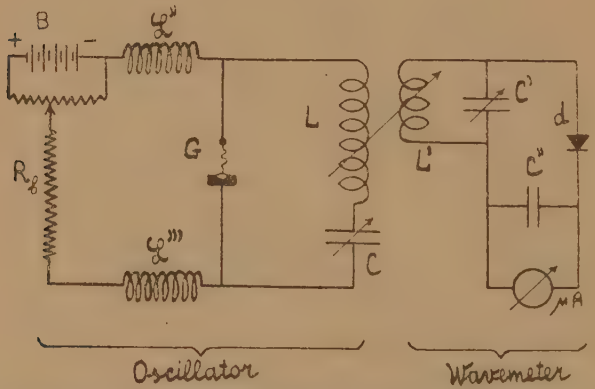

The scheme as used for short-wave reception; the circuit L′C′ has been calibrated by the method of stationary waves on Lecher wires; the coupling between L′ and L was loose.

(2) An investigation of temperature influence on generating contact showed that the value (abs.) of the negative resistance produced by the contact was strongly decreased by even comparatively small equable external heating (for example, on 60° C.; see fig. 11—both positive and negative branches of the characteristic curve are shown in the same quadrant). If the detector is generating the oscillations are stopped by heating. Decrease of the temperature gives the contrary effect †. Thus the contact of a generating detector,

* *T. i T. b. p.* no. 21, p. 349 (1923). Ref. by H. Pocock, 'Wireless World and Radio Review,' xiv. p. 299 (1924); M. Gausner et T. Quinet, *Radio Revue*, no. 30, p. 189 (1924); and by J. Podliasky, *Radioélectricité*, v. p. 196 (1924).

† *T. i T. b. p. n.* 18, p. 45 (1923). Ref. by C. N. Vinogradov, *L'Onde Electrique*, n. 33, p. 441 (1924).

under normal conditions, when working is very feebly heated.

The action of the contact of a zincite generating detector may be regarded as the result of a cold electronic process, but having certain properties of the voltaic arc * (*cf.* § 2). This is in accordance with the observations described above.

For the purpose of the present consideration we may introduce the conception of ohmic resistance (of touch at the contact †) R_s, which is in parallel to the hypothetic

Fig. 11.

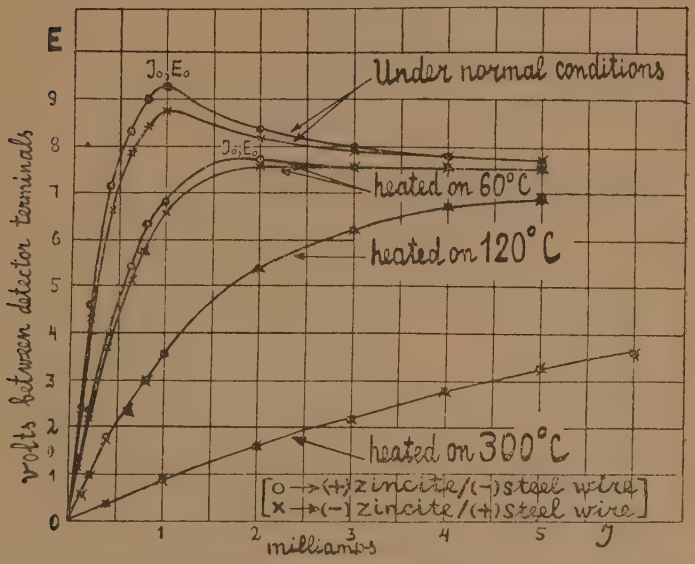

The curves $E = f(I)$ under varying conditions of temperature of zincite steel wire detector. The curve at the top and that third from top are plotted with the positive of applied current to the zincite, while the second and fourth were with negative to the zincite. Both the fifth and sixth curves indicate each two branches of characteristics which are considered. All curves were plotted from same oscillating point.

After cessation of heating (approach to normal conditions) initial properties of detector are restored.

(The oscillation circuit was disconnected during the time of plotting.)

---

* Partly similar to thermionic emission, but under a great deal lower temperature (see fig. 11). Due to the temperature, E_0 changes considerably (which may be somewhat analogous to break-down voltage of ordinary discharge in the gas). See *T. i T. b. p.* no. 18; C. Vinogradov, *loc. cit.*

† *See* G. Hoffman, *loc. cit.*

discharge and also takes into account the fact that the electronic discharge at I from O to $I<I_0$ is very small, and the current passes chiefly across R_s (*i. e.* $\tan\beta \doteq R_s$; see fig. 9 *a*).

For a space of characteristic $I>I_0$ an expression

$$E=\tfrac{1}{2}(IR_s+a\mp\sqrt{(a-IR_s)^2-4R_sb})+Ir, \quad . \quad . \quad (I.)$$

is obtained if it be supposed that cold electronic discharge at generating contact at $I>I_0$ is subject to the law $e=a+b/i$ *. Here e and i are tension and current of electronic discharge; a and b = constants ; r = resistance of crystal thickness ;

Fig. 12.

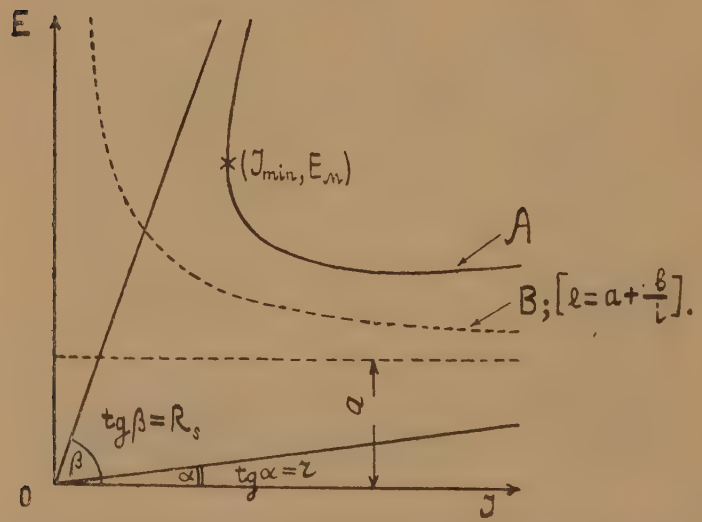

I = current across the whole detector ; E = tension on detector terminals † (*cf.* § 2). On fig. 12 is shown the curve which corresponds to expression (I.) (curve A). To each value of I correspond two values for E, but only one of them will be stable ($E<E_M$), since at $E>E_M-\frac{de}{di}>R_s$ (see fig. 12).

In most cases formula (I.) is near to experimental results. With regard to the order of magnitude of the constants in

* See Mrs. Ayrton, 'The Electric Arc,' London. V. Mitkevich, Journ. Russian Phys.-Chem. Society, p. 678, 1903, and p. 65, 1904.

† *T. i T. b. p.* no. 18, p. 45 (1923). C. N. Vinogradov, *loc. cit.* *Cf.* Gautherot, *Radio Revue*, no. 33, p. 278 (1925).

formula (I.) the following table may give some indications. The calculations are based on characteristics which are plotted from the oscillating points of the zincite.

Contact.	r_Ω.	R_Ω.	a.	$b\times10^3$ *.
Zincite N1—steel wire ...	98	20,000	5	1·7
,, ,, ,, ...	80	28,000	7·5	3·5
,, ,, ,, ...	76	10,000	3·3	0·9
,, ,, ,, ...	80	30,000	4·5	1·5
,, ,, ,, ...	50	25,000	3·5	1·5
,, ,, ,, ...	49	6,000	3·5	0·8
,, N2—steel wire ...	150	32,000	9	1·5
,, ,, ,, ...	170	40,000	10·5	3

"R_s" can be calculated approximately as

$$R_s \doteqdot \frac{2E_0-a}{I_0}, \quad . \quad . \quad . \quad . \quad . \quad . \quad . \quad (II.)$$

where E_0 and I_0 are coordinates of the plotted characteristic curve which corresponds to the commencement of the stronger discharge (see fig. 9 *a*).

When I_0 and E_0 of the curve taken are nearest to the values $I_{min.}$, E_M respectively (of the corresponding theoretical curve; see fig. 12 [A]), the calculations may be done with close approximation ($I_0 r$ neglected).

For one of such cases, on fig. 13 are shown the results of comparison of the slope value of straight line of calculated R_s (expression II.) for given characteristic (dotted line, $\tan\beta = R_s$ †) with the value of slope at its initial part (OA on fig. 13). In this case (see fig. 13) it is clear that they are near together, which is in accordance with the present consideration.

All negative resistances given by conductors with characteristics with negative slope, for the following consideration, may be divided, as was done by G. Ostroumoff ‡, into two different groups: (1) "a negative series-resistance" and (2) "a negative leak-resistance."

* "*a*" has a dimension of the potential; "*b*" has a dimension of power.

† For this case $R_s = 18{,}500_\Omega$.

‡ G. Ostroumoff, *T. i T. b. p.* no. 38, p. 465 (1926). One or another group of negative resistance is determined by characteristic rotation in regard to coordinates (which are displaced by constant components of both a direct current and tension; see fig. 9 *b*). By this the stability is determined in one circuit or another (G. Ostroumoff considers both the arc and the vacuum-tube). (*Cf.* H. Barkhausen, *Zeit. für Hochfrequenztechnic*, xxvii. p. 150 (1926). Also Kiebitz, *ibid.* p. 136 (1926) *T. i. T. b. p.* no. 14, p. 384 (1922) and no. 38, p. 436 (1926)).

From the form of static characteristic of the generating detector (see figs. 9 *a*, 11, 13 ; *cf.* also fig. 9 *b*) it can be seen that a generating detector may give "a negative leak-resistance." Thus a steady periodical process may be excited by a generating detector only, either :

(1) In a "capacity circuit" RC (fig. 14—the circuit consists of the capacity C and resistance R, where self-inductance is very small) with the period of impulses proportional to RC analogically to a multivibrator, Abraham and Bloch * ; or

(2) In an ordinary (Thomson) oscillating circuit (LC) connected *in series* to the detector G (see fig. 10) †. This was found to be so in all our experiments ‡.

In the following table are shown the observations of frequencies of "capacity oscillations" which are produced by a generating detector in circuit RC § (fig. 14).

R(Ω.)	C(μF).	Observed frequencies. f(cyc./sec.).	Value of coefficient k in expression $f=1/k$RC corresponding to observed f.
60	2·9	2200	2·61
40	4·9	1800	2·84
170	0·9	2100	3·12
170	2	850	3·46
170	2·9	620	3·28
170	4	460	3·19
240	2·9	560	2·56
240	2	790	2·62
220	0·9	2300	2·19
40	4·9	1550	3·29

* H. Abraham and E. Bloch, *C. R.* clxviii. p. 1105 (1919). 'Radio Review,' i. no. 2, p. 91 (1919). *Cf.* H. Barkhausen, *E. T. Z.* p. 1338 (1924) ; E. Friedländer, *Arch. für Electrotech.* xvii. pp. 1 and 103 ; B. Van der Pol, Jn., Phil. Mag. lii. p. 978 (1926). The latter author termed these oscillations "relaxation oscillations." In this paper they are termed "capacity oscillations" to distinguish them from another type of relaxation oscillations,—"self-induction oscillations,"—of which the period is proportional to L/R. "Self-induction oscillations" appear to be steady only in the presence of "negative leak-resistance" (see fig. 9 *b*) in the circuit containing self-induction and resistance, where capacity is very small.

† In the "Thomson circuit in parallel" it is possible to obtain stable oscillations only with "negative leak-resistance," for example, with vacuum-tube (see fig. 9 *b*).

‡ From a generating detector may also be obtained oscillations of which the period is regulated mechanically (quartz, camerton, and so on).

§ *T. i T. b. p.* no. 38, p. 446 (1926).

Fig. 13.

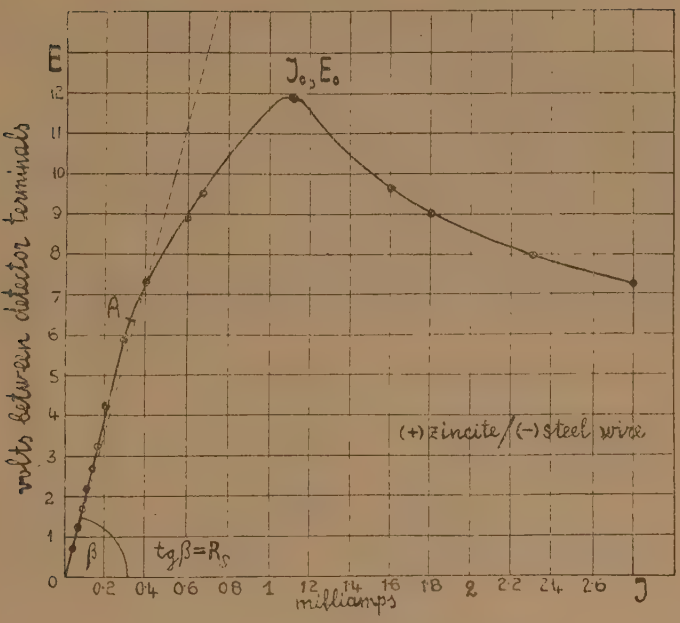
E
volts between detector terminals
J_0, E_0
A
β
$tg\beta = R_g$
(+) zincite / (−) steel wire
0 1 2 3 4 5 6 7 8 9 10 11 12
0·2 0·4 0·6 0·8 1 1·2 1·4 1·6 1·8 2 2·2 2·4 2·6
milliamps
J

Fig. 14.

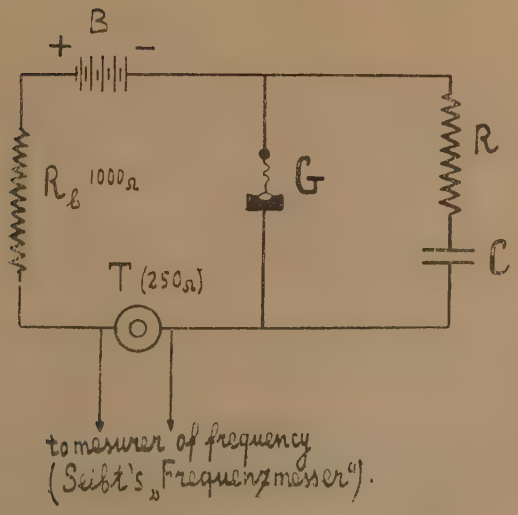
B
+
−
R_g 1000Ω
G
R
C
T (250Ω)
to measurer of frequency
(Seibt's „Frequenzmesser").

R = 1000$_\Omega$; ohmic resistance of the telephone = 250$_\Omega$; B = 12 volts = const.

In a "Thomson oscillating circuit in series" (LC) the generating detector G (as well as Duddel arc) produces, generally speaking, the oscillations of the "second type" * (see Pl. XIX. fig. 15).

Fig. 15 (Pl. XIX.) represents the oscillograms of oscillating current of low frequency. The oscillograph loop was directly connected to oscillating circuit LC. $C = 2\,\mu F.$; $L = 0{\cdot}1$ H.; ohmic resistance in the circuit $= 11_\Omega$; $R_b = 1000_\Omega$; B = 12 volts (see fig. 16).

The period of these non-sinusoidal oscillations will increase the more in respect to $2\pi\sqrt{L/C}$ (1) the greater C/L, (2) the smaller the resistance of the circuit, (3) the steeper the

Fig. 16.

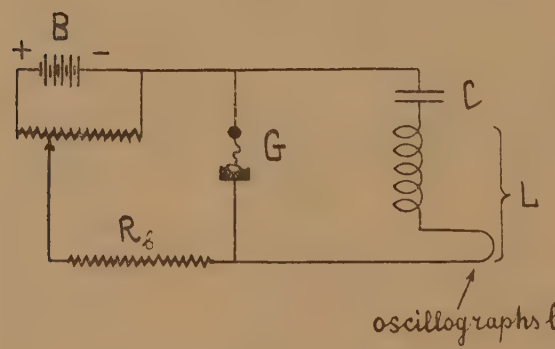

negative slope on a given space of detector characteristic. For example, with strong increase of direct current I (see fig. 9 *a*) the period may be decreased approximately to $2\pi\sqrt{L/C}$. Compare the curve "*a*" on fig. 15 (Pl. XIX.), which is plotted at small I ("*a*" at I = 2·5 milliamps.; E, on detector terminals, = 7·1 volts) with "*b*" plotted at large I ("*b*" at I = 4·9 milliamps.; E = 6·2 volts) across the generating detector.

But it may be mentioned that the production of "second type" oscillations cannot be taken as a factor to confirm either the thermal theory or the point of view on the

* *T. i. T. b. p.* no. 14, p. 375 (1922); 'Wireless World and Radio Review,' no. 271, p. 93 (1924). "By Second type" here is meant a large deflexion of the oscillating current in the circuit from a sinusoidal form. The oscillograms were kindly taken by Mr. A. M. Coogucheff.

electronic discharge. It is a consequence of the characteristic form (even if counted as "non-inert") of generating detector (see fig. 9 *a*), and also of its regimen and the properties of the connected oscillating circuit.

There are interesting thermal theories with respect to the actions of generating contact formulated by W. Eccles *, A. Petrowsky †, and G. Ostroumoff ‡, and as regards the sounding of detector by K. Lichtenecker §.

F. Seidl discovered an interesting phenomenon of the sounding of crystals, and investigated in connexion with this phenomenon different effects ‖ under the condition of larger currents than in the case of ordinary oscillation with crystal, and came to view the effect of sounding as a consequence of electronic discharge.

As it is with other sources of negative resistance, in the schemes with a generating detector the regimen of regeneration may be obtained. For practical purposes the detector is easy to connect directly to the aerial of the receiver ¶ (figs. 17 *a* & 17 *b*).

More than eighty different natural minerals have been investigated with regard to the oscillations, and it has been found that (besides zincite) tinstone (SnO_2) generated rather well.

The author desires to take this opportunity of expressing his gratitude to Mr. N. A. Smolianinoff for his kind presentation of many specimens of minerals.

For practical purposes the most satisfactory type was found to be a zincite crystal which was prepared by fusing with MnO_2 in an electrical arc furnace **.

Fusion of the crystals increases their conductivity. Fused crystals produce stable oscillations (which may be maintained for more than three days). With fused crystals, tension of d.c. source must not be too great—about 12 volts are enough

* W. Eccles, *loc. cit.* (cit. by A. Petrowsky).

† A. A. Petrowsky, *Morskoy Sbornic*, no. 10 (1911).

‡ G. Ostroumoff, *T. i T. b. p.* no. 24, p. 204 (1924).

§ K. Lichtenecker, *Zeit. für Tech. Phys.* viii. p. 161 (1927).

‖ F. Seidl, *Vien. Ber.* (II. *a*) cxxxv. H. 9 (1926); *Phys. Zeit.* xxvii. pp. 64 and 816 (1926). The effect of sounding of crystals has also been discovered by the radio amateur, A. Karpovsky, Nov. 1925 (*T. i. T. b. p.* no. 43, pp. 449–451, 1927).

¶ Lossev, *Technika Sviazi*, ii. nos. 3–4, p. 390 (1924). Ref. by V. Gabel, 'Wireless World and Radio Review,' vol. xv. no. 269, p. 50 (1924). *Cf.* Britch. pat. J. Smith and S. Pearce, No. 259005 (1925) (Exp. Wir. & Wir. Eng. iii. no. 39, p. 776 (1926)).

** *T. i T. b. p.* no. 21, p. 349 (1923). Also *Zeitschr. für Fernmeldetechnik*, no. 9, p. 132 (1925).

on the average. Signs of poles are important. Except for some cases, the branch of characteristic at (+) zincite and (−) steel wire has steeper negative slope (see, for example, fig. 11). Of course, stability occurs only when the resistance R_b (see figs. 8, 10, 14, 16, 17 *a* & 17 *b*) is not less than the absolute value of the negative resistance produced by the detector (at given I and E).

In conclusion, it may be mentioned that a considerable change of zincite detector characteristic may also depend on the Joule effect (*cf.* fig. 11). For example, when the oscillating point giving the characteristic curve is traced by the steady current, of order more than 10 milliamps., the

Fig. 17 *a*.

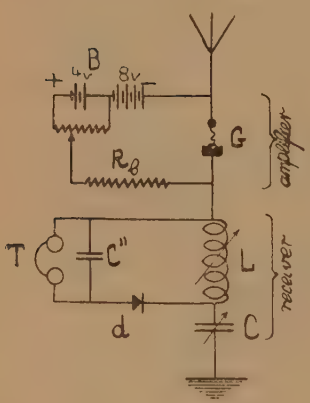

B=12 volts (4+8).

During the work of the scheme the current I across the detector G was usually taken of order 4 milliamps.

R_b=1000$_\Omega$.

Fig. 17 *b* *.

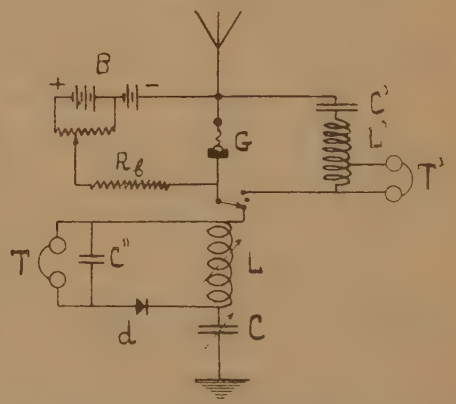

L'C' is "an auxiliary circuit" of low audio-frequency, used to find the oscillating points on the crystal.

$L'=0{\cdot}035$ H.; $C'=0{\cdot}25\,\mu$F.

To obtain the oscillations in the circuit LC after switching from L'C' to LC, the conditions

$$C/L \geqslant C'/L' \quad \text{and} \quad R \ll R'$$

must be taken.

R and R' are resistances in the circuits.

"hysteretic loop" depending on the Joule effect was observed (*cf.* fig. 11).

Setting the generating zincite detector in benzene, ether (generally in non-conductive intensively evaporating liquids) makes E_0/a greater, and enables the production of negative

* Russian Pats. 996, 75317 (1922); 472, 77717 (1923).

resistance to be greater in absolute value *. (See the influence of the temperature in fig. 11; *cf.* also § 2.)

§ 5. *Luminous Detector as a Light Relay.*

The luminescence of a carborundum detector may be observed, beginning with a current through the contact of order 10^{-4} amp. (see the characteristics on figs. 2, 3, & 7).

With strong current of order 10^{-1} amp. bright luminescence may be obtained, and it still remains on a red-hot (by the Joule effect) crystal. Fig. 18 (Pl XIX.) (orthochromatic plate) shows the piece of carborundum placed between two metallic rods; the current $=0{\cdot}2$ amp.; the potential difference between rods $=29$ volts. At the negative electrode a violet spot (fig. 18, on the right) of luminescence II. is marked on the red-hot crystal.

During observations of both luminescences (I. and II.) in a rotating mirror, if an alternating current passes through the contact separate flashes may be clearly seen at frequencies up to 78,500 cyc. per second (current $= 0{\cdot}23$ amp. R.M.S.). The limit of discernment of these flashes (frequency 78,500 cyc. per second) depends on the resolving power of the installation of the rotating mirror, but it was independent of "luminescence inertia." Even at frequency 78,500 cyc. per second the lengths of the black intervals were more than the lengths of the flashes, which indicated that the luminescence appeared and disappeared very quickly †.

The brightness of the luminescence may be made sufficiently great to render it possible to record on a moving photographic plate an alternating current of frequency order 10^2 cyc. per second. Fig. 19 *a* (Pl. XX.) shows the record of a current 500 cyc. per second (with luminescence II.; current through the detector $= 0{\cdot}24$ amp., R.M.S.; objective F: 3·5; F = 7 cm.); see also fig. 19 *b* (Pl. XX.).

Fig. 20 (Pl. XX.) represents the action of luminescence II. on a photographic plate for different times of exposure (objective "Collinear Voigtländer" F : 18; F = 18 cm.;

* *T. i T. b. p.* no. 18.

† With regard to small inertia, compare the very small (and typical for fluorescence) duration of after-luminescence in photo-luminescence; (of order 10^{-8} sec.; less than 10^{-6} sec.). See S. J. Wavilow and W. L. Lewshin, Journ. Russian Phys.-Chem. Society, lviii. p. 555 (1926); *Zeit. für Phys.* xxxv. p. 920 (1926). In the investigation of the photo-luminescence phenomenon it has been stated by the above-named authors that there are no intervening stages between fluorescence and phosphorescence.

the luminescence is projected in natural size; current through the detector=0·23 amp.; tension on terminals 28 volts). For comparison, in fig. 21 (Pl. XX.) are shown some results for "glimmering" neon lamp (also non-inertia source of light) Osram 125–139 volts, to which was applied d. c. 177 volts with value 15·1 milliamps. From this it is clear that the luminous detector acted more effectually than the lamp (*cf.* figs. 20 & 21, Pl. XX.).

It may be mentioned that with strong currents sometimes, in addition to the contact luminescence, luminescence at the place of contact of single little crystals occurred, in one place or in another, in the middle of the carborundum piece (*cf.* fig. 18). The intensity of these luminescences also depends on current direction, in meaning of item 1, § 2.

In conclusion, the author wishes to thank Professor W. K. Lebedinsky, M.Sc., for his valuable advice in connexion with the work on oscillating crystals.

Nijny-Novgorod, Radio Laboratory.

CIII. *On Jaeger's Method as Applied to the Determination of the Surface Tension of Mercury.* *By* R. C. Brown, *B.Sc.**

TWO years ago research was commenced with a view to determining, by a small variety of methods, the surface tensions of certain molten metals. As in the literature of the subject the maximum bubble pressure method, sometimes called Jaeger's method, is quoted as having been used extensively for high temperature work, it was decided to make use, in the first place, of this method. A few preliminary experiments were carried out using mercury, for obvious reasons, and difficulties began immediately to appear. Many of these have apparently been encountered also by Bircumshaw (Phil. Mag., Sept. 1928). Throughout the past two years the vagaries of the method have been studied by the present writer, not so much for their own sakes as with a view to their elimination. The observations described in the present paper in many cases fall in with those of Bircumshaw and also break a certain amount of new ground.

* Communicated by Prof. A. W. Porter, F.R.S.

Apparatus and General Manipulation.

The apparatus was of the usual type. The gas to be used for blowing the bubbles was contained in a glass reservoir the volume of which could be controlled by allowing mercury to run in or out of it. On leaving the reservoir the gas passed through rubber tubing, which could be restricted to any required degree by means of a screw-clip, and then to the jet and one arm of a water manometer, which consisted of a tube of 0·5 cm. bore, the other arm being a Woolf's bottle of 10 cm. diameter. Thus pressure changes read on the narrow arm were multiplied by 1·0025 in order to obtain the true pressure change in centimetres of water. During the preliminary experiments the jet was clamped and the mercury under experiment was raised or lowered beneath it on a levelling table fitted with a graduated vertical action. Thus the jet remained stationary and the mercury was set with its surface coinciding with the plane of the jet by visual observation ; it was then raised through a known distance. Later the jet was provided with a graduated screw for vertical motion and the mercury container, which was of silica, was fixed. The disposition of this part of the apparatus was such that the whole could be enclosed in a vertical electric furnace, the temperature of the mercury being measured with a calibrated Pt, Pt–Rh thermocouple. A drying tube of wide bore containing calcium-chloride lumps was incorporated between the manometer and the jet. The jets, in the first place, were made of glass, and it was found that these could be drawn and fractured satisfactorily after some practice, and there appeared no necessity to grind them. Later, jets of amalgamated copper, platinum, and monel metal were used. When possible, the setting of the plane of the tip of the jet in the mercury surface, preparatory to lowering it through a known distance, was done visually; but, when the furnace was in use, this became no longer possible and the following technique was adopted. The pressure inside the gas reservoir was reduced and the screw-clip adjusted so as to cause a slow current of air to flow up the jet. The latter was then slowly lowered until the manometer began to rise, showing that the jet orifice had been closed by the mercury surface. The settings of the screw-head thus obtained were found to be in better agreement with those obtained visually than were those obtained by the more generally used method of allowing gas to flow out of the jet, probably because in this last case the outflowing gas forms a depression in the mercury surface and the

movements of the manometer are correspondingly less definite. In the later and more accurate experiments the mercury for each day's readings was collected in the silica vessel direct from a single-stage vacuum still.

The equation used in the calculations was

$$T=\frac{rg}{2}\left[H\sigma-\left(h+\frac{2}{3}r\right)\rho\right],$$

where

T is the surface tension of the liquid in dynes per cm.

r the radius of the jet in cm.

g the acceleration due to gravity.

H the maximum corrected reading of the manometer in cm.

σ the density of the manometric liquid.

h the depth of the tip below the free surface of the mercury in cm.

ρ the density of mercury at the temperature observed.

Results.

During the first experiments the bubbles were blown with air, and it was immediately noticed that the detachment of the bubble from the tip of a glass jet in mercury corresponded, in general, to no definite pressure for any given jet. The first indication of reproducibility was given by a glass jet of internal and external radii 0·026 and 0·045 cm. respectively. Readings of maximum bubble pressure taken immediately after setting the tip 0·391 cm. below the free surface of the mercury always rose consistently, not from a consistent initial reading, but always reaching a definite maximum. A typical series of readings was 38 cm., 42·0 cm., and a maximum of 42·52 cm. of water, the maximum being consistent. If the jet was withdrawn and reset in the liquid a similar series was obtained with the same maximum. When corrected for the rise of water in the wide arm of the manometer 42·52 cm. becomes 42·63 cm. of water with a density of 0·999 gm./cc. Using the internal radius of the jet in the calculations the value for the surface tension of mercury comes out to be 478 dynes/cm., and using the external radius the value is 819 dynes/cm. Of course the bubble is quite invisible during the whole of its life, so that the evidence as to which edge of the jet it is clinging to when the pressure inside it reaches a maximum is derived from the values given when each of the radii is used in turn

in the calculations. Thus in the above case it would appear that the internal radius is the correct one to use, as 478 is a much more probable value for the surface tension of mercury at room-temperature than is 819.

A set of readings covering several days, during which the jet was not removed from the mercury, was taken with this jet. After the first day the readings remained consistently at the maximum, rising slightly with time. Thus on the first day the result was 470 dynes/cm. and on the fifth it was 477, using the internal radius (the external radius, if used in the calculations, will, of course, give 817 for the fifth day). Points to be noticed are :—

1. On the fifth day the maximum pressures were constant to 0·05 cm. of water in 42 cm., and in most cases no variation was noticeable at all on a scale graduated in mm.

2. On withdrawing the jet and re-immersing it on the fifth day the pressure assumed its maximum value after about two bubbles had been released.

3. The pressure at which the bubble became unstable depended not on the time elapsed since setting the jet in the mercury but on the number of bubbles blown since then.

4. The mercury was not protected from atmospheric contamination to any great extent, so that the accuracy of the method would appear to be singularly independent of the state of the free surface of the mercury when once the jet has been immersed below it.

Next a jet was made with thinner walls but larger radii [internal 0·0847 cm., external 0·0970 cm., thickness 0·012 cm.]. The jet was soaked overnight in chromic and sulphuric acids, washed in tap-water and distilled water and dried. The following set of uncorrected pressures, p. 1048 (cm. water) was obtained. A horizontal line separating two consecutive readings indicates that between these two readings the jet was withdrawn and reset in the mercury.

Thus with this jet it would appear that after two or three bubbles had been released, the bubble began to form on the outer edge of the jet, giving a pressure of 16·14 cm. of water (when corrected for the rise of the wide arm), since this pressure gives, when the external radius is used in the calculation, a value of 473 dynes/cm., which is very near to values obtained with other jets, and also those published by other observers. The low value of the pressure obtained with the initial bubbles of the series might be explained by

assuming the presence of an air-film adhering to the jet upon first lowering the latter into the mercury, and the subsequent partial or complete destruction of the film by movements of the mercury following upon the release of the first bubbles.

Uncorrected Pressures.

15·7
15·7 } with external radius gives 450 dynes/cm.;
15·7 } with internal radius gives 399 dynes/cm.
16·0
16·10
16·10 } with external radius gives 473 dynes/cm;
16·10 } with internal radius gives 419 dynes/cm.
16·11
16·60
16·10
16·14
16·45
16·3
16·4
16·5
16·55
16·64
16·63
16·78
16·63
16·83
16·91
16·88
16·95
17·01
16·93
17·09
17·14 (the highest reading) { with external radius gives 523 dynes/cm.
{ with internal radius gives 462 dynes/cm.
17·03
17·10
17·08
16·4
16·4
16·9
15·7
15·7

The presence of an air-film on the horizontal face of the tip might also explain the tendency of the pressures to rise above the value of 16·14 cm., since the film would lessen the adhesion of the mercury to the underneath face of the jet,

and so cause the bubble to spread to the outer edge. During its destruction, however, the adhesive forces would be increased, and the mercury-glass circle of contact might find itself nearer to the inner edge of the jet when the maximum bubble-pressure was reached. The maximum reading recorded (17·18 when corrected) gives 462 dynes/cm. with the internal radius, which would indicate that during this series the bubble never actually remained on the inner edge of the jet. An actual change in the value of the surface tension does not seem to be indicated, since the series could be repeated over again by merely withdrawing the jet and re-setting it in the liquid, and also it must be remembered that a fresh surface is formed for each bubble, so that a change in the surface tension could only be brought about by a change in the bulk composition of the mercury. Another possible cause of the phenomena might be the creation—instead of, or in addition to, the destruction of an air-film—of a layer, on the underside of the jet, of some combination of the glass mercury and oxygen molecules which might cause an increase in the adhesion of mercury for glass. It is significant that, as will be seen later, there appeared no tendency for the bubble to be released from any but the outer edge when nitrogen was used instead of air for blowing the bubbles. With other glass jets which were made (and when air was used) it was usually noticed that pressures corresponding to the outer edges were registered on beginning a series of readings, but in some cases these could not be repeated until the jet was cleaned again and fresh mercury was used.

A copper jet (internal radius 0·042 cm., external 0·064 cm.) was then constructed and the tip of it amalgamated with mercury. The object in view was not so much the obtaining of an accurate value of the surface tension as the seeing whether the same large variations in the readings would occur when using a jet which was "wetted" by the mercury. The largest variation noticed was 0·6 cm. in 25 cm. of water which is far less than most of those experienced with glass jets. Taking an average reading and using the internal radius in the calculation we get 397 dynes/cm., and using the external radius 615 dynes/cm. The actual values mean very little since probably the mercury forming the bubble had a considerable amount of copper dissolved in it; but the comparative consistency of the readings was striking when compared with readings taken with glass jets.

Experiments were next carried out using nitrogen instead of air and little or no tendency was shown for the readings

to rise continuously as successive bubbles were blown. Moreover, different jets gave consistent values of the surface tension only when the external radius was used in the calculation. The following is a typical set of readings obtained with a glass jet of radii 0·0450 and 0·0695 cm. :—

Cm. of water (uncorrected).	
19·76	
19·78	
19·77	
19·78	... Mean 19·78, which, when corrected, becomes 19·83 cm.
19·80	This, with the external radius, gives 469 dynes/cm.
19·76	at 19° C.
19·80	
19·79	
19·80	

The readings remained constant for periods as long as 24 hours when the jet was kept below the surface of the mercury for that period. After such long periods of immersion, however, it was sometimes noticed that the gas flowed out of the jet in a constant stream and passed continuously up the outside walls of the jet to the free surface of the mercury without forming bubbles in the usual way. When this happened, the manometer registered a pressure less than that caused by bubbles and the surface of the mercury was covered with a pattern of standing ripples. This failure to form the usual bubbles was possibly caused by a weakening of the adhesion of the mercury for the glass of the jet by the formation of a film of gas on the glass, since it could usually be remedied by lowering the tip of the jet to 0·600 instead of 0·400 cm. (which was the usual distance employed) below the free surface of the mercury, thus increasing the hydrostatic pressure on such a film. Sauerwald and Drath (*Z. Anorg. Chem.* cliv. p. 79 (1926) have noticed that consistent readings of bubble pressure cannot be obtained in general unless the jet is immersed to a depth greater than 0·3 cm. A platinum jet of very small thickness (radii 0·0325 and 0·0352 cm.) behaved very similarly. On changing the dimensions of the jet by turning it in a lathe it was readily seen that the external radius must be used in the calculations in order to give consistent results for the two sizes of jet. A few readings taken with a jet of monel metal of dimensions similar to those of the platinum jets were also satisfactory. The values obtained for the surface tension of mercury at an average temperature

of 18° C. with glass and platinum jets (using nitrogen) are here summarized :—

Jet.	Radii, cm.		T, dynes/cm.
	Int.	Ext.	
Glass 1	0·0415	0·0500	471
„ 2	0·0450	0·0695	469
			472
„ 3	0·043	0·061	475
Platinum 1	0·0325	0·0352	477
			477
			478
„ 2	0·0315	0·0379	476
			476

Mean values :—

Glass jets ..... 472 dynes/cm.

Platinum jets ..... 477 „

Further interesting results were obtained when higher temperatures than that of the air were used. For this the furnace and other arrangements previously referred to were brought into use. The furnace was kept at the temperature required for several hours so as to avoid any temperature lag. At first the second glass jet referred to in the table above was used. The readings were extremely consistent, variations in pressure rarely reaching 0·05 cm. in any determination. The values obtained indicated that the external radius was to be used in the calculations. Unfortunately the jet was chipped and the readings became indefinite after determinations at three different temperatures had been made. Glass jet number 3 was then used, and it was found that, in order to bring the results into line with those already obtained (which agreed well with those of other observers), it was necessary to use the internal radius at the temperatures which were used. The actual pressures were again as consistent as before and there appeared no tendency for the bubble to form on the outer circumference. On the whole, however, the actual results for the surface tension given by this jet were unsatisfactory. Number 1 glass jet was found to be very satisfactory and good values were obtained with this, the bubble appearing to come from the inner edge of the jet except for air temperature. These remarks also apply to a fourth gas jet which was made.

Summary of values obtained for the surface tension of mercury at temperatures up to its boiling point :—

Jet.	Radii, cm.		Radius used in calculation.	Temp., °C.	T, dynes/cm.
	Int.	Ext.			
Glass 1	0·0415	0·0500	Internal	178	436
			,,	218	427
			,,	272	411
			,,	326	396
Glass 2	0·0450	0·0695	External	78	460
			,,	162	443
			,,	333	397
Glass 4	0·0350	0·0496	Internal	87	458
			,,	118	450
	Mean of several glass jets.		External	18	472

Fig. 1.

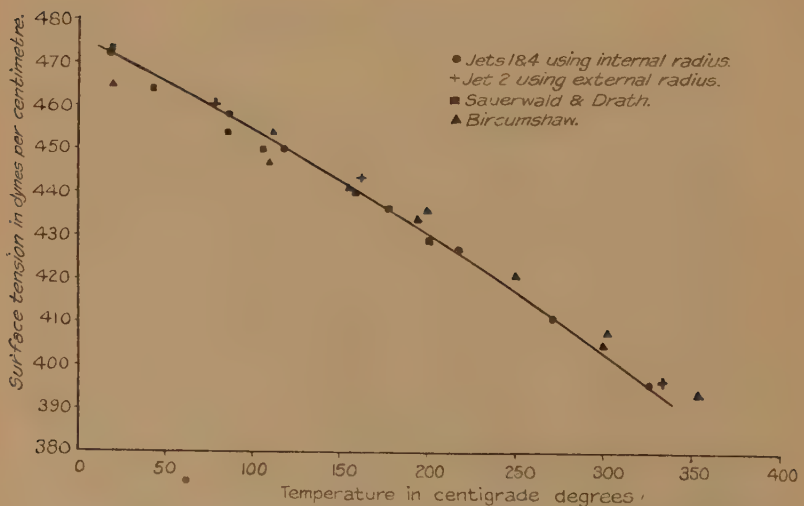

Fig. 1 shows these results graphically. The continuous line is drawn through the points obtained with jets 1 and 4. Results published by Sauerwald and Drath (*loc. cit.*) and by Bircumshaw (Phil. Mag. vii. 8, pp. 341 (1926) are also shown.

Collection of Results and Discussion.

When glass tips were used with air in the determination of the surface tension of mercury by the maximum bubble

pressure method, consistent readings were, as a rule, found only immediately after setting the jet in the liquid. After this the readings rose, but the initial reading could again be obtained by withdrawing the jet and setting it again in the mercury. By using tips of different radii it was found that these initial readings must be used with the external radius of the tip in order to give consistent values for the surface tension. On some occasions maximum pressures were reached which when used with the internal radius also gave fairly good results; but this was not general at air temperatures. Bircumshaw has recently noticed that there is difficulty in obtaining a definite bubble pressure when oxygen is used with glass jets; but that consistent results can be obtained with hydrogen and nitrogen. This (in the case of the nitrogen) was the experience of the present writer. When nitrogen was used, pressures given by any one glass jet were very constant except for one or two low ones usually to be found immediately after immersing the jet, a possible explanation of which is an air layer adhering to the walls of the jet. Thus there seemed little or no tendency for the bubble to detach itself from any but the external circumference of the jet when nitrogen was used. For reasons given earlier in this paper, there seems more possibility of a change in the radii of successive bubbles than of an actual change in surface tension. Platinum and monel metal jets gave similar results to those with glass jets.

When the mercury was heated certain glass jets always formed the bubble on the internal circumference even for temperatures less than 100° C., although one was discovered which formed the bubble on its outer edge right up to 330° C. This latter had a large wall thickness (0·025 cm. as compared with 0·009 cm. and 0·012 cm. of those in the former category). The deciding factor in the question as to which radius to use in the calculations was, for these high temperature measurements, the agreement of results with those of other observers. As a rule the radii were so different as to leave no doubt as to which radius should be chosen—the smallest difference between the two alternative results being about 30 dynes/cm. Certain it is that with several jets the actual bubble pressure was greater at high temperatures than at air temperature, which can only be interpreted in the above way, especially as the readings were so consistent.

The mechanism of the formation of the bubble on either of the two edges or at any line between them would appear to be obscure. It can only be said that when the adhesion

of mercury for glass is small, the bubble will certainly be formed on the outer edge, and when the adhesion is large it will not spread to the outer edge but will reach its maximum pressure and unstable state while still on the inner edge. These two cases correspond roughly to perfectly non-wetting and perfectly wetting liquids, *i. e.*, with liquids of angles of contact of 180° and 0°. Cantor (*Ann. der Phys.* xlvii. p. 399 (1892)) deals with the subject and expresses the opinion that for non-wetting liquids the radius of the bubble will depend on the angle of contact. Thus for this case he recommends jets of no thickness at their tip so that the internal and external radii coincide. It is found difficult to make such jets in practice, however.

Sauerwald and Drath consider that with liquid metals the bubble forms always on the external edge. Results described in the present paper seem to show that the bubble forms on the outer edge in the case of glass jets in mercury unless, either by the continuous blowing of bubbles with air or by heating the mercury, the adhesion between the two becomes large enough to prevent the bubble spreading to the outer edge. W. C. Baker (Science, lxvii. p. 74 (1928)) has shown that mercury at ordinary temperatures will adhere to a glass surface (in his case a spherical lens surface) which is withdrawn from it, and it was often noticed during the course of the present research that the mercury adhered to the jet when the latter was raised out of the free surface. Baker also mentions that, on raising his spherical lens surface, the line of contact did not move in a continuous way over the glass surface, but sometimes stuck and remained adhering at the same place for considerable up and down movements of the lens. This may correspond to the sticking which must take place when the bubble surface, having left the inner edge (it is on this edge during some period of its life since the mercury meniscus is first of all in the bore of the jet), does not spread completely to the outer edge but detaches itself while registering a pressure corresponding to a circumference lying between the two. When used at ordinary temperatures and with nitrogen, the bubble always comes from the outer edge, and in these circumstances the method is most satisfactory, especially in view of the facts that a fresh surface is blown for each bubble and that readings are constant for 24 hours or more even though the free surface of the mercury is exposed to contamination. The results obtained were 472 and 477 dynes/cm. for glass and platinum jets respectively at 18° C. These agree with the 473 at 19°C. of Sauerwald and Drath obtained with a silica

jet and CO_2; but not so well with Bircumshaw's most recent values, which cluster round 500 dynes/cm. The temperature curve in fig. 1 follows the results of Bircumshaw and Sauerwald and Drath.

I sincerely thank Dr. A. Ferguson and Prof. A. W. Porter for the assistance and encouragement which they have lent during the course of the work.

Carey Foster Laboratory,
University College, London.

CIV. *The Crystal Structure of Mercury, Copper, and Copper Amalgam.* *By* Henry Terrey *and* Cyril Maynard Wright *.

1. Crystal Structure of Mercury.

In connexion with some work on the crystal structure of amalgams it was necessary to know the crystal structure of mercury.

Two investigations have already been carried out: (1) by Alsen and Aminoff (Geol. For. Förh. xliv. 1922), who found that mercury at the temperature of solid carbon dioxide has a hexagonal lattice with $a_0=3{\cdot}84$ Å.U. and $c=1{\cdot}88$; and (2) by McKeehan and Cioffi (Phys. Rev. i. p. 444, 1922), who found that at a temperature of $-115°$ C. mercury has a rhombohedral structure.

In the present investigation the work was carried out at a temperature of approximately $-150°$ C., and the rhombohedral structure assigned by McKeehan and Cioffi fully confirmed.

Apparatus.

For the production of X-rays the Shearer type of tube was used, fitted with a copper anticathode and operated at 35,000–40,000 volts, the current being from 2–4 M.A.

The camera was constructed on somewhat similar lines to that used by McLennan and Wilhelm for their work on the crystal structure of solid carbon dioxide and solid oxygen (Trans. Roy. Soc. of Canada, May 1925, and Phil. Mag., Feb. 1922). The construction is shown in the sketches (figs. 1 to 5).

* Communicated by the Authors.

The main chamber of the camera was of heavy brass tube about 6 cm. in diameter, a cover being provided by a central,

Fig. 1.

Fig. 2.

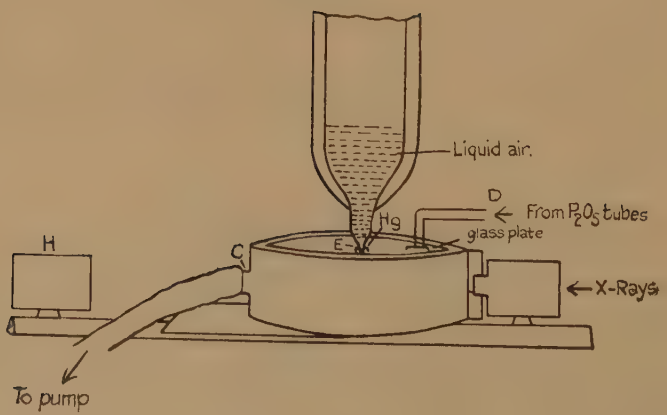

well-ground matrix, into which a double-walled vacuum flask fitted.

Fig. 3.

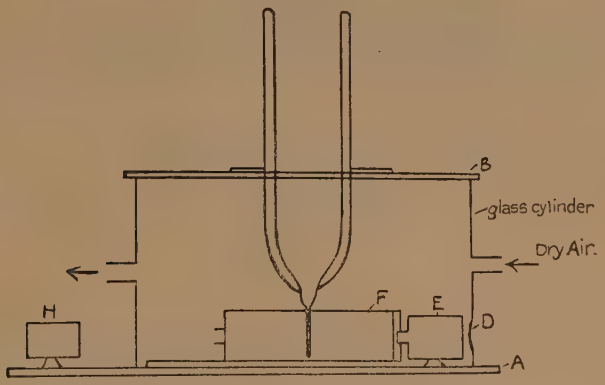

Fig. 4.

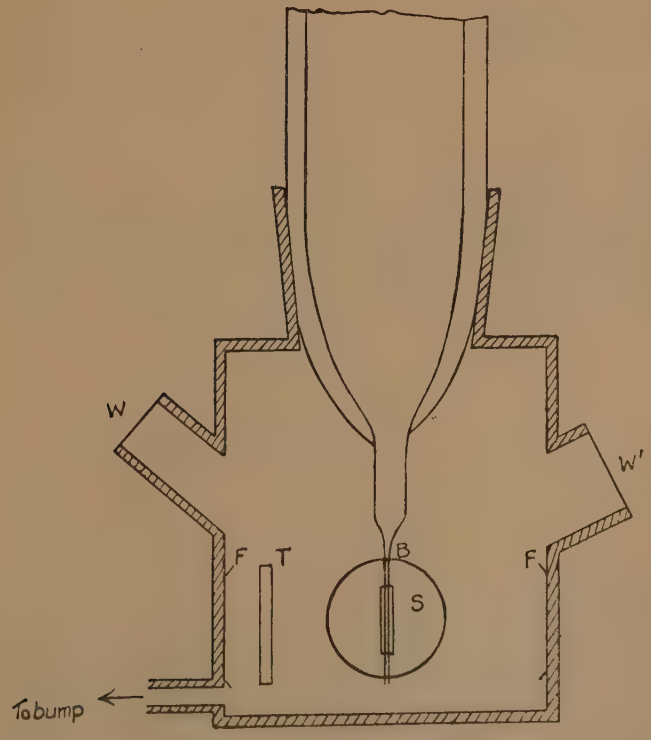

The slit, ·5 mm. wide, ·8 mm. high, and 3 cm. long, was cut from a brass cylinder 3 cm. long and 2 cm. in diameter, and was sealed into the wall of the camera.

A metal film-holder F, faced with nickel foil, ·03 mm. thick, was soldered on the inside of the brass tube, and the

Fig. 5.

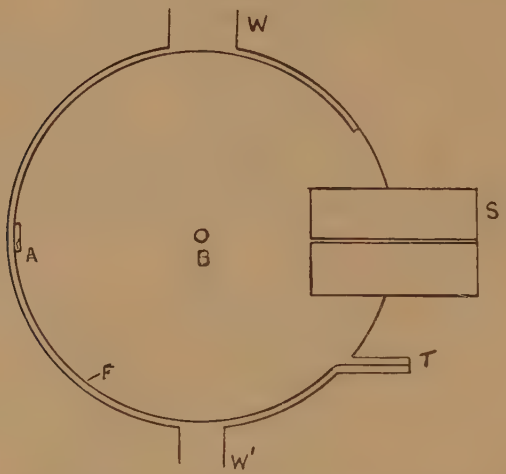

film was introduced at T, where the end of the film protruded through the brass tube. This joint was also soldered, so that the camera could be evacuated while the film remained at normal pressure. The films could thus be protected from mercury vapour in the camera.

Fig. 6.

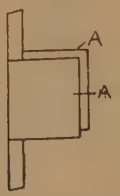

The holder consisted of a soft metal tube 12–13 cm. long, flattened out in the form of a narrow rectangular tube to allow the passage of the film. The holder was bent into an arc of a circle with the nickel on the inside, before introduction into the brass tube.

A strip of lead of the shape indicated in fig. 6, was fixed

at A to protect the film from the direct beam of rays, and the scattered rays were stopped by the "wings" AA. When the film had been introduced, the end of the holder at T was covered with plasticene to protect the film from the light.

The Dewar vessel of the pattern indicated was made, the tube A (of lead-free glass) being drawn out to a thin-walled fine capillary tube about ·8 mm. in diameter, the capillary being sealed at the lower end.

Experimental Method.

The capillary tube was lined up with the slit by rotating the Dewar vessel in the matrix. The position of the Dewar with respect to the camera was marked, so that this alignment need not be repeated with the same capillary tube. A piece of thin aluminium foil was waxed over the outside of the slit. The position of the camera was adjusted so that the X-rays passed through the slit, by viewing the fluorescence on a barium platino-cyanide screen placed in the centre of the camera (the Dewar being removed during this operation).

A little mercury was then placed in a small cavity in the bottom of the camera. The Dewar vessel was then replaced and the camera was evacuated with a Hyvac pump, a McLeod gauge being used to test the vacuum obtained. Liquid air was poured into the Dewar flask, and the base of the camera was very gently warmed. A film of mercury ·25–·5 mm. thick soon formed on the capillary tube, and the photograph was then started, an exposure of six hours being given. The lines on the film were quite distinct, but rather broad.

Before the values of d_{hkl} for the planes giving these lines could be calculated, an accurate measure of R, the distance from the film to the mercury surface, had to be obtained. This was found by filling the capillary tube with powdered sodium chloride, and with the Dewar vessel in the same position relative to the camera as for the mercury photograph another photograph was taken. Assuming the value of d_{hkl} for the sodium-chloride lines (Davey, Phys. Rev. xxi. 1923), the value of R was calculated. This did not give an absolutely accurate value for R for the mercury photographs, as the sodium chloride was in the capillary tube, while the mercury was on the outside, but the glass wall was as thin as possible, and it was the most accurate means of determining R.

Results.

Several photographs of mercury were taken, and the complete results from one measurement are included here (Table I.).

TABLE I.

Photograph of Solid Mercury.

Distance between lines.	Intensity.	R (from NaCl lines).	θ.	d_{hkl}.
cm.		cm.		
3·250	Strong.	2·877	16° 10¾′	2·760
4·050	,,	2·879	20° 10′	2·230
5·300	Weak.	2·875	26° 24′	1·730
6·364	Strong.	2·866	31° 48′	1·460
6·856	,,	2·863	34° 17′	1·365
7·789	Weak.	2·859	39° 1½′	1·221
8·724	Medium.	2·859	43° 43′	1·113
10·063	,,	2·854	50° 31′	·996
11·014	,,	2·852	55° 19′	·936
11·560	,,	2·852	58° 4′	·906

TABLE II.

Photograph of NaCl.

These values of R are used for the above determinations of d_{hkl}.

Distance between lines.	d_{hkl} (assumed).	R.
cm.		cm.
3·185	2·814	2·877
4·572	1·990	2·880
5·639	1·625	2·872
7·508	1·259	2·858
8·390	1·149	2 860
10·961	·938	2·852

By the use of Hull's plots (Phys. Rev. 1921, p. 17) it was seen that the diffraction given by mercury corresponded to a rhombohedral lattice with axial ratio 1·94. This structure confirmed the work of McKeehan and Cioffi.

Assuming the agreement between the spacings of the planes (111) and (110) to be exact, from the equation

$$d_{hkl}=\frac{(hx_1+ky_1+ly_1-1)\sqrt{1+2\cos^3\lambda-3\cos^2\lambda}}{\sqrt{(h^2+k^2+l^2)\sin^2\lambda+2(hk+kl+hl)(\cos^2\lambda-\cos\lambda)}},$$

referring the rhombohedron to three trigonal axes, where $\lambda=\mu$, it followed that

$$\cos\lambda=1\,3,$$

i. e. $$\lambda=70^\circ\,32';$$

knowing λ from the above equation, assuming $d_{111}=2{\cdot}233$, it followed that

$$a_0=2{\cdot}996\ \text{Å.U.}$$

Summary of Results.

A summary of results (Table III.) is given with the theoretical spacings, calculated from the above equation.

TABLE III.

Indices (hexagonal form).	Indices (trigonal form).	d_{hkl} (theoretical).	d_{hkl} (observed). 1.	2.	3.	Intensity.
10·1	100	2·735	2·766	2·760	2·760	s.
00·1	111	2·233	2·230	2·238	2·230	s.
10·2	110					
11·0	101	1·730	1·727	1·735	1·730	w.
20·1 10·4	111 211	1·462	1·445	1·466	1·460	s.
11·3 10·1 (2)	210 100 (2)	1·367	1·363	1·368	1·365	s
10·5	221	1·223	...	1·227	1·221	w.
21·1 00·0 (2) 10·2 (2)	201 111 (2) 110 (2)	1·116	1·106	1·115	1·113	m.
12·2	211	1·073	1·063	...	...	m. w.
10·0 20·5	211 311	·998	·988	·996	·996	m.
11·6 12·4	321 301	·938	·928	·935	·936	m.
10·1 (3) 10·7	100 (3) 322	·911	·901	·906	·906	m.

Rhombohedral system ..... $a_0=2{\cdot}996\times10^{-8}$ cm.
Hexagonal system..... $a_0=3{\cdot}460\times10^{-8}$ cm.
$c=1{\cdot}94.$

The results given in Table III. show very good agreement with the assumed structure. The calculated density, if one atom is associated with each cell (simple rhombohedral lattice), is 14·26 gm./cm.^{3}. The value here determined is in agreement with the values for its density, 14·193 gm./cm.^{3} at its melting-point (Mallet, Roy. Soc. London Proc. xxiii. p. 71, 1877), and 14·362 gm./cm.^{3} at the temperatures of liquid air (Dewar, Chem. News, lxxxv. p. 277, 1902).

2. Copper.

Considerable divergence exists in the literature with regard to the precise values for the plane spacings of copper, values between 3·597 A.U. and 3·634 A.U. being given (*cf.* Holgersson, *Ann. d. Physik*, iv. pp. 79, 35, 1926). Our value, 3·603, is slightly greater than the precision value of Davy (Phys. Rev. xxv. 1925), viz. 3·597.

Lattice Constant for Copper.

For the production of X-rays the Shearer type of tube was employed, photographs being taken with a Müller X-ray spectrograph, a slit of 0·2 mm. being used. The powdered substance mounted in the centre of the camera could be oscillated uniformly through an angle of 12° during exposure, which varied between 2–4 hours. The films were measured on a measuring machine graduated to 1/100 of a millimetre.

Experimental.

The copper was prepared by deposition from an aqueous solution of pure copper sulphate to which pure zinc and a little sulphuric acid had been added. The deposited copper was washed with water and alcohol, and kept under absolute alcohol to prevent oxidation.

In order to eliminate any uncertainty in the value of R, the distance from powder surface to photographic film, sodium chloride was used as a comparative standard.

The powders were prepared by grinding the halide or copper in an agate mortar and then rubbing through a 200-mesh silk handkerchief. The powdered samples were mounted in thin celluloid tubes, 0·6 to ·7 mm. in diameter. Two methods of packing the powders were tried—one where the sodium chloride and copper powder were intimately mixed before introduction into the tube, and the other where one half of the tube was filled with sodium chloride and the other half with copper. The first of these two

methods was found to give better photographs, and was used throughout this investigation.

Results.

The diffraction patterns of sodium chloride and copper were obtained on the films. Assuming the vales of d_{hkl} for the various sodium chloride lines (from W. P. Davey, Phys. Rev. xxi. 1923), the values of θ were calculated from the equation

$$n\lambda = 2d_{hkl} \sin \theta,$$

where θ is the angle of diffraction, d_{hkl} is the spacing of the reflecting plane whose indices are hkl, λ is the wave-length of the X-rays. Knowing θ, R can be determined, and these values of R for the sodium-chloride lines were plotted against the distance of the line from the mid-point of the film, so that the values of R for the lines of the substance under investigation could be read off from the graph.

The value of a_0, the side of the unit copper cube, was calculated from the expression

$$d_{hkl} = \frac{a_0}{\sqrt{h^2 + k^2 + l^2}}.$$

Several photographs were taken, using different samples of copper mixed with sodium chloride. The full results from one of these photographs are given in Table IV.

3. Copper Amalgams.

The first paper of note relating to copper amalgams was due to Becquerel (*Comptes Rendus*, lvi. p. 237, 1863, and lxxv. p. 1729, 1872), who prepared the amalgam electrolytically and examined its structure microscopically. He stated that the amalgam crystallized in rhombohedral prisms with pyramidal ends.

Guntz and Greift (*Comptes Rendus*, cliv. p. 357, 1912) carried out an extensive research on the preparation of this amalgam, and came to the conclusion that the final product depended on the mode of preparation and on the conditions of the experiment. This has certainly been confirmed in the present investigation, as it has been found that the metals readily unite in all proportions.

Regarding the chemical nature of this amalgam, there has been much difference of opinion. Joule (*Jahr.* 1863, p. 281) and others considered the amalgam, prepared by

electrolysis and by dissolving copper in mercury, as a simple compound, CuHg, but the evidence for the individuality of this product is meagre.

Puschin (*Z. Anorg. Chem.* xxxvi. p. 241, 1903), considerations of the E.M.F. of the cell $\begin{matrix}\text{Cu}\\\text{Hg}\end{matrix}\Big|\text{N . CuSO}_4\Big|\text{Cu}$, concluded that no compound was formed.

TABLE IV.

Distance between corresponding lines.	R for NaCl lines.	R for Cu lines.	sin θ.	d_{hkl}.	Plane.	a_0.
cm.	cm.	cm.				
*15·537	3·0015					
14·795	...	3·005	·3338	2·081	111	3·603
14·336	...	3·006	·3697	2·0795	111	3·601
*14·124	3·007					
13·599	...	3·008	·4269	1·801	100	3·602
*12·969	3·008					
*11·964	3·012					
11·110	...	3·009	·6034	1·274	110	3·602
*10·997	3·0085					
10·574	...	3·011	·6391	1·087	311	3·604
*10·098	3·013					
9·468	...	3·012	·7067	1·088	311	3·607
8·919	...	3·012	·7383	1·041	111 (2)	3·605

* NaCl lines.

Mean value..... 3·6035 Å.U.

λ_α for copper = 1·5374 Å U.

λ_β ,, ,, = 1·3889 Å.U.

A final mean value for a_0 was determined from eight different films, giving the following result:—

$$= 3{\cdot}603 \pm {\cdot}002 \text{ Å.U.}$$

More recently two papers have been published by Tammann and Mansuri (*Z. Anorg. Chem.* pp. 132–33, 1923–24)* on the properties of various amalgams, including copper amalgam. From a study of the cooling curves, E.M.F., change of volume on solidification, and the microstructure of copper amalgams (1–90 per cent. Cu), it is concluded in

* *Cf.* also Tammann and Stassfurth, *Z. Anorg. Chemie*, p. 143 (1925).

the latter paper that two series of amalgams exist. On continued heating of an amalgam (5–78 per cent. Cu) at 100° C. a crystallite X is slowly formed. On cooling, a crystallite $CuHg$ separates. At 20° C. neither of these forms is present, but another crystallite X′ appears. The two latter differ from the first in that, when heated, drops of mercury exude from them. It cannot be said that the evidence for the existence of these "crystallites" is very conclusive, but it certainly seems probable that copper amalgam can exist in more than one form, since the amalgams when first prepared are quite soft, but on standing set to a hard mass.

The purpose of this investigation was therefore twofold: firstly to determine the structure of copper amalgam, and secondly to see if there was any change in structure when the amalgam was first prepared and after it had hardened.

Preparation of Copper Amalgam.

An amalgam containing any desired amount of mercury could be obtained by rubbing together, in a mortar under very dilute sulphuric acid, the requisite quantities of the two metals. The copper was prepared as in the previous investigation, and pure re-distilled mercury was used.

These amalgams, which are quite soft and pasty when the mercury content exceeds 50 per cent., become much harder on standing. Even an amalgam containing as much as 75 per cent. of mercury will set to a fairly hard mass within 12 hours of its preparation. When the mercury content is less than 50 per cent. the amalgams harden within 3–4 hours of their preparation.

The amalgams—powdered by the same process as was used for copper—were mixed with from 1–2 times their weight of finely-powdered sodium chloride and mounted in thin-walled celluloid tubes. This method of filling the tubes could not be followed in all cases, as the amalgams of high mercury content, when freshly made, were too soft to mix with the sodium chloride, and for these the amalgam was packed in one half of the tube and sodium chloride in the other half.

Experimental.

The apparatus was exactly the same as was used in the previous investigation.

A series of amalgams was prepared from 90 to 20 per cent. copper, and at least two photographs were taken of each, one immediately after its preparation and another a few days later, when the amalgam had hardened. For

these second photographs, fresh samples of the amalgam and sodium chloride were made. The composition of each amalgam was accurately determined by estimating the copper present volumetrically with potassium iodide and standard thiosulphate.

Results.

The results obtained for the series of amalgams containing from 90 to 20 per cent. of copper can be briefly summarized in Table V.

TABLE V.

	Freshly prepared.		Hardened amalgam.	
Percentage of copper.	Copper lattice.	Amalgam lattice.	Copper lattice.	Amalgam lattice.
89.....	Strong.	...	Strong.	Weak.
79..... ..	,,	...	,,	,,
70.....	Fairly strong.	...	Fairly strong.	,,
57.....	Medium.	...	Medium.	,,
49.....	,,	Weak.	Weak.	Medium weak.
40.....	,,	,,	...	Medium.
27.....	,,	...	...	,,
18.....	,,	...	...	Medium weak.

This table shows that :—

1. The amalgams, when first prepared, are merely mechanical mixtures of the two metals, as in every case the diffraction pattern of copper was obtained on the film, and the intensity of the lines decreased with increasing mercury content. The appearance of a weak amalgam pattern in the freshly-prepared amalgams containing 40 and 49 per cent. of copper is probably due to the fact that these amalgams hardened in 3–4 hours, and the time of exposure was also of this order.

2. In the hardened amalgams a definite compound is found containing from 27–40 per cent. of copper. This pattern is masked in the amalgams of high copper content by the copper pattern.

However, in the above photographs there were never more than three or four lines measurable in the amalgam pattern,

although in the 40- and 27-per-cent. copper amalgams there were a number of lines faintly discernible on the films.

Several photographs were taken of the hardened amalgams of mercury content 50–70 per cent. to obtain a more distinct diffraction pattern of the amalgam. It was found that if the amalgam was prepared with a mercury content of

TABLE VI.

Amalgam. 32 per cent. Copper ; 68 per cent. Mercury.

Distance between lines.	Intensity.	d_{hkl}.
cm.		
15·957	v.w.	3·301
15·642	w.	2·977
*15·459	m.	
15·052	w.	2·512
14·953	w.	2·212
14·520	s.	2·212
14·249	v.w.	2·085
14·065	m.	2·006
*14·023	m.	
*12·846	w.	
12·603	w.	1·567
12·426	w.	1·526
11·870	w.	1·279
11·740	w.	1·393
11·546	w.	1·359
11·375	w.	1·334
11·019	m.s.	1·279
*10·879	m.	
10·375	w.	1·193
10·023	m.w.	1·153
*9·984	m.	
8·442	w.	1·012
8·139	w.	·991

* NaCl lines.

more than 70 per cent., and, after drying, it was compressed with the hand through fine-mesh cloth to remove the excess of mercury, an amalgam of composition ranging between 30 and 35 per cent. of copper was obtained. When photographs were taken of these powdered hardened amalgams, a large number of lines were visible and measurable on the films.

The results from two of these amalgams are given in Tables VI. and VII.

A photograph was taken of the pure hardened amalgam, and then of a mixture of the amalgam and sodium chloride, the object of this being to check the amalgam lines on the film of the amalgam-sodium chloride mixture.

The sodium-chloride lines were used, as before, to give an accurate measure of R, which was then employed in the determinations of d_{pkl} for the amalgam lines.

TABLE VIII.

Amalgam. 34 per cent. Copper ; 66 per cent. Mercury.

Distance between lines.	Intensity.	d_{hkl}.
15·153	w.	2·522
14·953	w.	2·203
14·530	s.	2·207
14·269	v.w.	2·082
14·073	m.w.	2·001
*14·049	m.w.	
12·597	w.	1·559
12·443	w.	1·524
11·890	w.	1·279
11·744	w.	1·390
11·551	w.	1·356
11·370	w.	1·329
11·033	m.s.	1·279
*10·894	m.	
10·383	w.	1·193
10·050	m.w.	1·153
*10·012	m.	
8·453	w.	1·011

* NaCl lines.

The diffraction pattern given by this amalgam did not fit exactly any of Hull's plots (Phys. Rev. 1921, p. 17) for the simpler crystallographic systems, viz. the cubic tetragonal and hexagonal (including close-packed and rhombohedral).

The best fit that can be obtained is for a simple tetragonal lattice with axial ratio ·64. The first five lines fit exactly, and almost all the others except the "2·006" line.

However, many more lines ought to be present which are not visible on the films, so that the most that can be done is to suggest this as a possible structure.

Conclusion.

It is evident that a change in structure occurs when the amalgam hardens; until this takes place the amalgams appear to be merely mechanical mixtures of the two metals. When the amalgam hardens, a definite compound is formed of composition 30–35 per cent. copper, and this compound is present all through the series of amalgams examined. Its structure cannot, however, at present be accurately determined, and it is only suggested that the amalgam possesses a simple tetragonal lattice with axial ratio ·64, and possibly of composition Cu_3Hg_4.

The Sir William Ramsay Laboratory
of Physical and Inorganic Chemistry,
University College,
London.

CV. *Proceedings of Learned Societies.*

GEOLOGICAL SOCIETY.

[Continued from p. 944.]

April 18th, 1928.—Prof. J. W. Gregory, D.Sc., F.R.S., President, in the Chair.

THE following communications were read:—

1. 'The Succession and Structure of the Borrowdale Volcanic Series in Troutbeck, Kentmere, and the Western Part of Long Sleddale (Westmorland).' By George Hoole Mitchell, Ph.D., M.Sc., F.G.S.

The area described lies in the eastern part of the Lake District south of the High Street range. It is drained by the Rivers Sprint, Kent, and Trout Beck, all of which flow in a southward direction.

The rocks described belong to the Borrowdale Volcanic Series. The estimated thickness of such members of the series as are exposed is approximately 3700 feet, but nowhere is the base seen. They are overlaid unconformably by the Coniston Limestone Series. Nine subdivisions are recognized:—

(*i*) Upper Rhyolites.
(*h*) Upper Andesites.
(*g*) Coarse tuffs.
(*f*) Wrengill Andesites.
(*e*) Kentmere Pike Rhyolites.
(*d*) Bedded tuffs, with andesite-flows.
(*c*) Harter Fell Andesites.
(*b*) Froswick Tuffs, with rhyolite-flow.
(*a*) Nan Bield Andesites.

There are also minor intrusions of rhyolite, quartz-porphyry, andesite, and lamprophyre.

The lava-flows range in composition from rhyolites to augite-andesites. In most cases flow-brecciation is evident and marked, while many of the andesites are intensely vesicular.

The tuffs, composed in the main of andesitic material, show in many deposits rhyolitic fragments in abundance, and range from very fine-grained and well-bedded examples to ill-assorted agglomerates.

The rocks have been subjected to severe earth-movements. Two systems of folding are recognized, an earlier one of pre-Bala age and a later one of Devonian age. The former system, of simple character, shows axes trending in a north-north-easterly and south-south-westerly direction. In the latter the folding was intense, with an east-north-easterly and west-south-westerly strike, while the pitch of the folds was determined by the folds of pre-Bala date. The rocks are steeply folded in the south-east of the area, and the folds are even overturned to the north. Northwards the folding is less severe, and is marked by the presence of a broad anticlinal fold.

No faulting of earlier date has been recognized, but several faults are referred to the Devonian system of earth-movements, while it is suggested that several north-and-south faults are of late-Carboniferous age.

The rocks are strongly cleaved, the strike of the cleavage coinciding with that of the Devonian folding.

2. 'The Geology of the Marquesas Islands (Central Pacific). By Lawrence John Chubb, M.Sc.

The Marquesas Islands are situated in about 10° lat. S. and 140° long. W. With one doubtful exception all are of volcanic origin. The southernmost, Fatu Hiva, consists of a caldera composed chiefly of lava-flows, within which an ash-cone has been built up. The western half of the whole structure has disappeared, apparently owing to submergence by faulting. Motane is a small ash island. Tahuata is larger, and it also is composed chiefly of ashes in its northern part; its south-eastern side has been faulted down. In Hiva Oa there are three great craters in the western part, some of the coasts are faulted, and there is an elevated plateau at a height of 1300 to 1500 feet above sea-level. Nuka Hiva has a structure similar to that of Fatu Hiva, and it bears a plateau at an elevation of 2600 feet.

A consideration of the directions of elongation of the islands, of the manner in which they are arranged, of the trends of the faulted coasts, and of the strikes of the dykes, leads to the conclusion that the group is situated, not on a crustal fold, but on a system of intersecting fissures.

The uplifted plateaux prove that elevation has occurred, but the embayment of the mouths of the streams that deeply dissect them

affords evidence of a later subsidence. All the islands are surrounded by a shore-shelf, now standing, owing to a recent fall in sea-level, 3 or 4 feet above high-water mark.

It is suggested that the poor development of coral-reefs in the group is due chiefly to periodic chilling of the water by extensions of the cold Peruvian Current, connected with cyclic climatic changes.

May 23rd, 1928.—Prof. J. W. Gregory, LL.D., D.Sc., F.R.S., President, in the Chair.

Prof. P. G. H. Boswell, D.Sc., F.G.S., delivered a lecture on the Geological Features of the New Mersey Tunnel. He said that the recent 'holing-through' of the highway-tunnel under the River Mersey, by which connexion was established between Liverpool and Birkenhead, makes the present time appropriate for giving an account of the features of geological interest which were revealed. The tunnel will be the greatest subaqueous tunnel in existence. The predictions of T. Mellard Reade regarding the existence of a buried channel beneath the River Mersey, and of G. H. Morton of a sub-Mersey fault, were verified in the driving of the Mersey Railway-Tunnel some fifty years ago. Subsequent records by local geologists have enabled greater precision to be given to the inferences, and the geological observations made during the operations now proceeding are, in the main, in accord with expectation.

The subaqueous portion of the tunnel (44 feet in diameter) and the two Birkenhead approach-tunnels lie in the Middle Bunter Sandstone ('Pebble-Beds'), which dips eastwards at about 3° to 5°. A fault-system, apparently of small aggregate throw, was met with at about 1828 to 1870 feet from the Liverpool shaft. The hade was eastwards, whereas in the case of the sub-river fault in the Mersey Railway-Tunnel it was westwards. On the Liverpool side, the presence of the 'Castle Street Fault', which throws down the Upper (Soft) Bunter Sandstone on the east, was confirmed. At the Old Haymarket entrance another north-north-west and south-south-east fault throws eastwards, and brings Lower Keuper Sandstone into contact with Upper Bunter.

From observations in the area of the docks and the environs of Liverpool, and the numerous exploratory borings carried out in connexion with the tunnel-works, it has been possible to construct exceptionally accurate profiles of the system of buried channels. They appear to be of subglacial origin, and do not deepen seawards; they are filled with gravel and sand, overlaid by boulder-clay. In place of the single channel found in the Mersey Railway excavations, two (or more) feeding-channels occur farther north.

Interesting, and at present unexplained, features have been observed in the levels of underground water. As would be expected, the fresh-water table rides on the back of the salt-water table in the neighbourhood of the Mersey estuary.

June 13th, 1928.—Prof. J. W. Gregory, LL.D., D.Sc., F.R.S., President, in the Chair.

The following communications were read:—

1. 'A Re-Excavated Cretaceous Valley on the Mongolian Border.' By Prof. George Brown Barbour, M.A., Ph.D., F.R.S.E., F.G.S.

The paper traces the history of successive infillings and renewed erosion of a buried Cretaceous valley 600 feet deep, discovered by the author in the course of a survey of the Kalgan district, on the Chinese–Mongolian border. The valley, originally cut in pre-Cretaceous lavas, was completely filled by the Nantienmen Beds, levelled off by erosion, and entirely covered by a heavy capping of plateau-basalts.

During late Pliocene times a stream followed part of this old Mesozoic valley-axis before striking off at an angle. The valley-bottom was again filled up by wind-blown lœss in mid-Pleistocene times, again partly excavated in late Pleistocene, and once more filled with very late Pleistocene or early recent gravels. At present, the course is being opened for the fourth time. The Cretaceous-valley deposit (Nantienmen Beds) has been left clinging to the side-walls in many places, so that it has been possible to trace the old landscape and to compare this with the present topography.

2. 'The Volcanic Complex of Calton Hill (Derbyshire).' By Sergei Ivanovich Tomkeieff, F.G.S.

The volcanic complex of Calton Hill shows two phases of vulcanicity:—

(i) Effusive phase—represented by, besides the agglomerate and tuff of the old volcanic cone, a highly decomposed lava. Petrologically and chemically it is comparable with the other contemporaneous Lower Carboniferous lavas of the district. The vesicles are filled up with a chlorite of delessite type.

(ii) Intrusive phase—represented by a fresh analcite-basalt, which has intruded into the old volcanic chimney and spread amœba-like in the volcanic cone, detaching large masses of vesicular lava. Besides abundant analcite, mostly in the form of spheroids, the basalt contains numerous inclusions of peridotite. These inclusions, apparently represent shattered fragments of a pre-existing rock, and contain, besides the normal pyroxene, a definite hydrous augite.

[*The Editors do not hold themselves responsible for the views expressed by their correspondents.*]

Fig. 1.

Luminescence I.

Fig. 4.

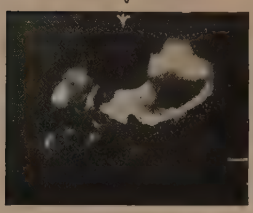

Luminescence II.

Magnified 30 times.

Fig. 5

Luminescence I. × 505.

Fig. 6.

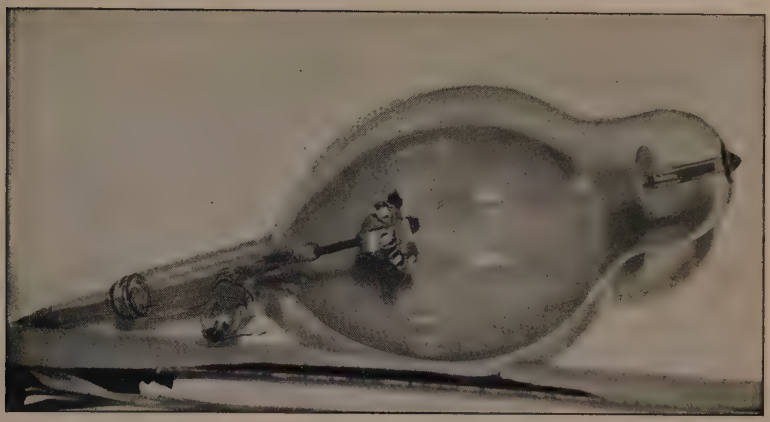

Discharge-tube, used for observations of cathodo luminescences.

Fig. 9 *b*.

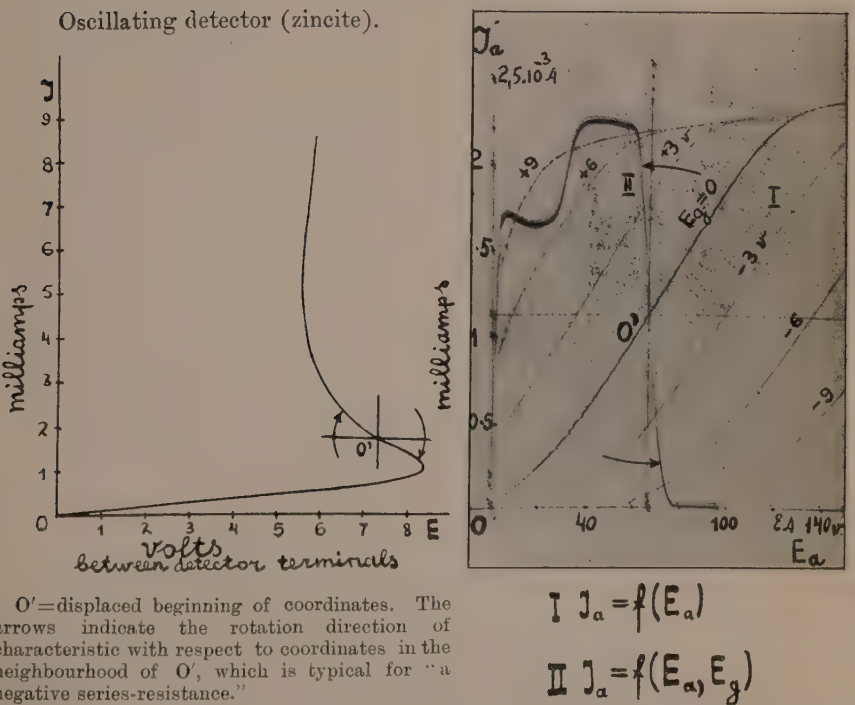

O′=displaced beginning of coordinates. The arrows indicate the rotation direction of characteristic with respect to coordinates in the neighbourhood of O′, which is typical for "a negative series-resistance."

I $J_a = f(E_a)$

II $J_a = f(E_a, E_g)$

II.=the "regeneration-characteristic" of vacuum-tube (with negative slope). The arrows indicate the rotation direction of characteristic with respect to coordinates in the neighbourhood of O′, which is typical for "a negative leak-resistance."

The characteristics of vacuum-tube were plotted by means of B. A. Ostroumoff's "characterograph" (*Zeit. f. Techn. Phys.* no. 4, p. 168, 1927).

Fig. 15.

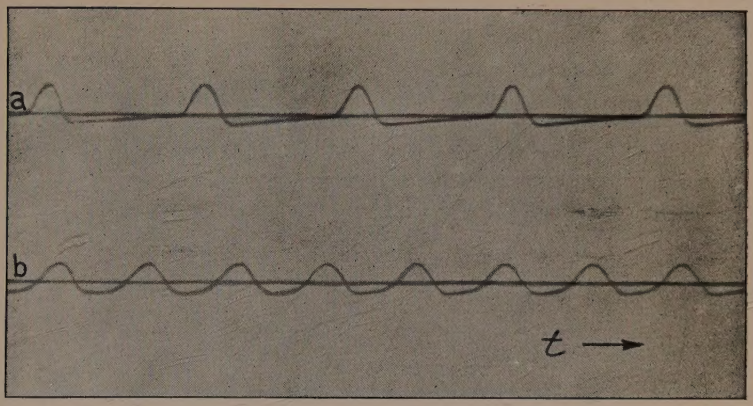

"a" at I=2·5 milliamps.; E=7·1 volts.
"b" at I=4·9 milliamps.; E=6·2 volts.
Both curves (a and b) were plotted from same oscillating point.

Fig. 18.

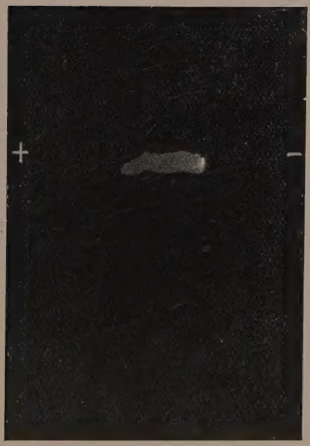

Glimm spot of luminescence II. on a red-hot crystal; the crystal is placed between two vertical metallic rods. 1½ natural size.

Fig. 19 *a*.

Record of current 500 cyc. per sec. on a moving photographic plate (with luminescence II.; value R.M.S. of current I = 0·24 amp.; objective F : 3·5).

Fig. 19 *b*.

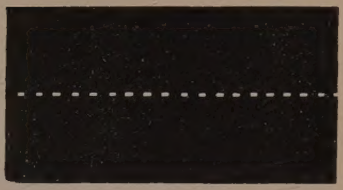

Record of fig. 19 *a*. Magnified from the original 3 times.

Fig. 20.

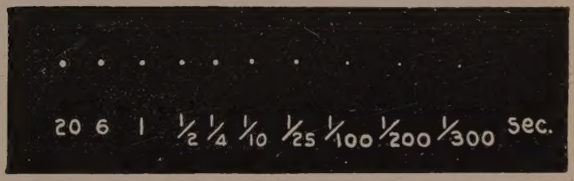

Detector luminescence (luminescence II.); I. = 0·23 amp.; E = 28 v.; (6·44 w.); F : 18. Natural size.

Fig. 21.

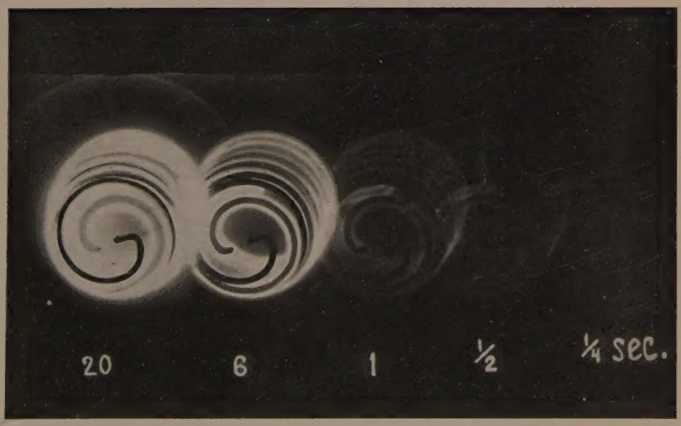

Neon lamp, at same optical conditions (cliché diminished 1·25 times); I = 15·1 milliamps.; E = 177 v. (2·67 w.); or 132·8 v.—without potential difference the ballast resistance = 2,930Ω, placed in the cap of lamp (2·0 w.).